# Urban Mining: A Systematic Approach to Separate Valuable Metals by Solvent Extraction

**Auteur :** Thonus, Sylvie
**Promoteur(s) :** Pfennig, Andreas
**Faculté :** Faculté des Sciences appliquées
**Diplôme :** Master en ingénieur civil en chimie et science des matériaux, à finalité spécialisée
**Année académique :** 2021-2022
**URI/URL :** http://hdl.handle.net/2268.2/15905

Prof. Dr.-Ing. Andreas Pfennig

Department of Chemical Engineering – Products, Environment, and Processes (PEPs)

# Protocol for solvent extraction experiments applied to nickel, cobalt and neodymium

Sylvie Thonus

Liège, August 2022

Sylvie Thonus, BSc in engineering


Protocol for solvent extraction experiments applied to nickel, cobalt and neodymium


Master-Thesis

to obtain the academic degree of

Master of Science

in

Chemical Engineering


submitted to

Université de Liège

supervisor:

Prof. Dr.-Ing., Andreas Pfennig

Université de Liège


Liège, August 2022

Master Thesis
for
Mrs. Sylvie Thonus

# Protocol for solvent extraction experiments applied to nickel, cobalt and neodymium

## Project Description

Recycling of precious metals and rare earths notably from electronic scrap is an attractive prospect. Such scrap is available in Europe and rich in those metals. However, the metals need to be separated from each other. To achieve this, a sequence of scrap comminution, acid leaching and solvent extraction is commonly put forward.

Solvent extraction process is specific to the metal extracted. To design processes, the development of numerical models is important, but it requires experimental parameters fitting for the system studied. For this purpose, standardized lab experiments must be conducted.

This aim of this work is to establish protocols for two kinds of solvent extraction experiments. The first is solvent extraction in shaken tubes. The extraction equilibrium is determined for a given $p$H based on this protocol. Several extraction experiments allow to determine the stoichiometry and equilibrium constant of the extraction reaction. The second experiment is dedicated to mass-transfer kinetics in a single-drop cell. The extractant organic solution is introduced dropwise in the equipment and maintained in contact with the metal aqueous solution for a determined residence time. With data points obtained for different residence times, the mass transfer rate is obtained for the system.

To measure metal concentration in aqueous phase, spectrophotometry is used in this work. The accuracy of the measurements is evaluated by comparing this work's results

with results from literature. The protocol is first tested out on nickel and cobalt extraction, two metals well-known in the literature, then on the less-studied rare earth metal neodymium.

# DECLARATION SUR L'HONNEUR

Je déclare sur l'honneur que j'ai rédigé le présent travail de manière autonome, que je n'ai pas utilisé d'autres sources/outils que ceux indiqués et que j'ai signalé comme tels les passages tirés des sources utilisées, tant littéralement que sur le fond.

Liège, le …………………………          ………………………………………………

      (signature)

## AFFIDAVIT

I declare that I have authored this thesis independently, that I have not used other than the declared sources/resources, and that I have explicitly indicated all material which has been quoted either literally or by content from the used sources.

Liège, ………………………          ………………………………………………

      (date) (signature)

# Acknowledgement

I am very grateful to Pr. Dr.-Ing. Andreas Pfennig for supervising my Master thesis and taking the time to answer any question I had. The experience he imparted was invaluable.

I am much obliged to Marc Philippart de Foy for assuring the day-to-day supervision and rereading this thesis. This thesis quality got genuinely better thanks to his contribution and, well, I hope I was not too much of a handful.

I would like to thank Thierry Salmon for his technical assistance at the laboratory. His help was both precious and reassuring.

The general procedure for solvent extraction experiments was imparted by Zaheer Shariff. It gave me a foothold to the subject.

Restarting and learning how to handle the mass transfer equipment was achieved with the assistance of Ezgi Uslu.

I also want to express my gratitude to all the PhD students working in the laboratory during my thesis. They took the time to placate me and to remind me that experimental failure is still valuable data.

# Résumé

L'extraction par solvant est une méthode hydrométallurgique de purification des métaux. Les métaux solubilisés dans une solution aqueuse sont extraits sélectivement dans une phase organique. Divers extractants organiques sont utilisés à cette fin, chacun convenant à la purification de métaux différents. Cette méthode est déjà largement utilisée dans l'extraction primaire de métaux comme le nickel, le cobalt et les terres rares. Elle est également de plus en plus adaptée au recyclage des métaux, de nouveaux procédés étant en cours de développement.

Les modèles sont un outil très important pour le développement des procédés. Pour garantir leur fiabilité, ils doivent être ajustés aux données expérimentales. Pour assurer la reproductibilité des expériences, celles-ci doivent être normalisées. Ce travail établit des protocoles pour deux types d'expériences d'extraction par solvant.

Le premier consiste à établir des courbes d'extraction. Les courbes d'extraction montrent l'évolution de l'extraction à l'équilibre en fonction du pH. Une phase organique contenant l'extractant est ajoutée à une solution aqueuse de métal dans un tube. Le pH de la solution aqueuse a été ajusté au préalable. Le tube est agité dans un bain thermostatique jusqu'à ce que l'équilibre soit atteint. Les phases sont séparées et recueillies. La phase aqueuse est alors analysée. Plusieurs mesures effectuées à différents $p$H permettent de construire une courbe d'extraction. A partir de celles-ci, la stœchiométrie et la constante d'équilibre de la réaction d'extraction peuvent être trouvées. Le protocole développé pour construire les courbes d'extraction est testé sur des systèmes connus : extraction du nickel avec D2EHPA, extraction du nickel avec Cyanex 272 et extraction du cobalt avec Cyanex 272. La spectrophotométrie est utilisée pour l'analyse de l'échantillon aqueux. Les courbes d'extraction obtenues sont confrontées aux résultats de la littérature. Ensuite, une courbe d'extraction est établie pour le néodyme extrait avec D2EHPA. Le néodyme est une terre rare qui a de nombreuses applications mais pour laquelle la littérature est rare.

La deuxième expérience est consacrée à la mesure de la cinétique du transfert de masse dans une cellule à goutte unique. La cellule à goutte unique est un équipement qui permet de faire léviter une goutte de diamètre souhaité dans une phase mobile continue. Dans la présente étude, la goutte contient l'extractant et la phase continue

le métal à transférer. Après contact entre la goutte et la phase continue, le métal contenu dans les gouttes récupérées est extrait à nouveau dans une autre phase aqueuse et sa concentration finale est mesurée. Par rapport à la concentration à l'équilibre, on obtient le taux de transfert du métal. Le protocole est appliqué à l'extraction du nickel avec D2EHPA et à l'extraction du néodyme avec D2EHPA.

Au terme de ce travail, il est clair que, si la spectrophotométrie présente des avantages évidents, elle manque de précision pour ce travail. Il s'agit d'une méthode rapide et peu coûteuse qui ne nécessite que de petits échantillons. Malheureusement, le spectrophotomètre ne semble donner des mesures précises que pour des concentrations comprises dans une gamme assez limitée. De plus, la phase aqueuse a tendance à se troubler à des degrés d'extraction élevés, ce qui rend les mesures de concentration par spectrophotométrie totalement erronées. Il est tout de même possible d'obtenir un ordre de grandeur sur une gamme de concentration modérée.

Pour l'expérience de transfert de masse, les conditions opératoires doivent être judicieusement choisies pour éviter la précipitation dans l'équipement tout en ayant une concentration en métal suffisamment élevée. L'interaction des phases doit être testée au préalable. Par exemple, la gélification de l'extractant a été observée avec le néodyme. La polymérisation des complexes néodyme-D2EHPA est causée par une charge métallique excessive. La formation de gel empèche la poursuite de l'expérience de transfert de masse.

En revanche, la gélification n'est pas apparue pour le nickel. Le transfert de masse du nickel-D2EHPA s'est avéré très lent, surtout par rapport au système standard zinc-D2EHPA. Le transfert de masse semble limité par la diffusion interne de la goutte. Il est possible que la vitesse de réaction ait aussi une contribution importante à ce phénomène.

# Abstract

Solvent extraction is a hydrometallurgical method to purify metals. Metals solubilized in an aqueous solution are extracted selectively in an organic phase. Various organic extractants are used for this purpose, each suitable for different metal purification. This method is already used widely in the primary extraction of metals like nickel, cobalt and rare earths. It is also increasingly adapted to metal recycling with new processes being developed.

Models are a very important tool for process development. To ensure their reliability, they need to be fitted to experimental data. To ensure the reproducibility of the experiment, they must be standardized. This work establishes protocols for two types of solvent extraction experiments.

The first is establishing extraction curves. Extraction curves show the evolution of the extraction equilibrium as a function of the $p$H. An organic phase containing extractant is added to a metal aqueous solution in a tube. The aqueous solution has its $p$H value adjusted beforehand. The tube is shaken in a thermostatic bath until equilibrium is reached. The phases are separated and collected. The aqueous phase is then analyzed. Several measurements conducted at different $p$H allow to build an extraction curve. From them, the stoichiometry and the equilibrium constant of the extraction reaction can be found. The protocol developed for building extraction curves is tested on well-known systems: nickel extraction with D2EHPA, nickel extraction with Cyanex 272 and cobalt extraction with Cyanex 272. Spectrophotometry is employed for analysis of aqueous sample. The resulting extraction curves are confronted to results from literature. Afterward, an extraction curve is established for neodymium extracted with D2EHPA. Neodymium is a rare earth metal that has plenty of applications but for which literature is sparse.

The second experiment is dedicated to mass-transfer kinetics measurement in a single-drop cell. The single-drop cell is a piece of equipment that allows levitates a drop of desired diameter in a continuous mobile phase. In the present study, the drop contains the extractant and the continuous phase the metal to be transferred. After contact between the drop and the continuous phase, the metal contained in the retrieved drops is extracted again to another aqueous phase and its final concentration measured.

Against the equilibrium concentration, it gives the metal transfer rate. The protocol is applied to nickel extraction with D2EHPA and neodymium extraction with D2EHPA.

At the end of this work, it is clear that, while spectrophotometry presents obvious advantages, it lacks precision for this work. It is a fast, inexpensive method that only requires small samples. Unfortunately, the spectrophotometer only seems to give precise measurements for concentrations that are comprised in a rather limited range. Moreover, turbidity tends to appear at high extraction degrees, which renders measurements by spectrophotometry completely unreliable. It is still possible to get an order of magnitude on a moderate concentration range.

For the mass transfer experiment, the operating conditions must be judiciously chosen to avoid precipitation in the equipment and at the same time having a sufficiently high metal concentration. The phases interaction should be tested beforehand. For instance, gelation of the extractant was observed with neodymium. Polymerization of the neodymium-D2EHPA complexes was caused by excessive metal loading. Gel formation prevented the mass transfer experiment from proceeding.

In contrast, gelation did not show up for nickel. The nickel-D2EHPA was proved to have very slow mass transfer, especially compared to the zinc-D2EHPA standard system. The internal mass transfer seems to be the major limitation to the mass transfer. It is possible that the reaction rate also has an important contribution to this phenomenon.

# Table of Content

# 1 Introduction

Due to environmental concerns, energy consumption is gradually shifting towards more renewable sources. Electricity is at the forefront of this transition. However, it implies a dramatic change in energy storage facilities and mobility solutions. Electronics and batteries are increasingly being developed, for instance in electric vehicles. A number of precious metals are thus already heavily employed and their consumption is expected to increase further. Cobalt, nickel and rare earths are part of those crucial metals.

It is already common sense that metal resources are limited. It is reason enough to worry about future raw materials shortage. On one hand, the European Union (EU) already depends on imports of nickel and cobalt for the overwhelming majority of its needs. All of the rare earths are imported from a market ruled by China. EU is thus dependent on foreign countries for its energy transition. On the other hand, electronical products and batteries are already used widely in EU countries and the disposal of end-of-life products is a challenge. Indeed, they are hazardous materials so treating them safely is expensive.

An alternative already employed to plain disposal is recycling. The advantages are obvious. The metals contained in these electronical and battery waste are in high demand to produce new electronics and batteries. They could be recovered in EU from waste, therefore both reducing the needs to import metals and reducing the amount of waste disposed of. The term urban-mining has been coined to designate the production of metallic raw materials from waste.

The processes already developed for urban-mining employ methods from pyrometallurgy, hydrometallurgy, or both. Pyrometallurgy is the production of metals by high temperature processes. Temperature can reach up to 2000 °C.

Hydrometallurgy is the treatment of metals and metallic compounds in a liquid media. Solid metals are dissolved in an aqueous solution and the different types of metals are separated to finally obtain the metal of interest at solid state. It can be collected in metallic state or as a compound: hydroxide, oxalate, etc. Pure products of cobalt, nickel or neodymium are typically obtained by hydrometallurgy, often by solvent extraction.

The general principle of solvent extraction is transferring selectively metals from one aqueous phase to an organic phase and vice-versa. The transfer is achieved by mixing the two phases together. The organic phase must be chosen non soluble in water, so the phases separate by settling. Solvent extraction allows to purify metals and, by adjusting the aqueous to organic phases ratio, the metal of interest can be concentrated in a solution. Moreover, the two phases can cycle through the plan.

Solvent extraction processes keep being developed and optimized for recycling electronical wastes. To scale up to an industrial process, models are an essential assist. To ensure that the results correspond to reality, the model parameters must be obtained from laboratory experiments. Those experiments must be conducted under conditions as close as possible to those in which the model is run.

The object of the present work is to establish a protocol to obtain data on extraction kinetics, stoichiometry and extraction degree in an efficient and reliable way. The use of the spectrophotometer is studied to analyze the extraction results. The protocol is validated using nickel and cobalt, which are well studied metals. Afterwards, the protocol is applied to a rare earth, the neodymium. All experimental results obtained are analyzed with respect to the literature.

# 2 Literature Review

## 2.1 Solvent Extraction

Solvent extraction refers to the transfer of components from one liquid phase to another. The phase that receives the metals from an aqueous phase is called the extractant. It is usually an organic phase. The type of solvent extraction of particular interest for this work employs a chemical reaction, typically located at the interface of the phases. The reaction allows to have a higher component concentration in the extractant phase than by simple physical extraction. It also promotes a higher selectivity and allows to work with smaller concentrations in the primary liquid phase.

Different types of extractant exist. They can be divided into families according to their working mode. The anionic exchanger extractant trades an anion in the aqueous phase with another it carries. The electrical charges are such that the loaded extractant is neutral. This type of extractant is obviously not used to extract metals as metallic ions are positively charged.

The solvating extractant is an organic ligand that works by replacing the hydration water around a metal cation and its corresponding anion. The complex formed is electrically neutral and hydrophobic, so it is transferred to the organic phase.

The cationic exchanger extractant is an organic acid. It presents a long organic tail that ensures its solubility in organic phases. The metallic cation is traded for hydrogen ions and a neutral complex is formed. The $p$H of the aqueous phase is the driving force of the extraction. The higher the pH, the more cations are transferred to the organic phase, and vice-versa. Carboxylic acids, sulfonic acids, phosphoric acid esters, phosphonic acids and phosphinic acids are possible cation exchangers. For instance, D2EHPA (Di(2-Ethylhexyl) phosphoric acid) is a phosphoric acid and Cyanex 272 (bis(2,4,4 trimethylpentyl) phosphinic acid) a phosphinic acid.

The last kind of extractant is chelatant extractant. It is a combination between cation exchange and solvation. Ligands trap a metal ion at the center of a metal organic complex and hydrogen ions are released during the reaction. Stoichiometry is followed and the resulting complex is neutral. This complex transfers to the organic phase. Oximes and crown ether are examples of chelating agents.

Those extractants are usually highly viscous because of their molecule size and interactions. To decrease the diffusion time, the organic phase viscosity is lowered by dilution with an organic solvent. Decreasing the viscosity also decreases the energy requirements in solvent extraction processes as pumping a liquid takes more energy when the liquid is more viscous. The type of diluent influences the reaction kinetics but hardly the equilibrium. Its concentration, however, has an effect on both kinetics and equilibrium.

The diluent selected should have a low viscosity and allow an efficient phase separation. It implies that it must have a low water solubility, does not tend to form emulsion and separates easily from the aqueous phase. Safety considerations are taken too. The volatility must be low, the flashpoint 25 °C above the operating range and the solvent must not be toxic. Finally, economic concerns dictate that the solvent must not decompose under operating conditions, the solvent must be inexpensive and sold by several suppliers. Generally, hydrocarbons either aliphatic or aromatic are chosen. Inexpensive crude oil fractions like kerosene are usually employed.

Sometimes the metal-extractant compound becomes non-soluble in the solvent and extractant mixture and a third phase is formed. In this case, either another diluent should be tested, or a phase modifier be added to solubilize the compound.

In hydrometallurgy, the extractant is organic and dissolved in an organic diluent. The metal is dissolved in an aqueous phase, generally by leaching. If a cation transfer extractant is employed, the $p$H of the aqueous phase is adjusted to obtain a compromise between quantity extracted and selectivity. The aqueous and the organic phase are non-soluble. They are mixed to increase the interface surface and thus speed up the metal transfer. Afterward, the two phases settle and are separated. The organic phase is charged in metals and the aqueous phase is depleted. The aqueous phase $p$H is adjusted again to a value adequate for leaching and is sent back to dissolve new metals. The organic phase gets depleted of the metals it contains by getting mixed with another aqueous phase. It is called the back-extraction. In a cation extraction, this new aqueous phase must be acidic. After the phase separation, the organic phase is recycled back into the extraction part. The aqueous phase after the back-extraction contains the purified metal in solution. It can then be further treated with other methods.

## 2.2 Cobalt and Nickel Uses

Nickel and cobalt are metals used in a plethora of applications. For instance, catalysts for hydrogenation contain nickel. Of the 1,838,000 tonnes of nickel mined in 2021 (Statista, 2022c), more than 75% is used in alloys (Statista, 2021). This includes not only stainless steel, but also cupro-nickel alloys and other nickel alloys known for their resistance to oxidation and their high strength at high temperature (Ahmad, 2006). Electroplating accounts for 5% of the total nickel use, and batteries for 9%. Nickel-metal hybrid battery (NiMH) is a type of renewable battery that is used for domestic applications or for some hybrid electric vehicles (Elwert *et al.*, 2015). The cathode is made of nickel oxyhydroxide (NiO(OH)) and the anode is made of an alloy containing rare earths and other metals like cobalt, nickel, manganese or aluminum (Elwert *et al.*, 2015). In recent years, lithium-ions batteries are supplanting the nickel-metal hybrid ones for electric vehicles and electronic devices (Elwert *et al.*, 2015).

Almost all types of Li-ions batteries contain cobalt (Elwert *et al.*, 2015; European Commission. Joint Research Centre. and Roskill., 2021). In 2021, 170,000 tonnes of cobalt were extracted (Statista, 2022a) and more than half of the cobalt was used for batteries (Roskill Consulting Group, commissioned by the Cobalt Institute, 2021). Cobalt has applications in metallurgy too. Around 10% of the cobalt is used in tool steel (Roskill Consulting Group, commissioned by the Cobalt Institute, 2021). Tool steel is a type of steel that boast high wear resistance, toughness and good shock-resistance. They are thus suitable to manufacture blade, chisel, drill bits, molds for plastics and so on (Jayanti, 2017). Nickel alloys also often contain cobalt. 13% of the total cobalt demand in 2020 was for manufacturing nickel-based alloys (Roskill Consulting Group, commissioned by the Cobalt Institute, 2021). Some pigments, catalysts and magnets also contain cobalt.

Despite these other applications, the main driver of the growing demand for nickel and cobalt is Li-ions battery production. Those are high capacity rechargeable batteries that are invaluable for the development of electric vehicles and electrical storage systems, which thus play an essential role in the ongoing energy transition (European Commission. Joint Research Centre, 2018).

A Li-ion battery has a graphite coated copper foil as anode and a lithium compound on an aluminum foil as a cathode. The two electrodes are surrounded by a liquid electrolyte that is an organic solvent with a conducting salt, typically $LiPF_6$. An organic membrane separates the electrodes. Once the battery is charged, lithium ions are stocked in the graphite of the anode. When the battery releases electricity, those lithium ions are transferred back to the cathode (Elwert *et al.*, 2015).

Several compositions exist for the cathode. The highest capacity is provided by a layered oxide structure using metals such as cobalt, nickel, aluminum and manganese. However, a damaged Li-ion battery using a layered oxide cathode presents fire and explosion hazards, so care should be taken (Elwert *et al.*, 2015). Safer cathode groups exist too, such as the spinel structure ($LiMn_2O_4$) or the phosphate group ($LiFePO_4$), though they both have a lower capacity.

Three main types of layered oxides cathodes are commercialized. $LiCoO_2$ (LCO) cathode is commonly used in electronic devices such as laptops and mobile phones (European Commission. Joint Research Centre, 2018). The other two types of cathodes are $LiNi_{0.8}Co_{0.15}Al_{0.05}O_2$ (NCA) and $LiNi_{0.33}Mn_{0.33}Co_{0.33}O_2$ (NMC). They boast a higher energy density and contain smaller quantities of the expensive cobalt (Elwert *et al.*, 2015). In consequence, they are employed in applications like electric vehicles and energy storage systems (European Commission. Joint Research Centre, 2018). As sales of electric vehicles are forecast to increase up to 30% a year from 2021 to 2025 (Roskill Consulting Group, commissioned by the Cobalt Institute, 2021), the world demand for cobalt and nickel is expected to increase significantly. For nickel, the demand for batteries application in EU27 is expected to reach 560 kt by 2040, from 17 kt in 2020. Worldwide, an increase by 2.6 Mt of nickel for batteries is forecast for 2040, whereas only 92 kt of nickel were dedicated to battery production in 2020 (European Commission. Joint Research Centre. and Roskill., 2021).

## 2.3  Primary Extraction of Cobalt and Nickel

Cobalt is a metal that is very rarely found alone in ores. It is usually extracted as co-product from copper or nickel extraction. In 2020, around 55% of extracted cobalt was produced alongside nickel and close to 30% as by-product of copper extraction (Roskill Consulting Group, commissioned by the Cobalt Institute, 2021). As cobalt and nickel

have similar chemical properties, solvent extraction is employed to promote high purity (Flett, 2004). Moreover, leaching followed by solvent extraction is suitable for low concentrations and ores that contain cobalt usually have a composition with less than 1% cobalt and around 2% nickel or copper (Dehaine *et al.*, 2021). The acid leaching is usually carried out using sulfuric acid, hydrochloric acid or a mixture of both (Rickelton, Flett and West, 1984).

Cobalt and nickel are present as cations in the post-leaching aqueous solution. Their extraction can be conducted by cation exchange. Long organic molecules bearing a functional group loaded with hydrogen cations are used as cation exchangers. The hydrogen cation is traded for metallic cations from the aqueous solution while increasing the acidity of the aqueous solution. The higher the initial $p$H, the higher the extraction driving force. The organic chains of the extractants are usually long, which decreases their water solubility (Pfennig, 2021). The extractants are dispersed in the aqueous phase by mixing. Once the extraction is finished, the two phases are left to settle and separated. To transfer back the metal cations to an aqueous phase, an acidic aqueous solution is mixed with the metal loaded organic phase.

The extraction equilibrium depends on the metal in solution, on the $p$H of the solution and on the extractant. As the equilibrium is different for each meal, some of them are extracted preferentially. It allows to extract metals selectively. Using an organophosphorus extractant, cobalt gets extracted by cation exchange at a lower equilibrium $p$H than nickel, for instance (Rickelton, Flett and West, 1984).

The extractants D2EHPA (Di(2-Ethylhexyl) phosphoric acid) and PC88A (2-ethylhexyl phosphonic acid-mono-2-ethylhexyl ester) were used industrially to extract cobalt from nickel ore leachates until more selective extractant were developed. Rustenbourg Refiners in South Africa set a process to purify cobalt using D2EHPA. The typical extraction curve of base metals using D2EHPA is presented in Figure 2-1. Usually, there is about twice as much nickel as cobalt in the ores. In this process, as D2EHPA is not very selective between cobalt and nickel, cobalt is made to precipitate from the leachate. A solid cobalt concentrate with a minimal 2:1 ratio of cobalt to nickel is thus obtained. Once the cake is acid leached, a solution concentrated in cobalt was obtained.

D2EHPA could then extract cobalt at commercial purity (Flett, 2004). Commercial purity nowadays means less than 1%-wt of other metals (MarketWatch, 2022). Leaching of a precipitation cake was also done by Nippon Mining. They used PC88A on a sulfide cake from nickel refining (Flett, 2004).

However, PC88A and D2EHPA present a major inconvenient. They tend to extract calcium over cobalt, and calcium can be present in cobalt ore gangue (Dehaine *et al.*, 2021) as seen in Figure 2-1. Moreover, if sulfuric acid is used for leaching, gypsum crud can form and cause extractant loss (Rickelton, Flett and West, 1984; Flett, 2004).
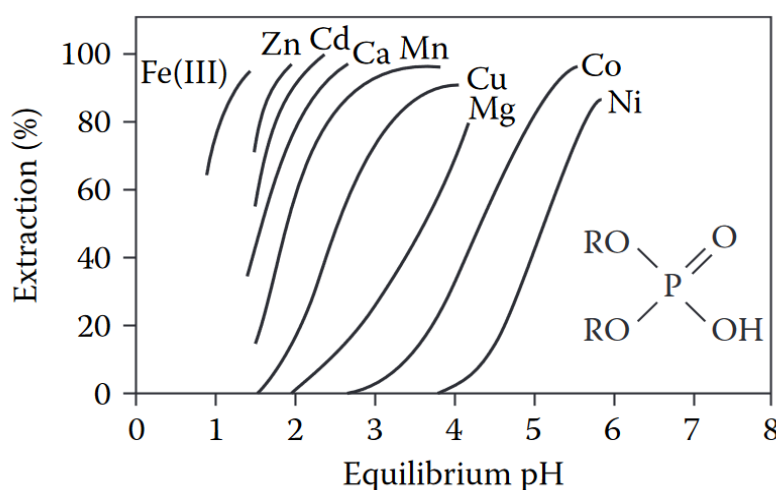


Figure 2-1: Typical extraction curves of base metal by D2EHPA (Sole, 2008)

Another extractant was thus developed in the 1980s, the Cyanex 272 (bis-(2,4,4 trimethylpentyl) phosphinic acid). Its typical extraction curves for common metals are shown in Figure 2-2. It extracts cobalt over calcium and has the highest known Co-Ni selectivity (Rickelton, Flett and West, 1984). It shows a Co/Ni separation factor of 7000, compared to factors of 14 and 280 for D2EHPA and PC88A respectively (Flett, 2004).

As the Co/Ni separation factor is overwhelmingly better with Cyanex 272, this extractant is the standard in the industry to recover cobalt from a nickel-cobalt ore leachate. However, other metals in solution can be extracted by the Cyanex 272. For instance, iron and copper are common impurities in ores and are extracted at lower *p*H than cobalt. (Olivier, 2011). Most of those metals must be separated from nickel and cobalt mixtures before solvent extraction. It is done by adjusting the *p*H with MgO, CaO or NaOH for instance, to precipitate the metals as hydroxides. This process is called the

neutralization. Iron is usually precipitated with other impurities for instance (Kursunoglu and Kaya, 2019). Once the concentrations of impurities are low enough, the rest of the refining can take place.
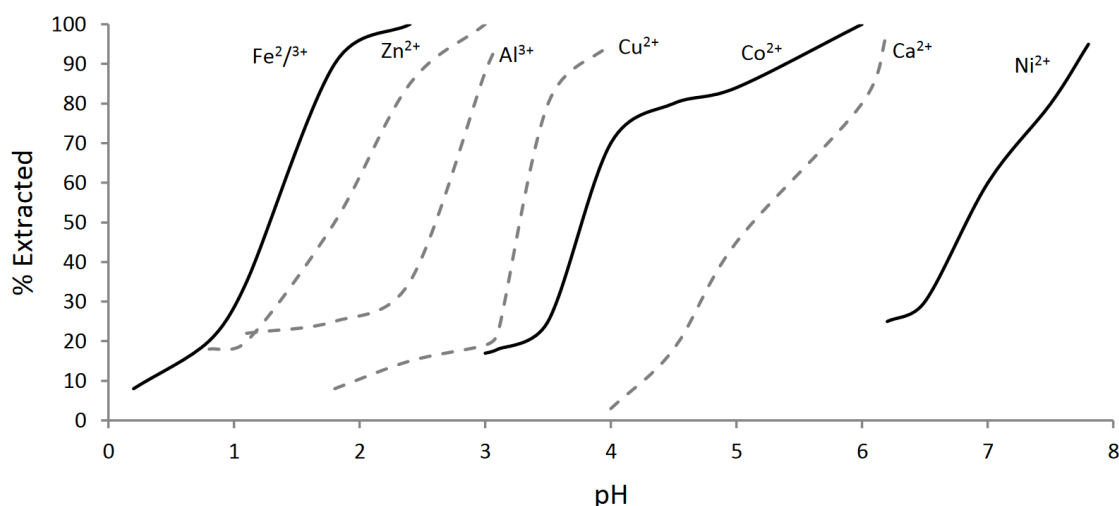


Figure 2-2: Typical extraction curves of base metal by Cyanex 272 (Olivier, 2011)

Several types of processes were developed. Direct solvent extraction is the one with the lowest capital and operating costs. Cyanex 272 extracts cobalt and some impurities directly from the leachate. Afterward, cobalt and nickel are refined separately (Kursunoglu and Kaya, 2019). Direct solvent extraction was operated at Bulong, in Australia between 1999 and 2003 (Donegan, 2006). The process started from a leachate with low level of iron, aluminum and chromium. After the solvent extraction, nickel was extracted from the aqueous phase using the extractant Versatic 10. That extractant is a tertiary-branched carboxylic acid. It allows to separate nickel from calcium and magnesium. Nickel cathodes are then produced by electrowinning. On the cobalt side, cobalt, copper and zinc precipitate from the loaded organic phase as sulfides. The obtained sulfide cake is then refined to get cobalt cathodes (Donegan, 2006).

If too much metal impurities are contained in the leachate, they may interfere with the cobalt extraction. A more adapted way would thus be to precipitate both nickel and cobalt. However, undesired metals will coprecipitate. In consequence, the intermediate nickel product is then leached again and solvent extraction performed on this concentrated leachate to produce high-purity cobalt and nickel.

Cobalt and nickel are either precipitated as hydroxides or as sulfides. Sulfide precipitation has some clear advantages over hydroxide precipitation. It is more selective than hydroxide precipitation (Kursunoglu and Kaya, 2019) thus less impurities will co-precipitate. Metal sulfides have very low solubility compared to metal hydroxides, hence less nickel and cobalt are left in solution after precipitation (Lewis, 2010). However, sulfide precipitation is riskier. Indeed, to precipitate metal sulfides, a hydrogen sulfide ($H_2S$) source must be added to the solution. The chemical breaks down and releases $H_2S$ gas that will react with the metal ions and form a metal sulfide precipitate (Lewis, 2010). Dosing this chemical is crucial to avoid excess $H_2S$ gas (Lewis, 2010). Indeed, this gas is both highly toxic and inflammable. Breathing it in is lethal to humans (INRS, 2014). Despite those hazards, sulfide precipitation is an important process in hydrometallurgy (Lewis, 2010).

An example of a plant using sulfide extraction is Murrin Murrin in Australia (Flett, 2004). The resulting mixed-sulfide cake is treated by oxidative pressure leaching. To obtain high purity cobalt and nickel, some unwanted metals such as iron, aluminum, copper or zinc must be disposed of. Adjustment of $p$H with ammonia allows to precipitate iron and aluminum. Copper and most of the zinc are removed via sulfide precipitation. The remaining zinc is then recovered through solvent extraction with Cyanex 272. In a second solvent extraction stage, the $p$H of the aqueous mixture is increased with ammonia, and cobalt is extracted with Cyanex 272. Both nickel and cobalt are reduced with hydrogen to obtain metal powders at the end of the process (Kursunoglu and Kaya, 2019).

If producing hydrogen and hydrogen sulfide on the plant is too expensive, nickel and cobalt are precipitated as metal hydroxides. Lime or magnesia can be used for $p$H adjustment (Kursunoglu and Kaya, 2019). It is to be noted that a wide range of metals precipitate as hydroxides. The intermediate product thus contains more impurities than when using sulfide precipitation.

The Cawse Nickel project in Australia uses ammoniacal releaching of a mixed-hydroxide cake (Ayanda *et al.*, 2013). As ammoniacal leaching results in a basic solution, nickel is extracted rather than cobalt in this process. The extractant used is LIX 841, a

hydroxime (Kursunoglu and Kaya, 2019). Metallic nickel is collected by electrowinning and cobalt precipitates via sulfide precipitation (Kursunoglu and Kaya, 2019).

## 2.4  Recycling of Cobalt and Nickel

Nowadays, recycling is a major concern for society. Metal recycling is no exception. Nickel alloys, like most alloys are recycled by pyrometallurgy. They are usually smelted and refined just enough to reuse it in an alloy. Metals in batteries have to be completely separated and purified to hope to reuse them in future batteries. Indeed, only high purity materials can be made into batteries (European Commission. Joint Research Centre, 2018; European Commission. Joint Research Centre. and Roskill., 2021). Hydrometallurgy is the most suitable method to treat them as high purity can be achieved (Neumann *et al.*, 2022).

Once batteries are collected, they must be sorted. Both NiMH batteries and LiBs are still in use nowadays (Elwert *et al.*, 2015; Porvali *et al.*, 2020) and get collected for recycling. As previously explained, their components are different and so should be recycled in an appropriate process. Indeed, not all metals have sufficient monetary value to justify recycling. For instance, cobalt, nickel and manganese are expensive enough while aluminum gets discarded (Pradhan, Nayak and Mishra, 2022). Moreover, as explained in the previous section, different chemical compositions are employed for the LiBs. It adds a layer of complexity and the fluxes contain variable amounts of metals to be recycled.

After sorting comes pretreatment. It allows to have access to the inside of the batteries and to make a first purification. It can either be a mechanical or a pyrometallurgical route (Neumann *et al.*, 2022). For the mechanical route, the batteries are discharged using a heat treatment or salt bath (Porvali *et al.*, 2020; Neumann *et al.*, 2022). Next, they are crushed and the product gets classified using sieving as well as gravity and magnetic separation (Pradhan, Nayak and Mishra, 2022). LiBs must imperatively be crushed under inert atmosphere because they ignite and explode when oxygen gets in contact their interior (Neumann *et al.*, 2022). Finally, the fraction rich in precious metals is treated by hydrometallurgy. This fraction is composed of the anode and cathode material crushed into powder and separated from their metallic supports (Porvali *et al.*, 2020; Neumann *et al.*, 2022). It is called the black mass (Brunn, 2021).

For the pyrometallurgical route, the batteries are smelted in a furnace (Georgi-Maschler *et al.*, 2012). A first refining is done and the process produces metallic alloys, slags and gases (Neumann *et al.*, 2022). This alloy is called matte (Neumann *et al.*, 2022). The carbon used for the reduction can come from the batteries themselves for LiBs recycling (Umicore, 2022). Matte is further purified using hydrometallurgy.

The methods for hydrometallurgy are similar to those used for primary extraction. The metals are leached, then purified using precipitations and solvent extraction. Inorganic acids are the most used chemicals for leaching. Sulfuric acid is usually the preferred acid because it is cheap, effective and compatible with metal separation techniques (Neumann *et al.*, 2022; Pradhan, Nayak and Mishra, 2022). For LiB black mass, a reducing agent is needed to solubilize cobalt and nickel from their oxide state. It is usually oxygenated water ($H_2O_2$) that is used (Neumann *et al.*, 2022).

To separate the metals in the leachate, purification by precipitation and solvent extraction are employed. For LiBs, manganese, nickel and cobalt must be separated. Manganese tends to be extracted using D2EHPA. The remaining cobalt and nickel are commonly separated with Cyanex 272 (Neumann *et al.*, 2022). For NiMH batteries, once the rare earth elements are out of the leachate, the cobalt and nickel are separated by solvent extraction (Rombach and Friedrich, 2014).

Several industrial processes are developed to recycle batteries. Umicore exploits the Ultra High Temperature (UHT) technology to treat Li-ion and NiMH batteries. It employs a pyrometallurgical pretreatment, and a copper, cobalt and nickel alloy is treated by hydrometallurgy. Slags are treated by external partners and have different uses according to the type of batteries fed to the process (Umicore, 2022).

Eramet is conducting the ReLieVe project in collaboration with Suez. The process passed the pilot plant trials in December 2021 (Eramet, 2022). The black mass is treated with hydrometallurgical methods to obtain battery-grade nickel, cobalt, lithium and manganese, with the smallest environmental footprint possible (Eramet, 2022).

Fortum in Finland recycles Li-ions batteries by hydrometallurgy too, after a mechanical pretreatment. A chemical precipitation methodology is applied to recover metals from the black mass. The metal products are sold as battery raw materials (Fortum, 2022).

The extraction of nickel and cobalt by solvent extraction is a mature technology. A range of usable extractants is available that covers almost all configurations, with Cyanex 272 being the standard choice. Not only is the extraction fast, but the metals are well separated (Rickelton, Flett and West, 1984). To increase the extraction kinetics even further, the trend is to study the synergic effect of several extractants mixed together rather than to develop new extractants (Chauhan and Patel, 2014). Those researches are less expensive and time-consuming than developing a brand-new extractant (Cheng *et al.*, 2016).

## 2.5 Neodymium Uses

No rare earth element (REE) is found on its own in its natural state. REE-bearing ores contain a wide mix of REEs. In 2021, 280,000 tonnes of REEs were mined worldwide (Statista, 2022d). As they are close in chemical properties, separation to obtain each REE at high purity is a very expensive process (Habashi, 1997).

The form of REEs that needs the least purification is called mischmetal. It is an alloy of rare earth metals obtained by fused salt electrolysis of rare earth chlorides (Habashi, 1997). Its rare earth metals proportion depends on the ore refined but it contains typically around 17% of neodymium (Habashi, 2013). Mischmetal has direct applications in metallurgy. Small quantities of mischmetal can be added to steel to promote flexibility and hot-formability (Habashi, 1997). Less than 1%-wt of mischmetal is beneficial for the mechanical properties of aluminum, copper and magnesium alloys too (Kippenhan and Gschneidner, 1970; Habashi, 1997). Despite these applications, only 8.6% of the total REEs consumption is dedicated to the metallurgy industry (Statista, 2022b). Other applications need higher purity elements, like permanent magnets, catalysts or glass production. As such, ores are leached using acids and the REEs are separated from the leachate. Two alternatives are possible for the separation. It is performed either by ion exchange on a cation exchange resin bed or by solvent extraction (Habashi, 2013). The REEs consumption share for permanent magnet, catalysts and glass production was respectively of 29.4%, 20.2% and 13.6% in 2020 (Statista, 2022b).

The REE that is mainly used in permanent magnet is neodymium, in neodymium-iron-bore (NdFeB) magnets. Figure 2-3 is a sample of this kind of magnet (Dalvin, 2006). The permanent magnet market accounted for 65% of the total neodymium market in

2020 (Grand View Research, 2021). Those magnets present a high magnetic flux density (Goonan, 2011). As a result, they can be very small and thus allow the manufacture of compact electronic devices. Mobile phones, laptops, desktops and so on contain voice coils actuators containing neodymium magnets (Ciacci *et al.*, 2019). Microphones and loudspeakers likewise involve NdFeB magnets for their acoustic transducers (Ciacci *et al.*, 2019). Hard disks also include NdFeB magnets (Choubey *et al.*, 2021).



Figure 2-3: NdFeB magnets (Dalvin, 2006)

At a larger size, generators mounted on wind turbines are based on NdFeB magnets (Ciacci *et al.*, 2019). Those magnets are found too in electric motors set up in electric cars and in some high-end electric bikes (Goonan, 2011; Ciacci *et al.*, 2019). To summarize, NdFeB magnets are essential for both scaling down electronics and undertaking the energy transition to electricity.

Neodymium also has several other uses apart from magnet manufacturing. Neodymium is used in glass coloring for instance. The addition of neodymium in the glassmaking results in colors ranging from blue to wine red (Habashi, 1997). It is also used to manufacture medical lasers, namely neodymium-doped yttrium aluminum garnets (YAG) lasers (Ciacci *et al.*, 2019). In 2020, around 50 kt of neodymium oxide were produced worldwide (Davis, 2020).

## 2.6   Primary Extraction of Neodymium

As stated earlier, it is only possible to find ores containing a broad range of REEs. To separate the elements from each other, hydrometallurgy is used. The ore is leached either with sulfuric acid or with sodium hydroxide (Habashi, 2013). Leaching with sodium hydroxide leads to the production of slurry. This slurry is filtered, washed and dried. A filtration cake made of rare earth hydroxides is thus obtained (Habashi, 2013). It can then be acid leached for further purification (Habashi, 2013).

The leachate made with acid can be refined either by ion exchange on resin column or by solvent extraction. Solvent extraction is the preferred way because the extraction column are more compact than the ion exchange column, and because the chelatants used for ion exchange are expensive and hard to retrieve (Habashi, 1997). Ion exchange is usually reserved for producing high purity salts or oxides, up to 99.9999%, because solvent extraction can only achieve 99.99% purity (Judge and Azimi, 2020).
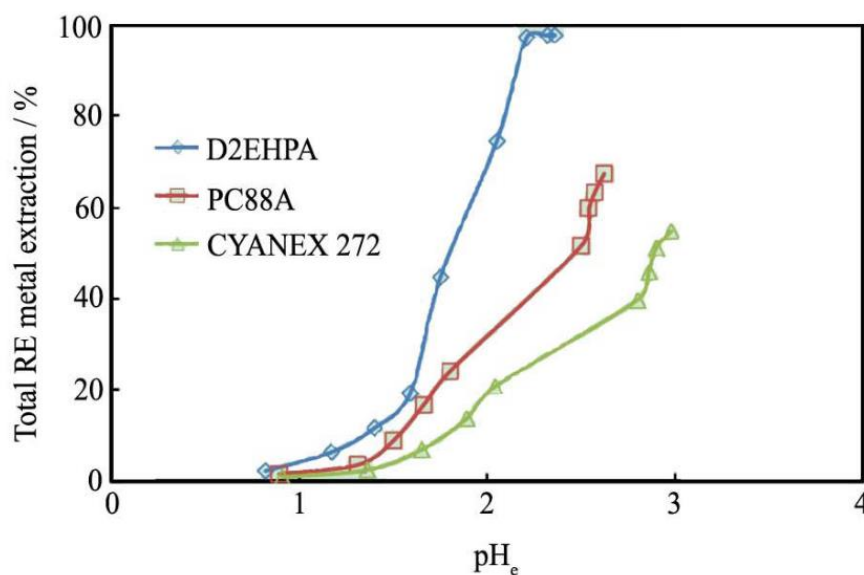


Figure 2-4: Typical extraction curves of rare earth metals by D2EHPA, PC88A and Cyanex 272 (Pahri *et al.*, 2015)

Usually, the extractant is a cation exchanger like carboxylic acids or organophosphorus acids (Judge and Azimi, 2020). The most employed acidic extractant for Nd extraction is D2EHPA (Habashi, 2013). Indeed, its behavior is well known and it is easily available. Moreover, it is very selective for REEs and separates well the different lanthanides (Habashi, 1997). Lately, PC88A has become a candidate to replace D2EHPA because

it presents higher separation factors for REEs (Zhang *et al.*, 2020). The typical extraction curves of rare earths by D2EHPA, PC88A and Cyanex 272 is represented in Figure 2-4 (Parhi *et al.*, 2015).

The extraction is achieved in several steps. The REEs are first extracted out of the ore leachate, while the impurities remain in the leachate. Then the REEs are back-extracted in a chloride medium and a second extraction is carried out to separate the different elements (Judge and Azimi, 2020). This second extraction is when neodymium is eventually separated from the other REEs.

Studies are currently conducted on how to diminish the left-over impurities. New extractants are being developed, new solvents are used and ionic liquids are investigated (Judge and Azimi, 2020).

## 2.7   Recycling of Neodymium

In 2021, 60% of the REEs were produced in China (Statista, 2022d) which controls the REEs market. As detailed earlier, electronics are highly dependents on REEs. Europe is a big consumer of electronics but does not dispose of a sufficiently large local primary source to meet its needs. To reduce this dependence on China, the recycling of REEs already present in Europe could be promoted. Moreover, ores are a finite resource and REEs demand keeps increasing (Zhang *et al.*, 2020). So, to ensure the sustainability of the REEs supply, recycling is essential. However, REEs recycling is not yet widespread. In 2011, less than 1% of REEs in end-of-life products was retrieved (Binnemans *et al.*, 2013).

Several reasons explain this situation. REEs from primary extraction used to be cheap enough that recycling and reuse of REEs was not competitive. Now that REEs recycling is worthwhile, the technologies are still under development. Efficient collection and sorting systems for waste containing REEs need to be established too (Binnemans *et al.*, 2013). Fortunately, recycling REEs has advantages other than environmental ones. In sorted waste, only certain REEs are present, while the full range is found in ores. Less separation steps are thus needed. Moreover, this waste is already thorium-free (Binnemans *et al.*, 2013). Radioactive thorium is commonly found in rare earth ores and is a health hazard (Habashi, 2013).

Neodymium can be retrieved mainly from NdFeB permanent magnets and from NiMH batteries to a lesser extent (Binnemans *et al.*, 2013). Permanent magnets contain 27-32%-wt of REEs, 67-73%-wt of iron and around 1%-wt of bore (Zhang *et al.*, 2020). The big magnets like those in wind turbines can be reused as they are. They are simply removed during dismantling and installed in new wind turbines. They weigh between 1 t and 2 t (Zhang *et al.*, 2020).

For electronics, permanent magnets are very small, they weigh around 1 g (Zhang *et al.*, 2020). Such small magnets make recycling neodymium from used electronic products quite complex because dismantling the electronics is time consuming and expensive. A lot of manual labor is involved (Ambaye *et al.*, 2020). Usually, they are shredded for recycling without removing the magnets. As the NdFeB magnets are brittle, they break down and stick to the ferrous parts (Binnemans *et al.*, 2013). Neodymium is thus mixed in very small concentration with other metals after the shredding. The state-of-the-art technique for recycling those shredded residues is smelting to retrieve metals like copper. However, REEs are lost in the slags as oxides (Binnemans *et al.*, 2013).

Research to recycle REEs from NdFeB magnets has focused on scrap from the manufacturing process, the so-called swarf. Hydrometallurgy is a serious contender for a potential recycling process. Indeed, it can treat oxidized and non-oxidized magnets as well as any magnet composition (Zhang *et al.*, 2020). Hydrometallurgy is also the way REEs are extracted from ore so the techniques are similar to the ones in current REEs production industry (Zhang *et al.*, 2020). Several hydrometallurgical ways explored to create a recycling process are introduced next.

All the studied hydrometallurgical processes start by leaching the scrap magnet. The leaching can be either selective or complete. For a selective leaching, a thermal oxidation is often carried out beforehand. It generates neodymium oxide ($Nd_2O_3$) and iron oxide ($Fe_2O_3$) out of the magnet phase ($Nd_2Fe_{14}B$). Neodymium is much more soluble than iron oxide in acidic solution, so when an inorganic acid is used for leaching, most of the iron stays solid (Zhang *et al.*, 2020). For the complete leaching, both organic and inorganic acids can be used. The goal is to put all of the metals in solution (Zhang *et al.*, 2020).

To retrieve neodymium from the leachate, precipitation, solvent extraction and extraction via ionic liquids has been studied. To precipitate neodymium from a highly acidic solution, precipitation reagents like oxalic acids are used. Neodymium oxides are obtained by roasting the oxalates (Zhang *et al.*, 2020).

Commonly employed extractants for REEs extraction are D2EHPA, PC88A and EHEHPA (2-ethylhexyl phosphonic acid mono-2-ethylhexyl). Those are all acidic extractants. Some experiments were done with extractants partially saponified with NaOH. Saponification allows to avoid gel formation and to diminish the acidification of the aqueous phase during the extraction. Using several extractants together to create a synergy is also being explored (Zhang *et al.*, 2020).

Extraction using ionic liquid solvent has been considered lately because it doesn't evaporate like organic solvent and it is environment friendly (Zhang *et al.*, 2020). Research for this technique is very new compared to the two others.

NiMH batteries are also a source of recycled REEs as they contain 8-10% mischmetal (Binnemans *et al.*, 2013). Lanthanum, cerium and praseodymium are present besides neodymium. A process to reuse the nickel and cobalt contained in these batteries already exists, but until now the REEs were discarded. In addition to the processes described in section 2.3, NiMH batteries were used as a cheap nickel source to manufacture stainless steel. REEs were discarded in the slags (Binnemans *et al.*, 2013).

Umicore and Rhodia developed a process based on Umicore's UHT process in 2011. It is named the Valéas recycling process. The slags are treated to retrieve REEs as a concentrate (Rombach and Friedrich, 2014). The concentrate is further separated by Rhodia by hydrometallurgy (Binnemans *et al.*, 2013; Rombach and Friedrich, 2014).

Research to elaborate a hydrometallurgical recycling process are ongoing. The electrodes are leached with inorganic acids and the leachate is treated (Binnemans *et al.*, 2013). Precipitation of REEs is achieved by using NaOH to change the *p*H or by precipitating REEs as oxalate for instance (Binnemans *et al.*, 2013; Jha *et al.*, 2021). This process is easy to operate and quite cheap, but it is not selective for the REEs (Jha *et al.*, 2021). To obtain each REE individually, a solvent extraction step is added in the process (Jha *et al.*, 2021). Like for primary extraction of REEs, D2EHPA and PC88A

are examined as extractants, as well as some less common ones such as Cyanex 923 or LIX 84 (Binnemans *et al.*, 2013; Jha *et al.*, 2021)

## 2.8   UV-Visible Spectrophotometry

Spectrophotometry is an analytical method that provides information on the composition of a homogeneous liquid and the concentration of its constituents. The analyzed solution is placed in a small transparent vessel and a light beam is emitted at one side of that vessel. The light beam passes through the sample and the intensity of the beam reaching the end of the vessel is measured. The components contained in the sample may absorb partially the energy transmitted by the light beam. The spectrophotometer measures the absorbance, which is related to the ratio between the intensity of the emitted light and the light intensity after the beam has passed through the sample. The absorbance can be linked to the concentration of the components contained in the sample. The wavelength of the emitted light beam can be varied around the UV-visible range, so between 320 and 800 nm here.

To determine the constituents present in the sample, the spectrum of the absorbance per wavelength is measured with the spectrophotometer. Indeed, different constituents have different spectra, so knowing the spectrum allows to characterize the components contained in the sample. Light energy absorbance is caused by the electrons in atoms that get excited to the next energy levels. These excited states can only be reached when specific amounts of energy are absorbed by the molecule. The energy needed by the electrons to reach an excited state depends on their atomic orbital and whether or not they are part of a molecular liaison (Jeffery *et al.*, 1989). Therefore, depending on the energy of the light beam, electrons can reach an excited state or not. The measurement conducted with the spectrophotometer consists in measuring the absorbance of the solution over a range of wavelength. The light energy being inversely proportional to its wavelength, varying the wavelength is tantamount to varying the energy supplied to the molecules in the sample. The absorbance per wavelength spectrum is plotted, and absorbance peaks can be observed for wavelength at which the electrons could be excited. As each molecule has different energy states for its electrons, the wavelengths at which absorbance peaks occur are characteristic of each molecule.

Knowing the absorbance spectrum allows thus to determine the components contained in the sample.

The intensity of the absorbance is determined by two factors: the concentration of the absorbing components in the liquid solution and the length of the path travelled by the light beam. The medium consists in the liquid sample and the wall of the transparent vessel in which the liquid is analyzed. This vessel is called the "cuvette". The thicker the cuvette, the higher the measured absorbance as the light has to cross a longer path before reaching the point where the remaining beam intensity is measured. Hence cuvettes are sold in different sizes to allow working in different absorbance ranges. The absorbance increases with the concentration of the sample too. The decrease in color intensity of a sample with dilution is a straightforward illustration: the lighter the solution, the less energy is absorbed from the light beam.

The Beer-Lambert's law gives a mathematical expression to those phenomena for a monochromatic light beam. The absorbance $A$ is proportional to the concentration $c$, the path length through the media $l$ and the molar absorption coefficient $\varepsilon$ (Jeffery *et al.*, 1989). The equation is the following:

$$A = \varepsilon c l \quad .$$

$\hspace{1em}$ (2-1)

The molar absorption coefficient depends on the nature of the sample. It is determined experimentally and given for a path length of 1 cm and a concentration of 1 mol/L.

Beer-Lambert's law can be applied to a specific system, to determine the concentration in a given component. A calibration curve is drawn for this purpose. The absorbance spectra are generated for different known concentrations in the analyzed component. As stated in Beer-Lambert's law, the absorbance is proportional to the concentration. For a fixed wavelength, usually chosen at a peak in the spectrum, a point of the calibration curve is drawn. The complete calibration curve is the function between the absorbance at that wavelength and the concentration of the component in the sample. The calibration curve is the interpolation found based on the experimental points, and its slope is the product between the molar absorption coefficient and the path length. Once done, the calibration curve allows to determine any concentration in a sample

from its absorbance measurement, as long as it belongs to the same range of concentration.

The spectrophotometer consists in four main parts: a light source, a monochromator, a slot for the cuvette and a photoelectric cell. The light source is usually a tungsten lamp to cover the 800 to 320 nm range. To reach the far UV range, a hydrogen or deuterium lamp is needed. Those can reach wavelength down to 200 nm (Jeffery *et al.*, 1989). Spectrophotometers capable of working in the far UV are usually equipped with both a tungsten lamp and a deuterium lamp. The device uses one or the other, depending on the wavelength.

The light emitted by the lamp is not monochromatic but includes a range of wavelengths. The monochromator is a mechanism that selects a wavelength and focuses the light on a smaller area. A diffraction grate is employed to select one wavelength. It is a metal plate with series of parallel grooves. Those grooves create tilted parallel surfaces that reflect light on the plate. The light rays that hit the grate change path and it generates light interferences. A light ray at a single wavelength is left. The wavelength is selected by changing the angle between the grate and the light source. The light is then focused with a curved aluminum mirror.

The sample is contained in a clear cell that is put into the light path. The cuvette is usually made of glass, styrene or Polymethyl methacrylate (PMMA). Those materials are suitable for wavelengths from 340 nm to 1,000 nm. At smaller wavelengths, the light is almost fully absorbed by the cuvette material. A cell made of quartz is necessary at such low wavelengths.

Before measuring any sample, the intensity of the light is measured for an empty cuvette. Indeed, the cuvette in itself has an impact on the light intensity which is inherent to all measurements using similar cuvettes. That intensity is used as the baseline of all measurements.

The UV-visible spectrophotometry is a characterization method that has undeniable advantages. It is non-destructive for the sample. Depending on the size of the cuvette, the measurement can be achieved with only 1 mL samples. The analysis is fast as a measurement can be done under one minute. The device handling is also easy and

does not need much training. However, the calibration curve takes time to be established and the precision is not as high as titration or atomic absorption spectroscopy.

# 3 Material and methods

In this work, metal extraction tests are performed using shake flask extraction. The quantity of metal in the aqueous phase after extraction is measured using UV-visible spectroscopy. As the quantity of metal introduced in the system is known, the quantity transferred from one phase to the other is deduced via a mass balance.

All the solutions are prepared on an analytical balance. Mass fractions are used in the calculations to describe the quantity of metal in a phase.

## 3.1 Chemicals

Nickel and cobalt solutions are prepared by dissolving salts. Nickel chloride hexahydrate ($NiCl_2 \cdot 6H_2O$) is supplied by Sigma-Aldrich. Cobalt chloride hexahydrate ($CoCl_2 \cdot 6H_2O$) is supplied by Roth. To adjust $p$H, sodium hydroxide (NaOH) provided by Sigma and hydrochloric acid 5 M (HCl) supplied by Fisher Chemicals are used.

Neodymium (III) oxide ($Nd_2O_3$) provided by Alfa Aesar is used as neodymium source in this work. It is put in solution using concentrated hydrochloride.

Deionized water (DI) is obtained by tap water distillation in the laboratory.

For the organic phase, kerosene provided by Total Fluid France is used as a diluent. Two extractants are used in this work: di-(2-ethylhexyl) phosphoric acid (D2EHPA) that is provided by Sigma-Aldrich and bis-(2,4,4-trimethylpentyl) phosphinic acid (Cyanex 272) supplied by Solvay.

## 3.2 Densimeter

Density of all stock solution is measured using a DMA 5000 M densimeter from Anton Paar. The "Density & Sound" method preset in the device is employed. It gives the density using the oscillating U-tube method. A borosilicate U-tube is made to vibrate and its characteristic frequency depends on the density of the liquid it is filled with (Anton Paar, 2011). A built-in thermostat allows to control the temperature during the measurement. As ambient temperature fluctuates between 19 and 21°C, the densimeter is set at 20°C for all measurement.

## 3.3 UV-Visible Spectroscopy

A spectrophotometer of model DR 3900 commercialized by HACH is used in this work. It uses a single beam produced by a tungsten halogen lamp (Hach, 2020). All the disposable cuvettes are made of PMMA and have a pathlength of 10 mm. For each measurement the cuvette is filled with 1 mL of the sample and the absorption spectrum between 320 and 900 nm is recorded. An empty cuvette is used to set the zero spectrum for the analysis. The spectrum obtained is the difference between the measured absorbance and the zero spectrum.

The shape of the spectrum depends on the metals inside the sample. The number of peaks and the wavelengths at which they occur are characteristic of the metal. The height of the peaks on the other hand indicates the metals concentration. To remove external disturbances that could shift vertically the spectrum, it is not the absorbance at the peak that is used to find the concentration but the difference in absorbance between a peak and a valley of the spectrum. One wavelength for the peak and one for the valley are fixed for each metal once and for all. They don't vary between the measurement.

Samples of fixed concentrations are used to make a calibration curve. It is a function obtained by interpolation between the concentration in metal and the absorbance difference. Once this curve is established for a metal, the concentration in this metal of any solution can be found using its absorbance difference. Of course, the curve is only reliable in the range it was built in.

To draw a calibration curve, samples of known concentrations are analyzed starting from the highest concentration and ending at the lowest one, namely DI. The samples are prepared from a stock solution by dilution using an analytical balance. A new cuvette is filled for each sample. Once a measurement is done, the cuvette is kept until all the calibration curve data are obtained. They are disposed of afterward. The main peak absorbance is surveyed during the analysis. If the absorbance evolves in an illogical way between the samples, the previous sample is measured again in the same cuvette.

Once the spectrum for each sample is obtained, the absorbance difference for each metal mass fraction is computed. Then, the absorbance difference is plotted against the metal mass fraction and an interpolation is worked out. The ordinary least squares method is employed. The curve can be linear or quadratic. The relative error is also evaluated. If it is lower than 3 % for all points, the precision of the calibration curve is considered adequate.

## 3.4   Extraction Procedure

The extraction is carried out in a 24 mL glass tube closed by a screw cap with a septum. 20 mL of liquid are poured in the tube. The organic phase is prepared in advance by mixing the diluent and the extractant in the predetermined proportion. It is then added as it is in the glass tube. The aqueous phase is prepared in the tube by diluting a stock solution of the metal. The $p$H of the aqueous phase is adjusted during the dilution.

Once the tube is ready, it is closed tightly. It is then shaken at 74 rpm in a rotating basket plunged in a thermostatic bath. It is left rotating as long as needed to reach the extraction reaction equilibrium. The agitation is then stopped, the basket is opened and the phases are left to separate, still in the thermostatic bath.

After the two phases are separated from each other, they are collected one after the other using single-use syringes. The organic phase is first sucked out and set aside. Next the interface is taken out with the same syringe to have as little organic phase as possible left in the tube. While collecting the interface, some aqueous phase is sucked inside the syringe too, so the syringe content is discarded. Finally, with a new syringe the aqueous phase is sucked out of the tube. The quantity of metal in the aqueous phase is measured by UV-Visible spectroscopy. The quantity of metal in the organic phase is then computed with a mass balance. The extraction degree is calculated too.

The $p$H at equilibrium is measured using a Knick Portamess $p$H-meter equipped with a Hamilton Single Pore Glass probe. The $p$H-meter is calibrated once a day either with buffer solutions at $p$H 1 and $p$H 7 or at $p$H 7 and $p$H 10. The expected $p$H of the solution must be between the $p$H values of the chosen buffer solutions. The buffer solutions AVS Titrinorm for $p$H 1 and 7 are supplied by VWR. The buffer solution for $p$H 10 is a

ROTI Calipure buffer solution supplied by Roth. Knowing the equilibrium $p$H and extraction degree for several points, the extraction curve can be built.

The metal mass fraction after extraction is determined using the spectrophotometer and the metal calibration curve. It is assumed that the volume of each phase stays constant throughout the extraction. The following function is used to compute the degree of extraction E:

$$E = \frac{c_{M,\alpha} - c_M}{c_{M,\alpha}} \quad . \tag{3-1}$$

The variable $c_{M,\alpha}$ is the concentration of metal $M$ before extraction and $c_M$ is the concentration of metal $M$ at equilibrium after extraction. Those are concentrations in the aqueous phase. As the aqueous phase volume is considered constant, the degree of extraction can also be expressed in the following way:

$$E = \frac{m_{M,\alpha} - m_M}{m_{M,\alpha}} \quad . \tag{3-2}$$

In this form, variable $m_{M,\alpha}$ is the mass of metal $M$ before extraction and $m_{M,\alpha}$ is the mass of metal $M$ at equilibrium after extraction.

The equilibrium reaction for the extraction by cation exchange is written as following:

$$M_i^{m_i+} + \overline{\frac{n_i}{p}(RH)_p} \rightleftharpoons \overline{MR_{m_i}(RH)_{(n_i-m_i)}} + m_iH^+ \quad . \tag{3-3}$$
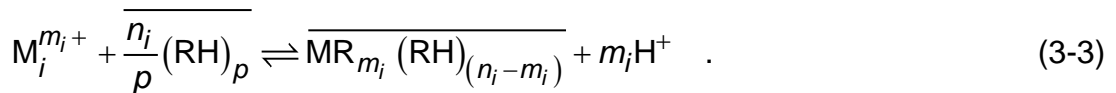
One extractant molecule is written as *RH*. Depending on the diluent polarity, the extractant can be in monomeric or in dimeric form in the reaction. As a result, the $p$ parameter is either 1 for the monomeric form or 2 for the dimeric form.

The metallic atom is written $M$. The metal $M$ on the left of the reaction is in the aqueous phase, the hydrogen cation on the right likewise. Both the extractant and the metal-extractant complex are in the organic phase. The molecules in the organic phase are noted with upper bars. This reaction takes thus place at the interface.

$n_i$ is the number of extractant molecules needed to extract one metallic cation $i$. The parameter $m_i$ is the charge of the cation, and so the number of hydrogen ions that are

released during the extraction of one metallic cation. The minimum number of extractant molecules to make a neutral metal-extractant complex is equal to the number of charges $m_i$. However, additional extractant molecules are often needed to transfer the cation to the organic phase, hence the number of extractant molecules per cation extracted $n_i$ can be higher than the number of charges $m_i$.

The equilibrium reaction allows to write the equilibrium constant $K_c$:

$$K_c = \frac{c_{MR_{m_i}(RH)_{(n_i-m_i)}}\, c_{H^+}^{m_i}}{c_{M_i^{m_i+}}\, c_{(RH)_p}^{n_i/p}} \quad , \tag{3-4}$$

where all concentrations $c_i$ are expressed in mol/L.

The number of extractant molecules $n_i$ that react per metal cation can be found in the literature. If the articles are contradictory or none are found for the studied system, a slope analysis can be performed. Extraction experiments are made with different extractant concentrations but at constant equilibrium $p$H. The partition coefficient $K$, which is the concentration ratio between the extracted metal and the metal still in the aqueous phase, is computed. The logarithm of the partition coefficient $K$ is plotted against the logarithm of the concentration in free extractant $c_{(RH)_p}$. A straight line is obtained, with a slope of $n_i / p$:

$$K_c = K\frac{c_{H^+}^{m_i}}{c_{(RH)_p}^{n_i/p}} \quad , \tag{3-5}$$

$$\log(K) = \log(K_c) + \frac{n_i}{p}\log\left(c_{(RH)_p}\right) + m_i p\text{H} \quad . \tag{3-6}$$

In case the $p$H cannot be kept constant during the experiment, stoichiometry can be deduced from an alternative way. Two extraction experiments using different extractant concentrations must be conducted, preferably with a degree of extraction close to neither 0 nor 1. As a first step, only one of the experiments is considered. Several values for $n_i$ are tested. The equilibrium constant $K_c$ is calculated for each $n_i$ value. Afterward, the result of the second experiment is predicted using each couple of value $n_i$

and $K_c$. The $n_i$ that gives the closest result to the actual measured data is the correct stoichiometry.

Once the stoichiometry is determined, the equilibrium constant value is calculated from the extraction curve using the (3-4) equation. Once the $K_c$ is known, the metallic cation concentration in the aqueous phase at equilibrium can be computed from the initial concentration of free extractant and the equilibrium $p$H.

## 3.5   Single-drop cell

The single-drop cell is an apparatus used to study mass transfer in a two-phase system. In this thesis, solvent extraction of metal is carried out. A light phase, called the dispersed phase is introduced dropwise in the cell, and removed from the system. A heavier phase, called the continuous phase, fills the cell. The contact time and the system temperature are set by the experimenter. In the present work, the diluted extractant is the dispersed phase and the metal aqueous solution is the continuous phase. The dispersed phase is analyzed after the experiment to assess the amount of metal transferred from the continuous phase towards the dispersed phase.

The single drop cell has a specific shape. It is schematized in Figure 3-1. The bottom of the single-drop cell consists of a conical part, then the cell widens on the upper part. The drop rises in the conical part and can be stabilized at the top of the conical part by pumping continuous phase from top to bottom. The stabilization time can be specified. Once the desired residence time has elapsed, the pump stops and the drop rises. It is collected into an upside-down funnel placed at the top of the cell. A capillary tube connected to that funnel carries the dispersed phase out of the cell.

The single drop is part of a bigger system. Three separated circuits are combined in the equipment, for three different fluids: the dispersed phase, the continuous phase and water used for temperature control. Those circuits are represented in color in Figure 3-2. They are respectively in green, red and dark blue.

The continuous phase is pumped in a closed circuit. Both the single-drop cell and a settling cell are in the circuit, but only one experiment can be conducted at a time, either a settling or a mass transfer experiment. Only the single-drop cell was used for this master thesis.
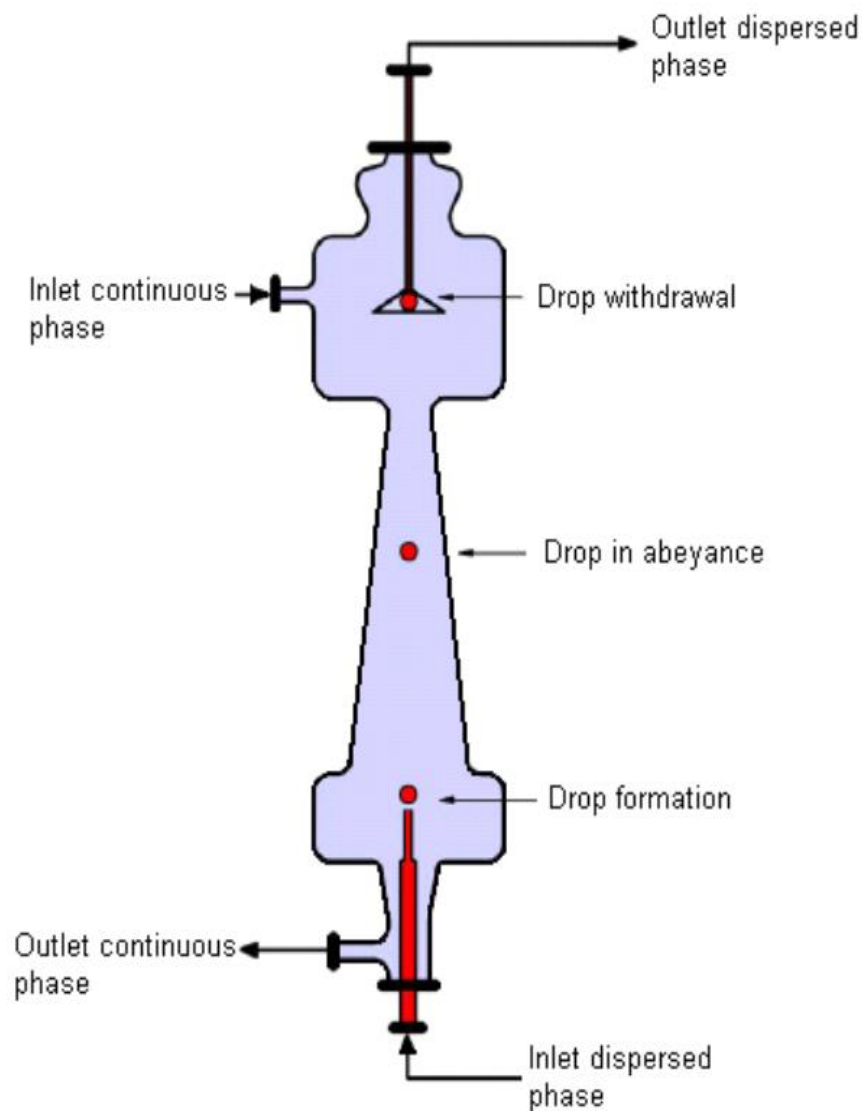
Figure 3-1: Diagram of the single-drop cell (Bronneberg, 2007)

When the single-drop cell is used, the settling cell serves as a tank. It is filled with the continuous phase which then flows through the circuit. The continuous phase is pumped into a rotameter to measure the volume flowrate, then passes through a heat exchanger before reaching the single-drop cell. The continuous phase then returns into the settling cell. A valve allows to remove air from the system between the rotameter and the heat exchanger. An overflow vessel is placed after this valve to avoid spills of the continuous phase.
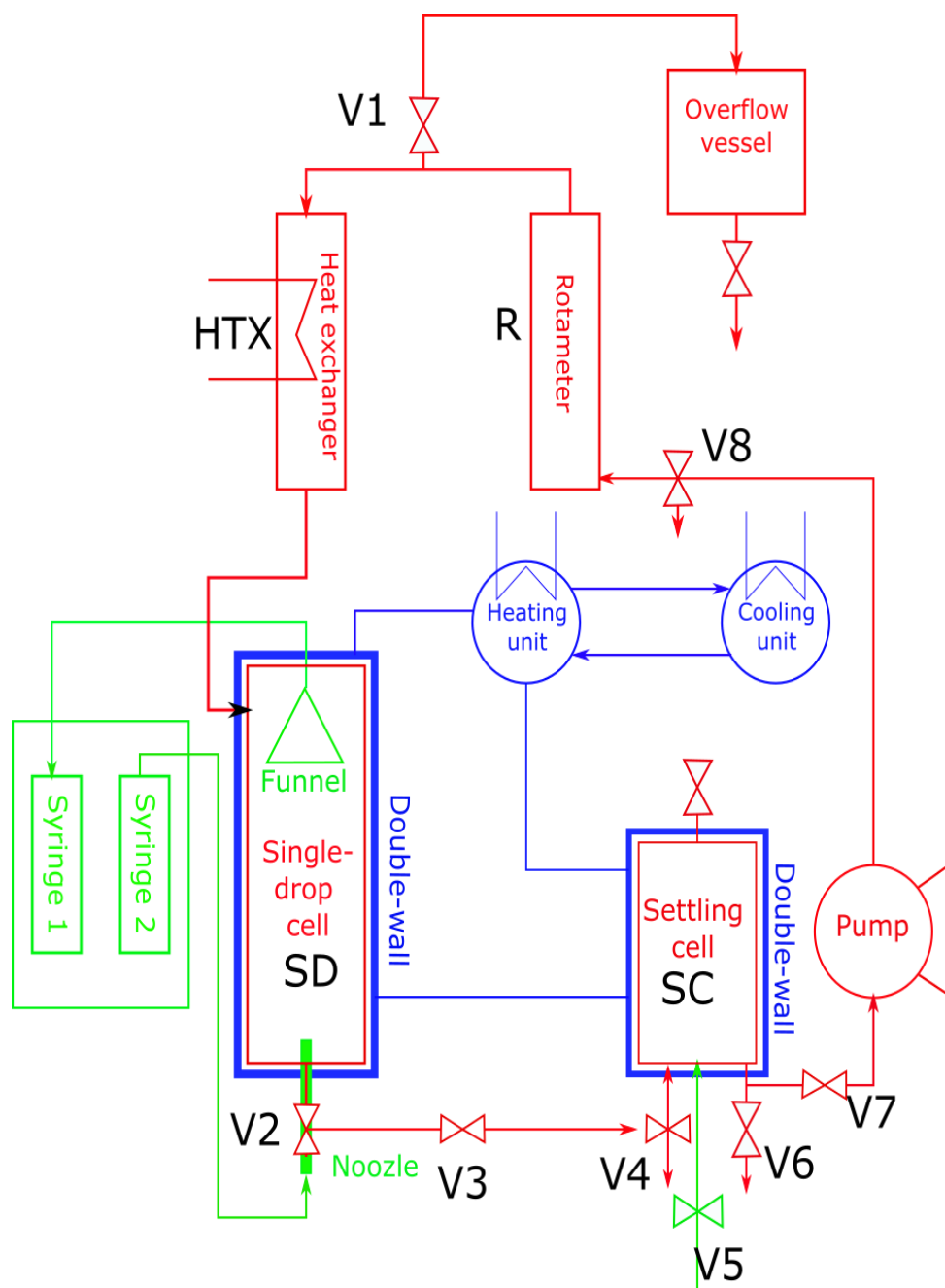
Figure 3-2: Flowsheet of the equipment

The dispersed phase circulates via a dosage unit. It consists in a double syringe pump with two Hamilton syringes connected to capillaries. A syringe is in charge of the inlet of the dispersed phase, and the other of the outlet. For the inlet, the syringe is first filled with the dispersed phase contained in an external bottle via a capillary. The pump is then used to fill in a nozzle completely with the dispersed phase. This nozzle is used to generate the drops. It is a long thin glass tube with a conical end and a screwed capillary at the other end. It is introduced in the cell from the bottom. The dispersed phase is pushed into the nozzle through the capillary and drops are formed and re-leased at the tip. The second syringe sucks the drop once it has reached the funnel. The collected drops are stored in the second syringe during the experiment. Once enough drops are collected, they are pushed from the second syringe into a glass tube via a second capillary. The collected dispersed phase is then analyzed. The syringe pump is shown in Figure 3-3.
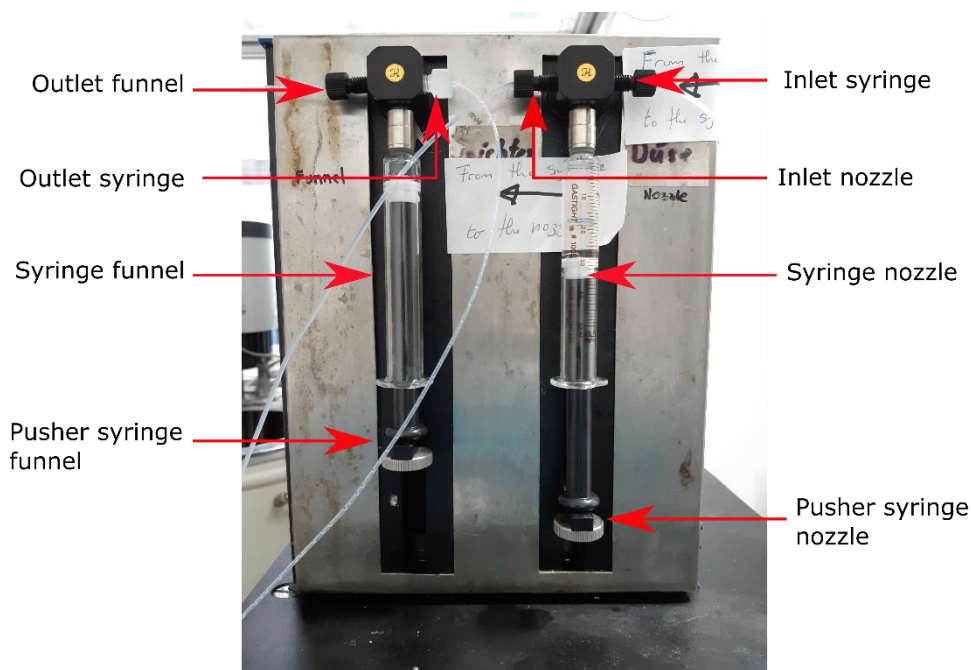


Figure 3-3: Dosage unit with its connections

The syringe pump is actioned using steps. The total height of a syringe corresponds to 2,000 steps. Two parameters are controlled for any movement of the syringe: the num-ber of steps and the time required to lift the pusher. The number of steps determines

the volume pushed through the nozzle. The following formula links the volume of a drop $V_d$, the syringe volume $V_s$ and the number of steps $S$ (Leeheng, 2014).

$$V_d = \frac{V_s S}{2000} \quad .$$

(3-7)

Assuming that the generated drops are perfect spheres, the volume of a drop is equal to

$$V_d = \frac{\pi D^3}{6} \quad ,$$

(3-8)

where $D$ is the drop diameter. The drop diameter $D$ is chosen by the experimenter before the experiment. The number of steps required to create drops of such diameter is thus computed from these two equations as follows:

$$S = \frac{1000 \pi D^3}{3 V_s} \quad .$$

(3-9)

Several nozzles of different diameters are available. As a rule of thumb, the diameter of the nozzle is half the drop diameter. Trial tests are carried out to find the appropriate nozzle diameter and speed of the lift, to always generate one drop of the desired diameter per injection. The appropriate injection speed should be such that the dispersed phase injected detaches from the nozzle in one single drop. The drop formation is also dependent on the viscosity of the dispersed phase, so it varies with the system temperature. It is imperative that no dispersed phase remains stuck to the tip in order to ensure that the desired drop volume is released. To prevent wetting of the tip of the nozzle by the dispersed phase, the tip of the nozzle must be perfectly clean and flat. No traces of organic phase should remain. No nick on the glass tip can be tolerated.

Both the settling cell and the single-drop cell have double walls. Distilled water circulates in that envelope to keep the system at constant temperature. The temperature is controlled by a heating unit and a cooling unit. Together, they allow to regulate temperature with 1°C precision.

The equipment is operated via a custom software on Visual Designer. The user interface is represented in Figure 3-4. The timing of each operation is programmed on the right and it is run for a chosen number of drops. Each syringe is controlled separately

and the set up can be modified mid-run. An approximative volume flowrate can be set on the software though it is only a guide value. It modifies the frequency of the pump, which changes the volume flowrate of the continuous phase. The exact volume flowrate is measured with the rotameter. The volume flowrate can be changed mid-run too.
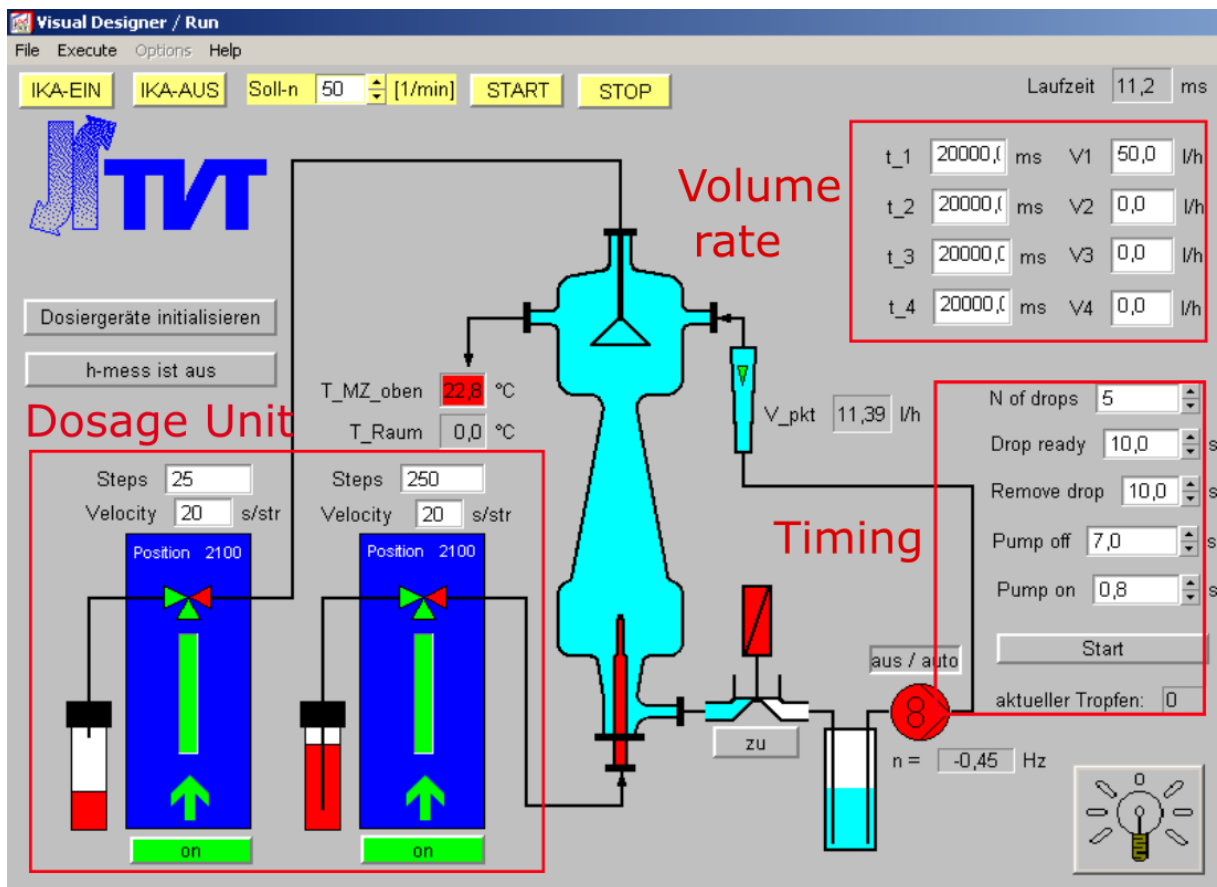


Figure 3-4: User interface on Visual Designer

To avoid transfer of one phase into the other, both phases are saturated with each other beforehand. Each phase is put into contact with a small quantity of the other phase for 12 hours. The phases are then separated and used in the experiment. The dispersed phase for the experiment is a mix of extractant and of diluent, kerosene in the master thesis. The continuous phase is a metal solution whose $p$H is adjusted at a suitable $p$H for solvent extraction. The dispersed phase is saturated with deionized water and deionized water is saturated with kerosene before making the metal solution. The metal concentration and the $p$H must be chosen to achieve more than 50% extraction at equilibrium, and to avoid metal precipitation in the equipment. Moreover, the metal concentrations to be measured after the experiment must be included in the

range covered by the calibration curve for the spectrophotometer. The *p*H of the continuous phase is adjusted with a NaOH or a HCl solution and is measured being poured into the equipment. The continuous phase is circulated for an hour in the system before a sample of the continuous phase is collected. The *p*H is analyzed to confirm the experiment parameters before carrying out the experiment.

Once all measurements are done, the organic phase is back-extracted with a strong acid in a glass tube. The *p*H needed to transfer all metals in the aqueous phase is determined using the extraction curve. Hydrochloric acid is used. It is assumed that 100% of the metal is back-extracted. Once the mixing and settling is done, the two phases are separated and the aqueous phase is analyzed by spectrophotometry.

The concentration of metal in the drop is presented in a dimensionless form. The time dependance of the concentration on the droplets is written $y^+$. Its expression is given by Altunok et al. (Altunok, Kalem and Pfennig, 2012) as the following:

$$y^+ = \frac{y^* - y(t)}{y^* - y_0} \quad .$$

(3-10)

The equilibrium mass concentration in the droplets is written $y^*$. The mass concentration in the droplets at a time $t$ is written $y(t)$. The initial mass concentration in the droplets is $y_0$. The extraction is done with clean dispersed phase, so $y_0$ is always equal to 0 g/L.

The molar equilibrium concentration is computed using the stoichiometry and the equilibrium constant found using the method detailed in section 3.4. Several assumptions are made. The *p*H and the metal concentration of the continuous phase are considered constant during the entire experiment. It is plausible because the volume of continuous phase is much greater than the volume of dispersed phase in the equipment, and the continuous phase is mixed when it is pumped through the equipment.

The initial extractant concentration form is computed from the volume fraction of extractant %-vol$_{(RH)_p}$, its density $\rho_{(RH)_p}$ and its molar mass $M_{(RH)_p}$:

$$c_{(RH)_{p,t_0}} = \frac{\rho_{(RH)_p}}{M_{(RH)_p}} \text{\%-vol}_{(RH)_p} \quad .$$

(3-11)

The stoichiometry allows to write the equilibrium free extractant concentration as a function of the metal-extractant complex concentration, as the drop volume is assumed to remain constant during the experiment:

$$c_{(RH)_p} = c_{(RH)_{p,t_0}} - \frac{n_i}{p} c_{MR_{m_i}(RH)_{n_i-m_i}} \quad .$$ (3-12)

Those assumptions applied to the equilibrium constant $K_c$ give the following equation:

$$c_{MR_{m_i}(RH)_{n_i-m_i}} = K_c \frac{c_M^{m_i+}}{c_{H^+}^{m_i}} \left( c_{(RH)_{p,t_0}} - \frac{n_i}{p} c_{MR_{m_i}(RH)_{n_i-m_i}} \right)^{\frac{n_i}{p}} \quad .$$ (3-13)

The equation is computed using Excel's solver. The equilibrium concentration of the metal-extractant complex $c_{MR_{m_i}(RH)_{n_i-m_i}}$ is the variable $y^*$ in equation (3-10).

To wash the equipment once empty, an acidic solution is prepared to get rid of the precipitates if needed. The equipment is then completely filled with an HCl solution and the pump is run for 1 hour. The system is then emptied completely. The same procedure is repeated 3 times with deionized water at 40°C. A sample of the third rinse water is collected in the settling cell and analyzed before pouring the continuous phase. The pH is measured to check if no acid is left in the equipment. If the pH is the same as for clean deionized water, the washing is finished. Otherwise, a new rinse with hot water is needed, and the pH is controlled again in the end. Such water rinses are repeated as many times as needed.

# 4 Results and discussion

## 4.1 Calibration curves

The concentration of metals in the aqueous phase is measured with a spectrophotometer. This device gives the absorbance of the solution at different wavelengths. To link the absorbance to a metal concentration, a calibration curve is needed. It is a function between the exact metal concentration and the absorbance of the solution.

For each calibration curve, several samples are prepared by dilution. Their concentrations are known exactly. The full spectrum of each concentration is taken. From the spectrum, the wavelengths of one peak and of one valley are selected to build the curve. The deionized water absorbance is subtracted from all the absorbances. Care is taken to have concentration with low enough absorbance. Indeed, the spectrophotometer cannot give precise measurement if the absorbance is over 3 (Hach, 2020). The lower absorbance limit is around 0.

### 4.1.1 Nickel

The spectrum of nickel was taken for nickel concentrations ranging from 30 g/L to 0 g/L. A difference of 3 g/L of nickel is kept between the samples, except for the 1 g/L sample. As shown in Figure 4-1, nickel spectra present two peaks, one at 393 nm and the other at 720 nm. The absorbance difference between the peak and the bottom wavelengths should be proportional to the concentration, according to Beer-Lambert's law. It is noted in section 2.8 as equation (2-1). This law states that there is a linear relation between the concentration in metal and the absorbance. However, at higher concentration, the increase in absorbance is not proportional to the increase in concentration. A polynomial expression therefore fits the absorbance versus concentration curve better. In Figure 4-1, it is visible that the 393 nm peak increase in absorbance is not proportional to the concentration increase. The behavior of the spectrum for 12 g/L of nickel in particular is not explainable by a concentration increase. On the one hand, its peak at 393 nm is much too low compared to the spectra of higher concentration solutions. On the other hand, its 720 nm peak height is as expected compared to the higher and lower concentrations peaks. In the absence of other reasons, a lack of precision in the measurement at 393 nm is strongly suspected. As a result, the calibration

curve is built based on the peaks at 720 nm. The lowest point to compute the absorbance difference is fixed at 501 nm, as shown in Figure 4-1.

As explained earlier, it is possible to build a calibration curve with a polynomial function
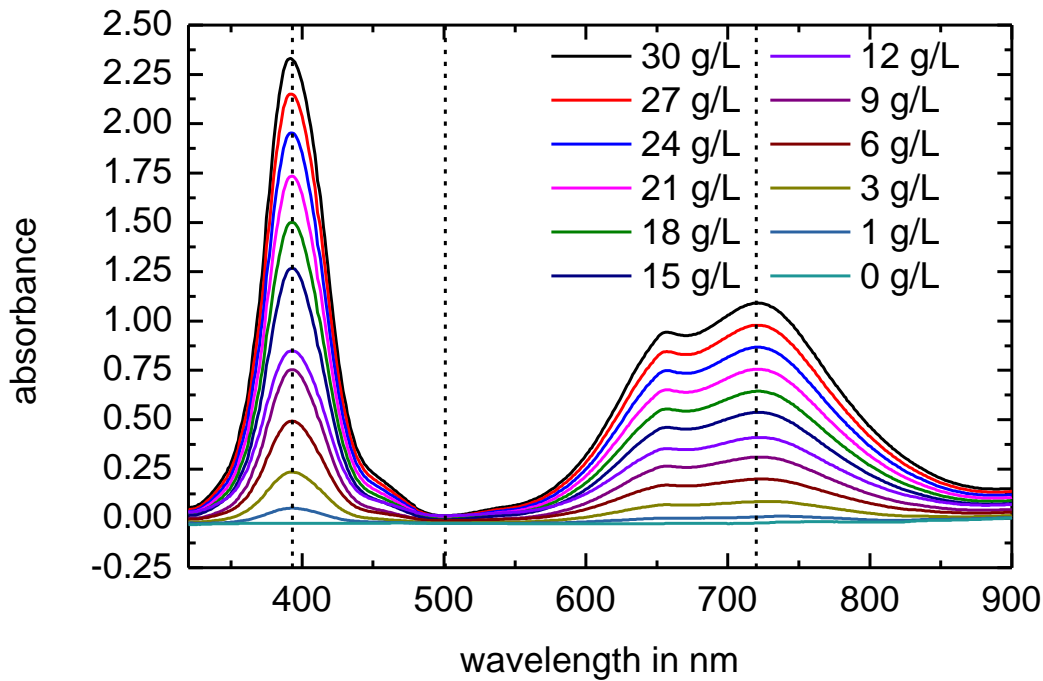


Figure 4-1: UV-vis nickel spectra at all concentrations, from 320 nm to 900 nm

even if the Beer-Lambert's law states that the relation should be linear. Case in point, the interpolation that best fits the points is a second-degree polynomial function. This interpolation is drawn in Figure 4-2, along with the experimental points. The coefficient of determination $R^2$ is 0.9998. The function expression is the following, with $F$ the metal mass fraction and $A$ the absorbance difference between the peak at 720 nm and the valley at 501 nm.

$$F = -0.002373 A^2 + 0.029258 A \quad . \tag{4-1}$$

The relative error of the calibration curve is computed in

Table 7-1 in Annexes. This is the relative error between the metal mass fraction predicted by the calibration curve and the metal mass fraction measured with the spectrometer for a sample obtained by dilution of a stock solution prepared on an analytical balance.
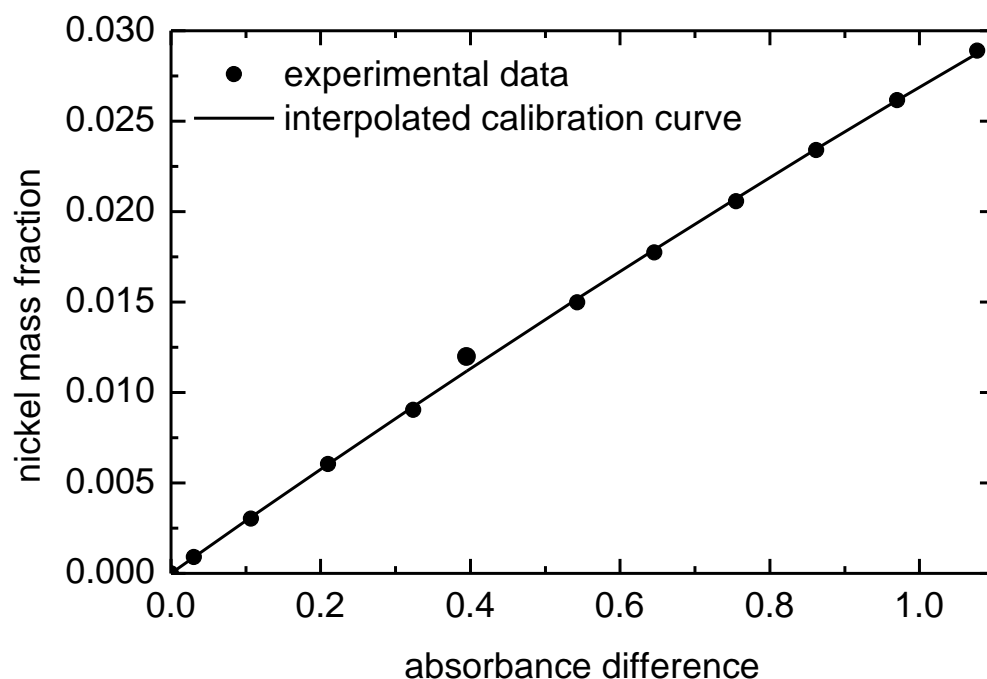
Figure 4-2: Calibration curve of nickel between 720 nm and 501 nm for a nickel concentration range between 30 g/L and 0 g/L

The absolute relative error on each point is less than 3% for each concentration, except for the 12 g/L nickel concentration. It was already the spectrum that looked abnormal in Figure 4-1. Based on the spectra, it was thus expected that that point would slightly diverge from the calibration curve. The range of concentration in which the concentrations are preferentially measured is thus from 30 g/L to 0 g/L. The experiments are designed to reach such concentrations in the aqueous phase.

## 4.1.2 Cobalt

The calibration curve for cobalt is established between 10 g/L and 0 g/L of cobalt. The maximum concentration is lower than for nickel because cobalt solutions present a much higher absorbance at identical mass concentrations. The spectrophotometer used is also not reliable at absorbances larger than 3 (Hach, 2020). A 10 g/L cobalt solution has a maximum absorbance much lower than 3 and such concentration is enough for the extraction experiments.
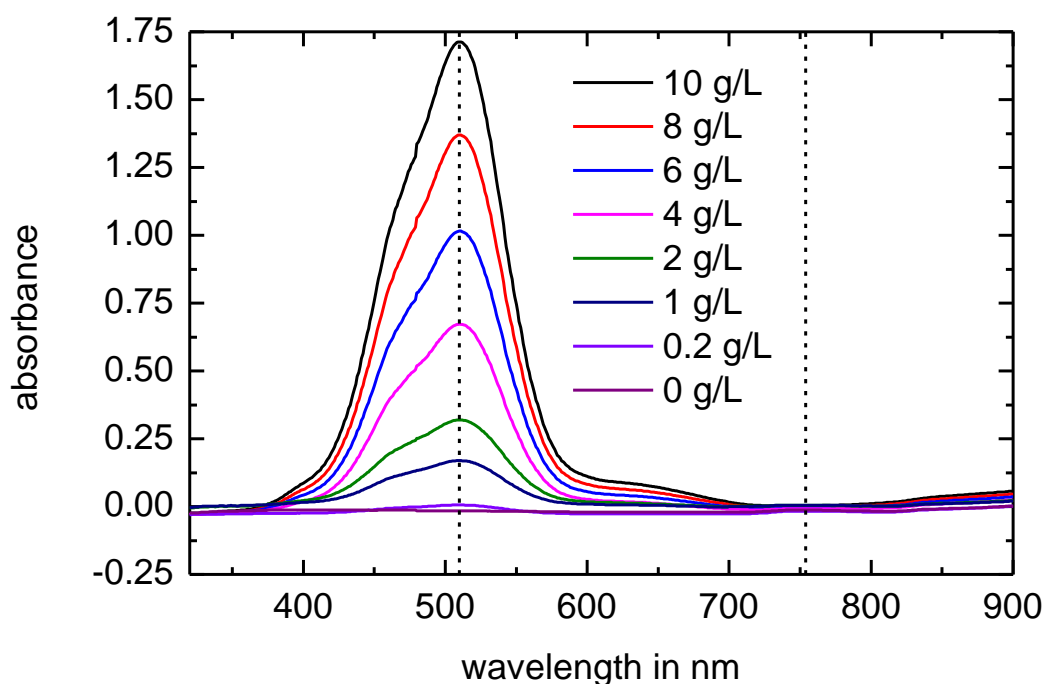


Figure 4-3: UV-vis cobalt spectra at all concentrations, from 320 nm to 900 nm

The cobalt spectrum shows only one peak at 510 nm. The valley wavelengths are 754 nm and 320 nm. 754 nm is selected because, from co-worker's experience, the precision at the edges of the spectrum is not guaranteed.

Each sample was measured twice to check for inconsistencies and both measurements are used in the interpolation. As seen in Figure 4-4, the absorbance differences obtained from both measurements of each sample are practically identical. The interpolation fitting the point best is a second-degree function with a coefficient of determination of $R^2$ of 0.9999.

This calibration curve has the following expression, using the same variables as for the nickel calibration curve:

$$F = -0.000243\,A^2 + 0.0060558\,A \quad .$$

(4-2)

The relative errors between the points and the calibration curve are computed in

Table 7-2. The precision is good above 2 g/L of cobalt as the relative error is below 3%. The range in which the concentrations are preferentially measured is thus between 2 g/L and 10 g/L of cobalt. The experiments are designed so that the aqueous phase concentrations are within this range.
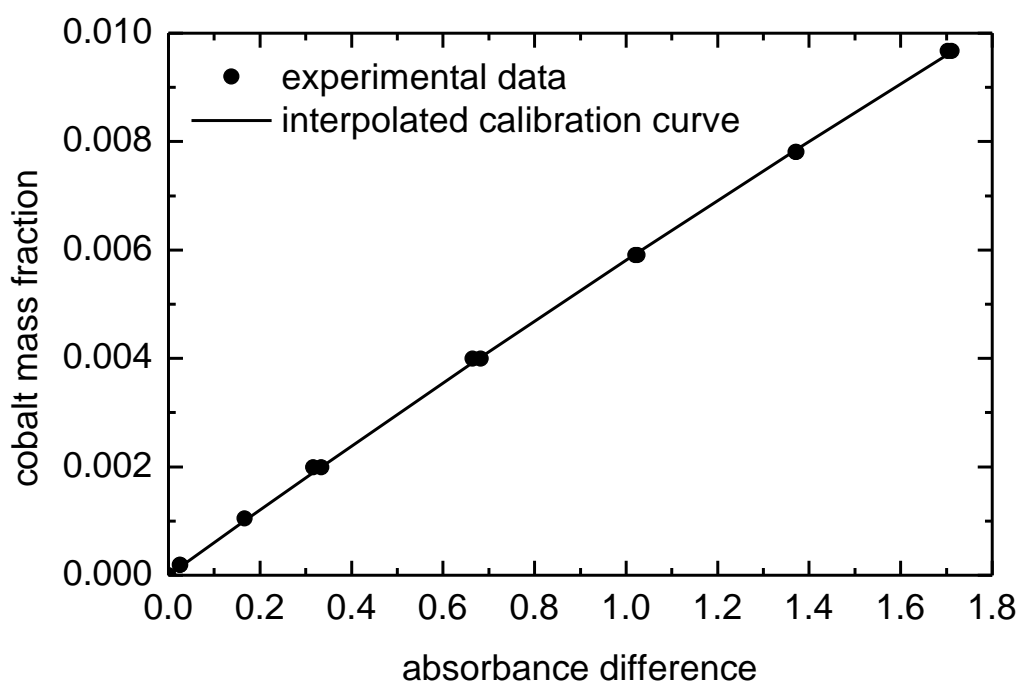


Figure 4-4: Calibration curve of cobalt between 510 nm and 754 nm for a concentration range between 0 g/L and 10 g/L

## 4.1.3 Neodymium

A calibration curve for neodymium is built between neodymium concentrations ranging from 7 g/L to 0 g/L. All spectra are visible in Figure 4-5. Seven peaks appear over the range of wavelengths covered, but only the three highest are considered: at 573 nm, 741 nm and 794 nm. At these wavelengths, the difference in absorbance will be larger between the different curves, which will increase the precision of the calibration curve.
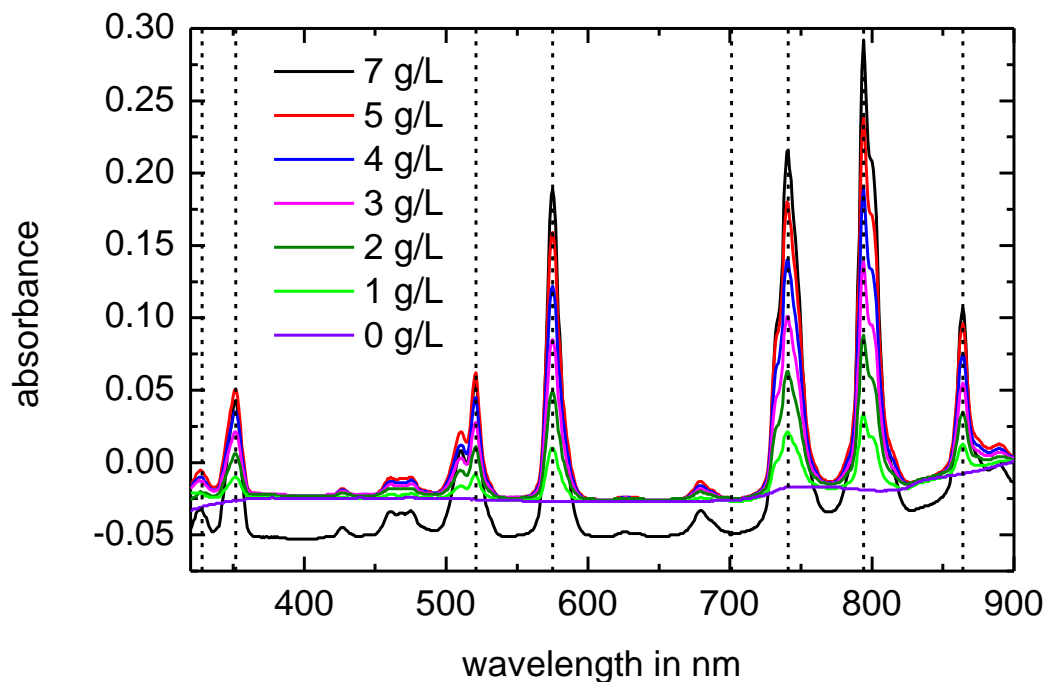


Figure 4-5: UV-vis neodymium spectra at all concentrations, from 320 nm to 900 nm

A calibration curve is built for each peak with 701 nm as the wavelength of the valley. The one with the highest precision is kept. The calibration curve with the highest precision is based on the peaks at 741 nm. The coefficient of determination $R^2$ is 0.9995 for the linear interpolation. The equation of the calibration curve is the following, using the same variables as before:

$$F = 0.027135\,A \quad .$$
(4-3)

Figure 4-6: Calibration curve for neodymium between 741 and 701 nm for a concentration range between 0 g/L and 7 g/L

Above 0.5 g/L of neodymium, the precision is good, with relative errors of less than 3%. The range of concentrations in which the concentrations are preferentially measured is thus between 0.5 g/L and 7 g/L. The experiments are designed to reach such concentrations in the aqueous phase.

## 4.2   Extraction curves

The extraction curves are made in 24 mL glass tubes closed with a septum cap. 10 mL of the aqueous phase is prepared in 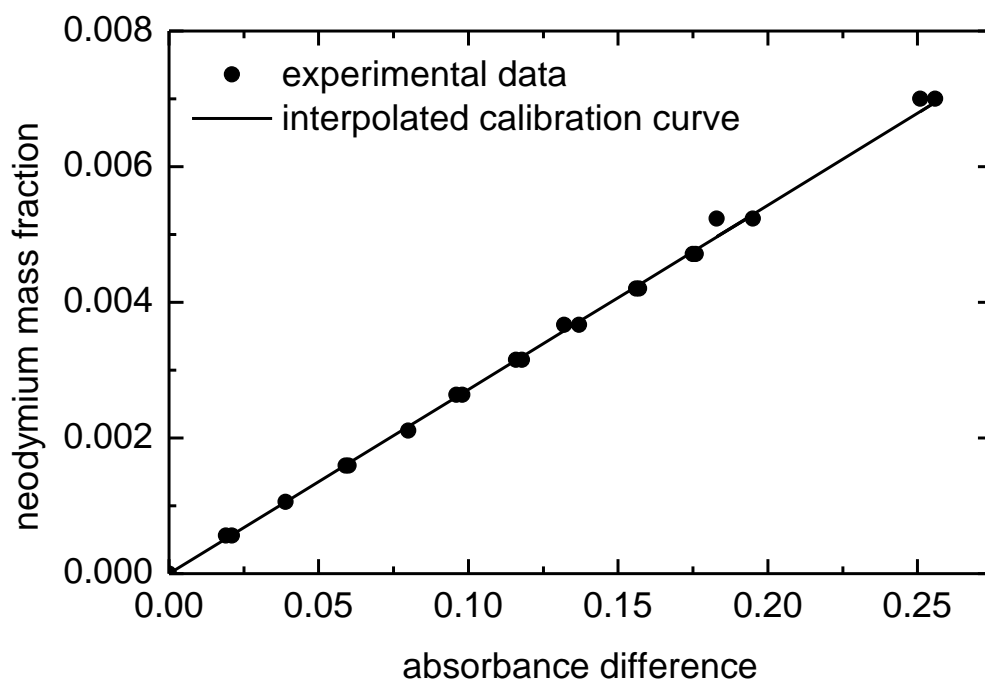the tube itself. The $p$H of the aqueous phase is adjusted before the extraction with either a sodium hydroxide solution or a chloride acid solution. The organic phase is prepared in advance and 10 mL of it is added to each tube once the aqueous phase is ready.

The same initial concentration in metal is targeted for each point of the extraction curve. The extraction is carried out in a rotating basket plunged in a water bath set at 25 °C. It can only rotate at 74 rpm. The extraction time is set for each system to ensure that equilibrium is reached, based on the literature. After extraction and settling, the two phases are separated and the concentration in the aqueous phase is measured using spectrophotometry. The calibration curves established above are used to compute the metal concentrations. The amount of metal in the aqueous phase before and after the extraction is then known. It allows to compute the degree of extraction in each tube. The $p$H at equilibrium is also measured. Finally, an extraction curve is established by plotting a curve through the data points of the degree of extraction versus equilibrium $p$H.

### 4.2.1   Nickel and D2EHPA

D2EHPA is readily available and quite cheap compared to other extractants. To build the extraction curve, all extraction experiments are performed with an aqueous solution containing 3 g/L of nickel. To decrease viscosity and use less extractant, the organic phase is prepared by mixing the extractant with kerosene as a diluent. The organic phase is made of 20%-vol D2EHPA and 80%-vol kerosene. For all experiments, a 1:1 ratio is chosen between the volume of aqueous phase and the volume of organic phase.

To detect settling issues, preliminary experiments are conducted. Deionized water is used as aqueous phase and is mixed with the organic phase in the same conditions as for the extraction experiments. During these preliminary tests, a stable dispersion of the aqueous phase occurs, causing the organic phase to turn white and opaque. As D2EHPA is known to form emulsion easily (Chauhan and Patel, 2014), this issue is not

unexpected. It can be prevented with an appropriate headspace in the tube. Indeed, droplets tends to get smaller in the rotating tube if a bigger headspace is left and the smaller the droplets, the more emulsion is favored. No emulsion is noted if less than 5 mL is left empty in a 24 mL tube, so 10 mL of each phase is used for all extractions.

The $pH$ of the aqueous solution is adjusted before adding the organic phase. In the base case, the 3 g/L Ni initial aqueous solution is at around $pH$ 6. After extraction, the $pH$ at equilibrium is 2.4. To build the full extraction curve, several samples of different starting $pH$ are prepared for extraction. The $pH$ is changed using a 40 g/L NaOH solution. The amount of NaOH solution added increases by 0.2 mL between the sample tubes. The last tube contains 1 mL of NaOH solution and is at $pH$ 10. Increasing the $pH$ induces precipitation in the aqueous phase with as little as 0.2 mL of NaOH solution added. Nickel hydroxide particles are thus in the aqueous phase before extraction. During extraction, D2EHPA exchanges hydrogen ions for nickel ions. Therefore, the aqueous phase gets more acid, its $pH$ decreases, and the nickel hydroxide dissolves. At equilibrium of the extraction reaction, the aqueous phase no longer contains any solid, except for very small amounts stuck at the interface.

The extraction is carried out in tubes for 10 minutes. Equilibrium can be reached with as little as 5 minutes for nickel extraction with D2EHPA (Rickelton, Flett and West, 1984), so 10 minutes provides a sufficient safety margin. The aqueous phase is analyzed, and the degree of extraction is computed. The $pH$ after extraction is also measured. The extraction curve is then built. It is presented in Figure 4-7.

A model is built on the extraction curve. The extraction stoichiometry is first established. From literature, D2EHPA forms dimers in a non-polar organic solvent (Mohammadi $et$ $al.$, 2015). The extraction equation can thus be written as the following, with RH being D2EHPA and $R_2H_2$ its dimeric form:

$$Ni^{2+} + \overline{\frac{n}{2}R_2H_2} \rightleftharpoons \overline{NiR_2\left(RH\right)_{n-2}} + 2H^+ \quad . \tag{4-4}$$
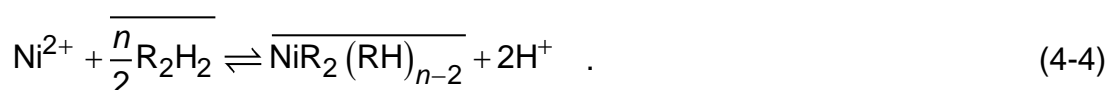
The $n$ parameter is the number of D2EHPA monomeric molecules needed to extract a nickel cation. From literature, 4 D2EHPA molecules in a monomeric form are needed to transfer one nickel cation to the organic phase, so $n$ is 4 (Daiminger $et$ $al.$, 1996;

Darvishi *et al.*, 2005; Talebi *et al.*, 2015). The equilibrium constant of the reaction can be written in the following formula:

$$K_{c,Ni} = \frac{c_{NiR_2(RH)_{n-2}} \, c_{H^+}^2}{c_{Ni^{2+}} \, c_{R_2H_2}^{n/2}} \quad . \tag{4-5}$$

Using the extraction curve data, the equilibrium constant is computed for each data point. The equation (4-5) is used. The constants obtained are slightly different from each other because of experimental errors but they are still of the same order of magnitude. They are averaged to obtain the equilibrium constant for the nickel extraction using D2EHPA in kerosene at 25°C. It is found that

$$K_{c,Ni} = 5.1 \times 10^{-6} \quad . \tag{4-6}$$

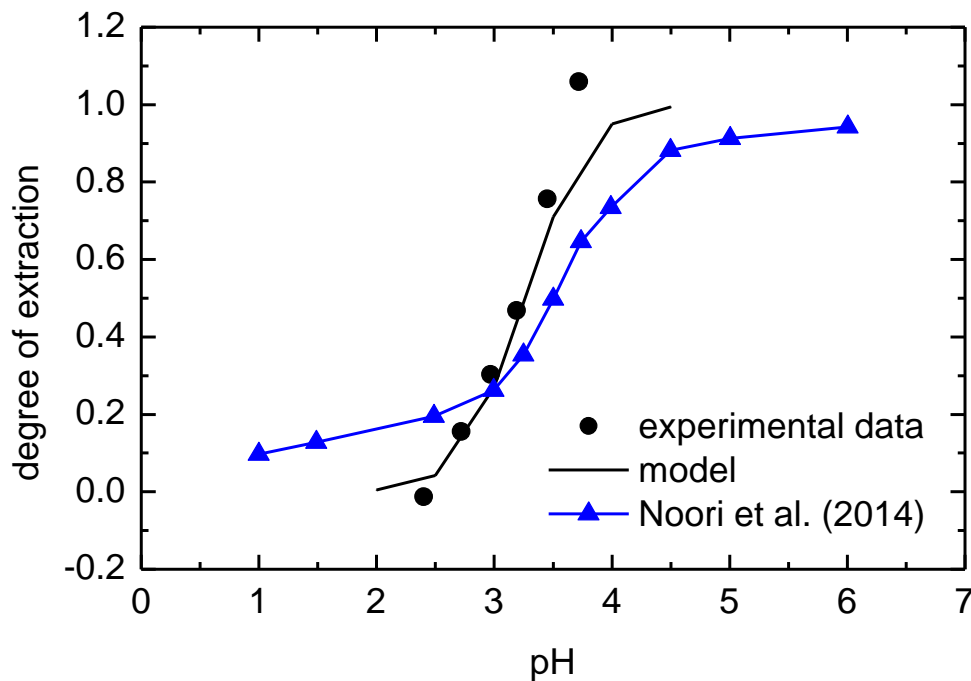Using the nickel extraction equilibrium constant, the extraction curve is modelled in Figure 4-7.



Figure 4-7: Extraction curve of nickel with 20%-vol D2EHPA, its model and an extraction curve from Noori et al. (2014)

The modelled curve matches pretty well the data points, except for the point at $p$H 3.7. However, this point is obviously illogical as its degree of extraction is above 1. It means that more metal is measured with the spectrophotometer then what is put in the tube. The problem is thus the absorbance difference measured with the spectrophotometer.

The issue lies in the presence of small amounts of organic phase remaining in the aqueous phase after the extraction. The aqueous phase appears clear to the naked eye, but the absorbance measured with the spectrophotometer seems to be impacted by these organic traces. In Figure 4-8, the spectrum of the aqueous phase at $p$H 3.7 is tilted. The absorbance increases when the wavelength decreases. This general behavior is typical of the organic phase. Using the calibration curve, a lower concentration than the real concentration is computed. At higher $p$H, this issue worsens and the aqueous phase becomes opaquer.

Turbidity can be present in the aqueous phase because some organic phase is emulsified in the aqueous phase. It doesn't coalesce and settle. Ions in the aqueous phase have an influence on settling. Some preliminary experiments show that 1 g/L of nickel ions in the aqueous solution prevents visible turbidity because it facilitates a good separation of the two phases. Above $p$H 3.5, less than 1 g/L of nickel is left in the aqueous phase and it could be why turbidity appears. When only deionized water and the organic phase are in the tube, the turbidity issue is prevented by keeping a small headspace. It looks like the exchange between hydrogen ions and nickel ions worsen the issue and a small headspace is not enough anymore. Turbidity can be diminished using centrifugation, but some organic phase is still detected using the spectrophotometer.

The calibration curve is compared with literature. Noori et al. article shows an extraction curve built in similar operating conditions. 2 g/L of nickel is extracted at 25 °C with different concentrations of D2EHPA in kerosene (Noori *et al.*, 2014). The volume ratio of the aqueous and organic phases is 1. The extraction is made in a sulfate medium. The extraction is measured using EDTA titration of the remaining nickel in the aqueous phase. This method is known as a reliable and precise way to measure nickel concentration when no cobalt, manganese, iron or copper are present in the solution. None of those impurities are present in the work of Noori et al., so the titration is a suitable

method. The extraction curve given by Noori et al. is thus reliable. The extraction curves for 0.6 M of D2EHPA is compared to the extraction curve built in this master thesis. 0.6 M of D2EHPA corresponds to the 20%-vol of D2EHPA used in this work. Both curves are drawn in Figure 4-7.

Below *p*H 3, the literature curve shows an extraction increasing from 10% at *p*H 1 to 30 % at *p*H 3. The increase is much more abrupt in this thesis extraction curve. It goes from 0% at *p*H 2.4 to around 30% around *p*H 3. This 10% difference compared to the literature may be caused by the precision of the spectrophotometry. By shifting the spectrum after extraction on the spectrum of deionized water, it is visible in Figure 4-8 that the baseline shifted compared to the deionized water and the calibration curve.

The spectra at bigger wavelength are higher for the aqueous phase after extraction than for the calibration curve. It could give a bigger absorbance difference between 501 and 720 nm, thus the concentration would be computed higher than it really is. Measuring a higher concentration would give a lower degree of extraction.
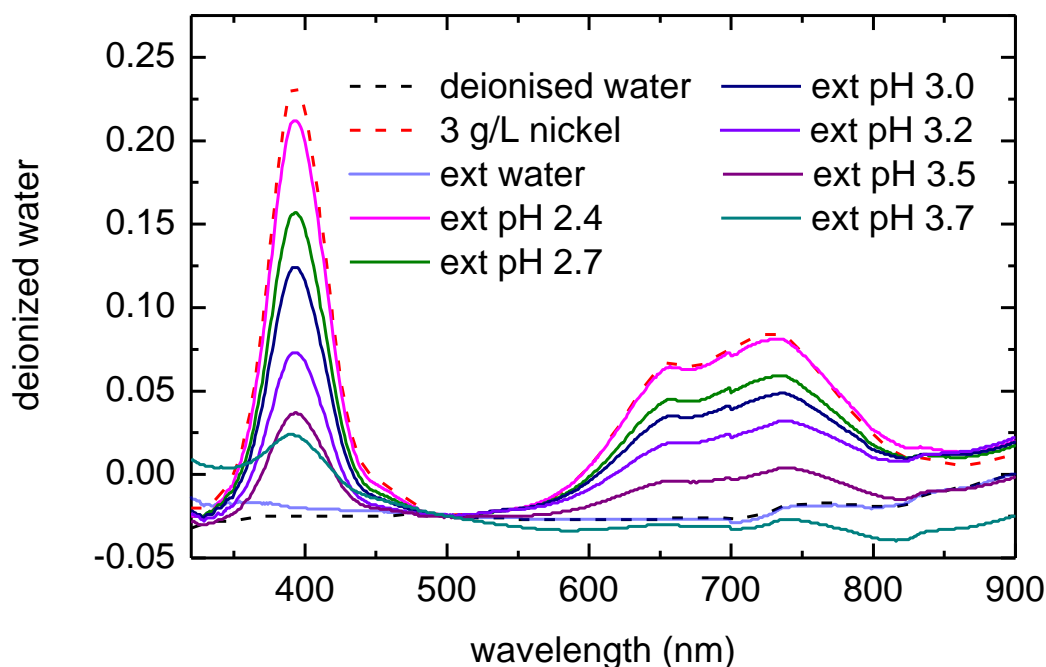


Figure 4-8: Superimposed spectra of deionized water post extraction, clean deionized water, nickel aqueous solution after extraction and 3 g/L nickel solution

Between $p$H 3 and 3.5, the extraction curve from Noori et al. presents a smaller slope than the curve of this work. It means the concentration obtained from the spectrophotometer at the same $p$H is lower than what would be expected from Noori et al. Beyond precision issues found with the spectrophotometer, the difference in media for the aqueous phase could have an influence on extraction. Noori et al. work uses nickel sulfate while this thesis uses nickel chloride. The concentration of sulfate or chloride does have an influence on extraction with D2EHPA (Shibata and Nishimura, 1977) but its exact magnitude is not entirely clear.

## 4.2.2  Nickel and Cyanex 272

For extraction with Cyanex, the metal concentration is taken identical to the one used for the D2EHPA extraction experiments. The same extractant percentage is taken too, of 20%-vol of extractant. It is commonly considered a high percentage of extractant. As Cyanex 272 viscosity is quite high with 0.142 Pa.s at 25°C (Rickelton, Flett and West, 1984), it is better to avoid too high viscosity for easier mixing and settling.

The tubes are prepared in the same way as for the D2EHPA extractions, with 4 mL headspace. The $p$H is adjusted with a NaOH solution before extraction and the precipitate formed dissolves during the extraction. The extraction lasts 10 minutes. It is long enough to reach equilibrium as 5 minutes are already sufficient (Rickelton, Flett and West, 1984). After analysis of the aqueous phase, the degree of extraction is computed. The degree of extraction versus the equilibrium $p$H is shown in Figure 4-9.

The aqueous phase is a bit turbid after extraction if it does not contain enough metal. It is observed in the preliminary tests conducted with deionized water as aqueous phase. The settling of the two phases is not perfect. Indeed, ions influence settling. This phenomenon was already observed for D2EHPA where nickel ions favorized the obtention of a clear aqueous phase. When the extraction is made at too high $p$H, the aqueous phase eventually becomes turbid with Cyanex 272 too. The reason is probably that almost all metal is extracted, so that not enough metal remains to ensure a clear aqueous phase. Above $p$H 6, the aqueous phase gets opaque and colorless after extraction. As nickel ions tint the solution green, it supports the assumption that almost

no metal ions are in the aqueous phase. Anyway, the spectrophotometry is unusable in that case because the sample turbidity influences the absorbance. From preliminary experiments, centrifugation cannot fully solve this turbidity. Experiments above $pH$ 6 are not used to establish a model from the extraction curve.
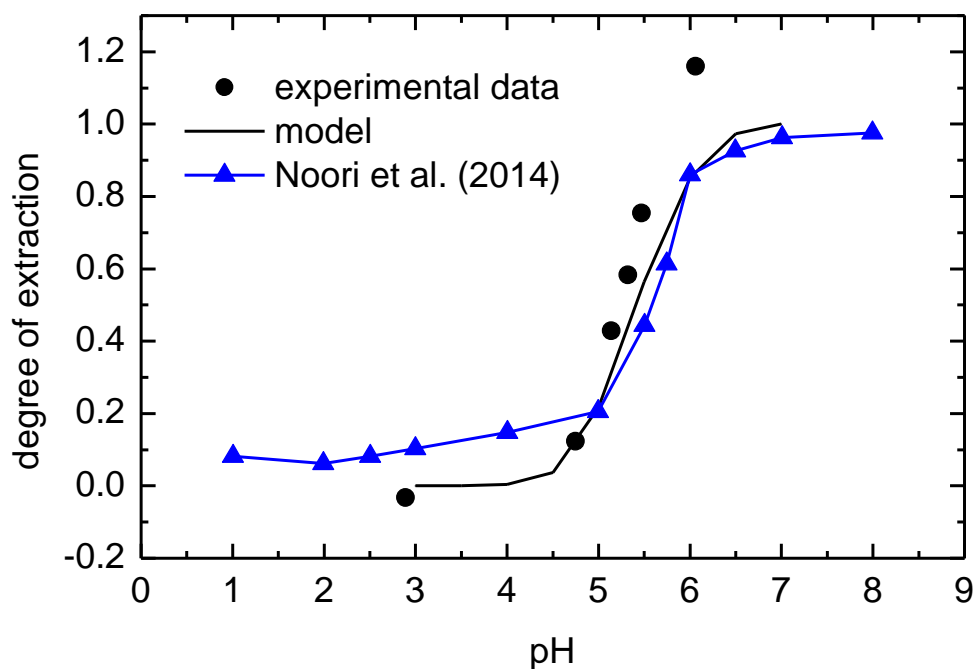


Figure 4-9: Extraction curve of nickel with 20%-vol Cyanex 272, its model and an extraction curve from Noori et al. (2014)

The reaction stoichiometry is established using literature. Cyanex 272 in solution in a low-polarity diluent form a dimer (Nguyen, Nguyen and Lee, 2020). If the extractant in a dimeric form is written as $R_2H_2$ and $n$ is the number of Cyanex 272 monomeric molecules needed to extract one nickel cation, the equilibrium reaction is as follows:

$$Ni^{2+} + \overline{\frac{n}{2}R_2H_2} \rightleftharpoons \overline{NiR_2\left(RH\right)_{n-2}} + 2H^+ \quad . \tag{4-7}$$
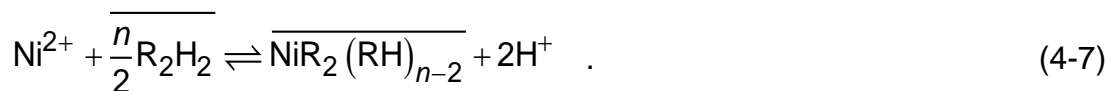
From literature, 3 dimers of Cyanex 272 are needed to extract nickel (Xun and Golding, 1987; Tait, 1993). It means that the value of $n$ is 6. The equilibrium constant is written from the reaction:

$$K_{c,Ni} = \frac{c_{NiR_2(RH)_{n-2}}\, c_{H^+}^2}{c_{Ni^{2+}}\, c_{R_2H_2}^{n/2}} \quad .$$  (4-8)

As previously, the equilibrium constant is computed from the extraction curve. It is

$$K_{c,Ni} = 1.5 \times 10^{-9} \quad .$$  (4-9)

The equilibrium constant is used to plot the model on the extraction curve in Figure 4-9.

The extraction curve is compared with the literature. Noori et al. studied the extraction of nickel and vanadium with Cyanex 272 diluted in kerosene at different concentrations. The aqueous solution contained 2 g/L of nickel and 2 g/L of vanadium in a sulfate medium. Sulfuric acid and ammonia were used to modify the $p$H (Noori *et al.*, 2014). 20%-vol of extractant is equivalent to 0.6 M. Between 20% and 80% of extraction, both extraction curves are very similar to each other. The model made from this work matches particularly well the curve from Noori et al.

Below 20% extraction, the curves differ. It is clearly an issue with the spectrophotometry because the extraction measured at $p$H 2.9 is - 6%. From observing the spectrum of the aqueous phase, the baseline didn't shift as much as in the D2EHPA extraction of nickel, yet the peaks are higher than expected from the calibration curve. No explanation for this phenomenon is found.

## 4.2.3   Cobalt and Cyanex 272

This extraction experiment encountered issues related to the metal spectrum and the initial concentration. These are outlined below and possible explanations given.

For the extraction of cobalt with Cyanex 272, the amount of extractant is kept at 20%-vol. The cobalt concentration is different from the nickel concentration used in the previous section. The calibration curve is only usable between 2 and 10 g/L cobalt.  Keeping the same molar concentration of cobalt as the nickel molar concentration used for the nickel extractions would give 1.5 g/L cobalt. A 4 g/L concentration is thus arbitrarily chosen for the experiment.

5 mL of the aqueous phase is prepared directly in the tube. A cobalt stock solution is used and $p$H is increased with a 40 g/L NaOH solution before the extraction. Afterward, 5 mL of the organic solution made of 20%-vol Cyanex 272 and kerosene is added. Cobalt hydroxide precipitates in the tube as soon as sodium hydroxide is added. Indeed, cobalt precipitates as a hydroxide at $p$H of around 7 or higher. The NaOH solution is added in 0.2 mL increments, and only an addition of 0.2 mL is sufficient to exceed $p$H 7. As the $p$H is lowered during the extraction, cobalt hydroxide solubilizes until only remain some particles stuck on the aqueous-organic interface. This extraction lasts 10 minutes. It is more than enough because cobalt extraction with Cyanex 272 can reach equilibrium in 5 minutes (Rickelton, Flett and West, 1984).

At the end of the extraction, the organic phase turns dark blue due to the formation of the cobalt complex. Bubbles are found in the aqueous phase after extraction while the organic phase is in one block. The bubbles are dark blue. Judging from their color, the membranes of the bubbles are made from the organic phase and contain the aqueous phase. Those bubbles coalesce and settle. However, the coalescence is not complete for the higher $p$H values. Membranes made of the organic phase stay stable and split the organic phase into several big compartments.
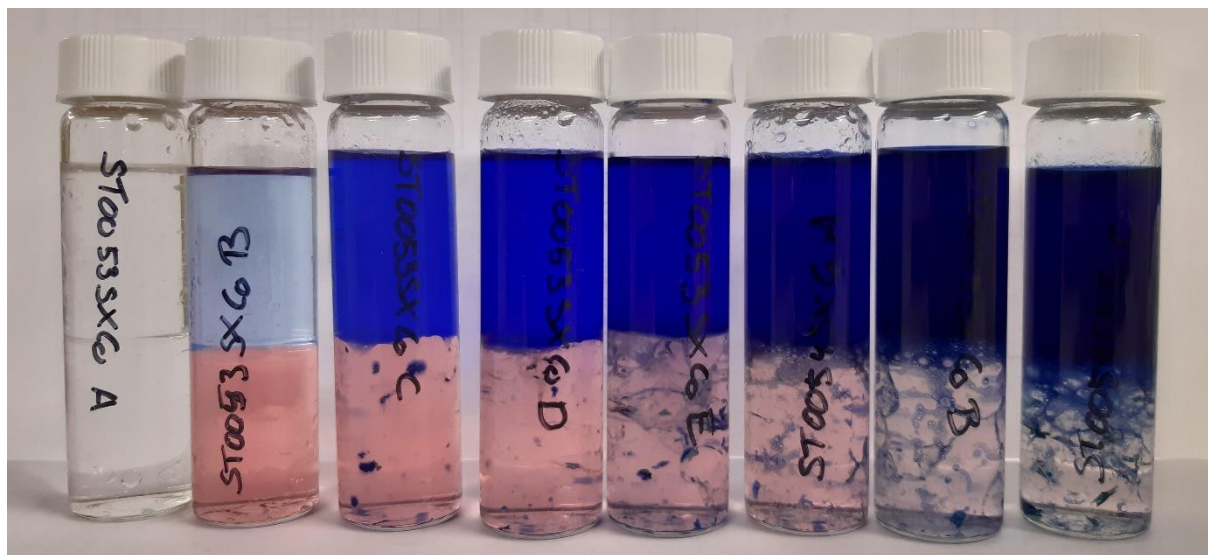


Figure 4-10: Tubes after extraction of cobalt with 20 %-vol Cyanex 272

Examples of tubes obtained after an extraction experiment and left to settle for 2 hours are shown in Figure 4-10. All tubes have been treated similarly during the extraction experiment. Only the initial conditions of each tube differ. The tube on the leftmost only

contains the organic phase and deionized water. The coalescence issue is not encountered in that tube. The other tubes contained initially a cobalt aqueous solution of around 2 g/L of cobalt and the organic solution. They are placed in from left to right by increasing $p$H value, from $p$H 2.7 to 5.0. The higher the $p$H, the more cobalt is extracted. The root cause of the settling issue is thus related to the extraction loading. Cyanex 272 increases in viscosity when its cobalt loading increases (Xun and Golding, 1987). Xun and Golding claim that it is caused by an aggregation of the metal extractant complex, and that the viscosity increases sharply from 70% loading.

As the coalescence is not complete, the tubes must be centrifugated for phase separation. 5 minutes centrifugation at 4,000 rpm allows to separate the phases. However, the degree of extraction at low equilibrium $p$H values clearly presents an issue. Indeed, the degree of extraction computed from the spectrophotometer measurement is of -0.188 at $p$H 2.6. Negative degrees of extraction are of course not physically possible as cobalt is not created in the closed tube during the extraction. Moreover, the blue color of the organic solution attests that some cobalt is already extracted. This issue arises because the absorbance measured after extraction is higher than for a 4 g/L cobalt solution without extraction. This can be seen in Figure 4-11.
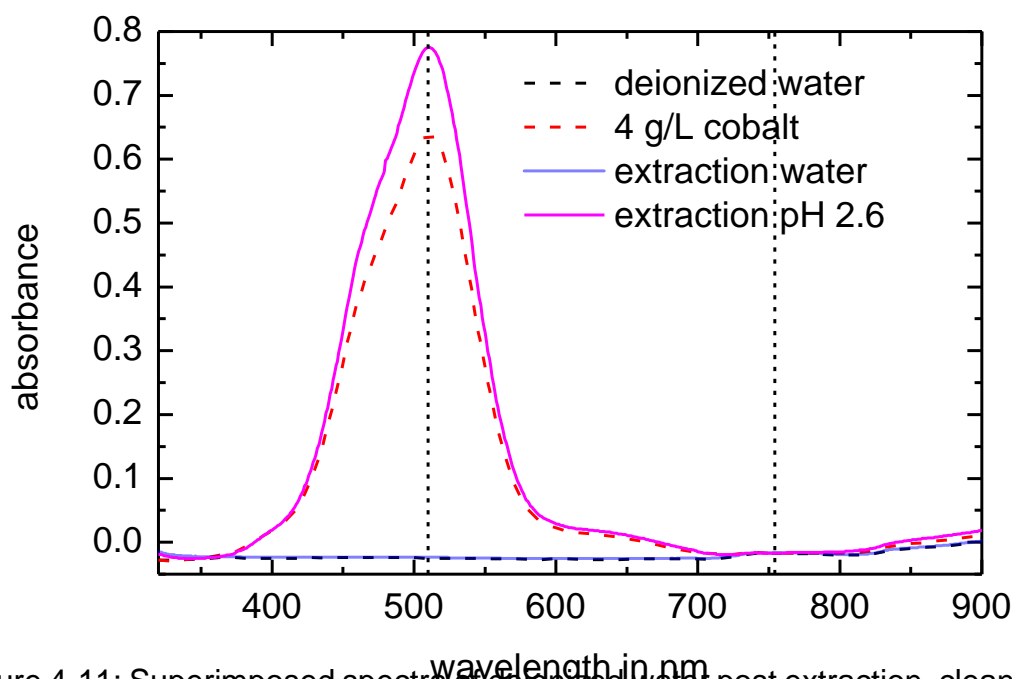


Figure 4-11: Superimposed spectra of deionized water post extraction, clean deionized water, cobalt aqueous solution after extraction at $p$H 2.6 and 4 g/L cobalt solution

In Figure 4-11, the spectra of the deionized water mixed with extractant, the extraction sample at an equilibrium $p$H of 2.6 and the 4 g/L cobalt aqueous phase are plotted along with the spectrum of clean deionized water. It is obvious that the extraction sample has a peak much higher than the 4 g/L sample. Yet, the baselines of all spectra superimpose well. It is the same unexplained issue that arises for the lower $p$H values for nickel. It is here amplified, probably because there is a 2.5 times higher molar concentration of metal in solution. Using the spectrophotometer for extraction of relatively high metal concentration is thus inadvisable.

The extraction reaction of cobalt with Cyanex 272 can still be given from literature. HR is the extractant in monomeric form and $n$ the number of such molecules needed to extract one metallic cation. Cyanex 272 in solution tends to form dimers, so its dimeric form is considered in the equilibrium reaction:

$$Co^{2+} + \overline{\frac{n}{2}R_2H_2} \rightleftharpoons \overline{CoR_2(RH)_{n-2}} + 2H^+ \quad . \tag{4-10}$$
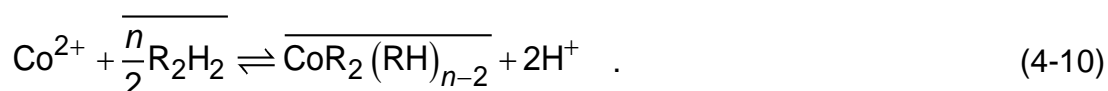
From literature, 2 dimeric Cyanex 272 form the cobalt extractant complex (Xun and Golding, 1987; Tait, 1993). The $n$ parameter is thus 4. The equilibrium constant is written as following:

$$K_{c,Co} = \frac{c_{CoR_2(RH)_{n-2}}\, c_{H^+}^2}{c_{Co^{2+}}\, c_{R_2H_2}^{n/2}} \quad . \tag{4-11}$$

As the extraction curve is clearly wrong, no model is made from it. For extraction curve made with cobalt at relatively high concentration, spectrophotometry does not work properly. Another analysis method must be used, such as EDTA titration, which has been proven to work.

## 4.2.4 Neodymium and D2EHPA

D2EHPA is a common extractant for neodymium. In this experiment, neodymium is extracted from a chloride medium. The initial concentration is selected to be in the range where the calibration curve is precise, which is between 0.5 g/L and 7 g/L. 7 g/L is arbitrarily chosen as starting Nd concentration in the aqueous phase for all extraction experiments. The extractant amount in the organic phase is fixed at 10%-vol and is

diluted in kerosene. The ratio between the volume of aqueous phase and the volume of organic phase is fixed at 1, as in previous experiments.

The issues with the behavior of D2EHPA were already solved in the experiments with nickel. Only a 4 mL headspace is kept in the 24 mL tube to prevent emulsion between the two phases and no separation issues are encountered.

The aqueous phase is made by dilution of a stock solution. Neodymium oxide is used to prepare the neodymium solution. Neodymium oxide is insoluble in ordinary distilled water. The $p$H must be close to 1 to ensure complete solubilization. It is achieved by adding 5 M hydrochloric acid. The stock solution has a 14 g/L concentration in neodymium ions. After dilution to 7 g/L, $p$H is around 1.3.

Before extraction, dilution and $p$H adjustment are made directly in each tube. Increasing $p$H is achieved with a 40 g/L NaOH solution, which corresponds to 1 M NaOH. In each tube, different amounts of the basic solution are added, with 0.2 mL increments. A lavender precipitate is produced as soon as the NaOH solution is added. It is particles of neodymium hydroxide ($Nd(OH)_3$). This solid dissolves during the extraction because the $p$H decreases due to the exchange of metal ions for $H^+$ between the extractant and the aqueous phase. Only tiny amounts of solid stay stuck at the interface between the two phases. The quantity is so small that it is assumed to be negligible in the metal mass balance.

Unlike in nickel extraction, D2EHPA extraction without $p$H adjustment already gives a degree of extraction of 58%. To obtain the other half of the extraction curve, $p$H is lowered before extraction. A solution of 1 M HCl is prepared by diluting a 5 M HCl solution. It is added by 0.4 mL increments to diminish $p$H before extraction.

The tubes are shaken for 20 minutes in a water bath at 25°C. From literature, it is enough time to reach equilibrium (Mohammadi *et al.*, 2015; Batchu and Binnemans, 2018). The basket is rotating at 74 rpm. Once time is up, the phases are left to settle. They are then separated and the aqueous phase is analyzed by spectrophotometry. The extraction curve is plotted in Figure 4-12.
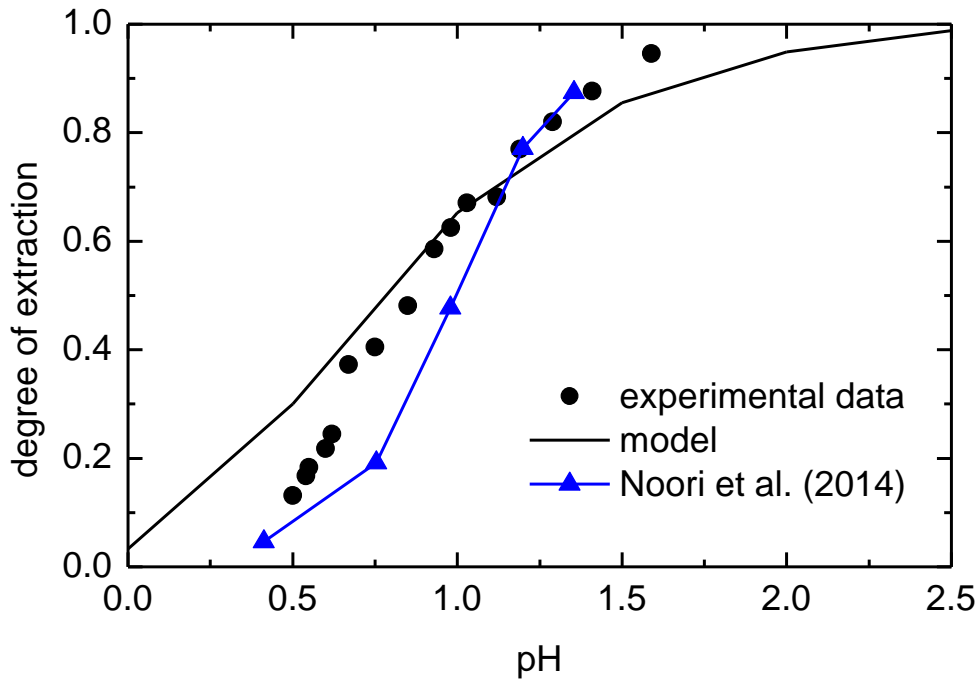
Figure 4-12: Extraction curve of neodymium with 10%-vol D2EHPA, its model and an extraction curve from Mohammadi et al. (2015)

A model is established using stoichiometry from literature and an equilibrium constant obtained from the extraction curve. As mentioned earlier, D2EHPA forms dimers when mixed with a non-polar diluent. Its monomeric form is written RH in the equilibrium reaction and its dimeric form $R_2H_2$:

$$Nd^{3+} + \overline{\frac{n}{2}R_2H_2} \rightleftharpoons \overline{NdR_3\left(RH\right)_{n-3}} + 3H^+ \quad . \tag{4-12}$$
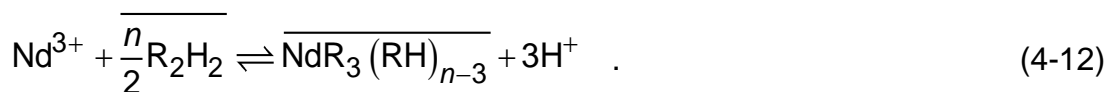
From literature, 6 monomeric molecules of D2EHPA are used to transfer one neodymium cation (Sato, 1989; Gupta and Krishnamurthy, 2005; Mohammadi *et al.*, 2015; Yin *et al.*, 2015). It means that *n* is 6 in the equilibrium reaction. It allows to calculate the equilibrium constant with the following formula and the extraction curve, like in the other experiments. The computed equilibrium constant is $K_{c,Nd} = 11.2266$.

$$K_{c,Nd} = \frac{c_{NdR_3\left(RH\right)_{n-3}}\, c_{H^+}^3}{c_{Nd^{3+}}\, c_{R_2H_2}^{n/2}} \quad . \tag{4-13}$$

The extraction curve computed from the equilibrium constant is drawn in Figure 4-12. It corresponds to the experimental data in an admissible way but diverges strongly at a $p$H below 0.5.

The extraction curve is compared with the literature in Figure 4-12. Mohammadi *et al* article presents a calibration curve of neodymium for 0.15 mol/L of D2EHPA in n-heptane (Mohammadi *et al.*, 2015). The diluent n-heptane is aliphatic like kerosene, so they should have similar influence on extraction (Batchu and Binnemans, 2018). The aqueous solution is prepared by dissolving REE oxides in hydrochloride acid and followed by dilution with deionized water. The $p$H is adjusted with hydrochloride acid and ammonia. The extraction starts around $p$H 0.5 and is at more than 80% when $p$H 1.5 is reached. The extraction behavior is similar between the extraction curve of this work and the article by Mohammadi *et al*. This work has a higher extraction at the same $p$H, but 10%-vol D2EHPA corresponds to 0.3 mol/L. It was observed for nickel that a lower extractant concentration needs a higher $p$H to reach the same extraction than with a higher concentration (Noori *et al.*, 2014). It is thus possible that the shift of this work extraction curve to the left is caused by a difference of extractant concentration.

This curve shows that neodymium can be extracted into the organic phase at low $p$H. To perform a back-extraction, a strong acid is thus needed.

## 4.3   Mass transfer experiments

Mass transfer experiments are done in the single-drop cell described previously. The equipment is filled with 2.5 L of an aqueous solution containing the metal to be transferred at desired concentration and $p$H. The $p$H is adjusted before pouring the solution into the equipment. Care must be taken to avoid any precipitation. The aqueous phase is pumped in the equipment and is considered homogeneous. Any local modification of the concentration or $p$H will be quickly absorbed by the big volume of aqueous phase. The concentration and $p$H in the aqueous phase are thus assumed constant.

Next, an organic phase containing an extractant is introduced dropwise via a nozzle at the bottom of the cell. The drop is stabilized for a residence time fixed by the operator. 250 drops are generated, collected and analyzed for each residence time.

For the analysis, the organic phase collected is mixed for an adequate time with a strong acid. The metal is extracted from the organic phase towards the acidic phase. The resulting aqueous phase is then analyzed by spectrophotometry.

## 4.3.1   Nickel and D2EHPA

The equipment is filled with a nickel chloride solution at 10 mmol/L, which corresponds to 0.58 g/L of nickel. The aqueous phase is prepared by diluting around 50 mL of a stock solution to obtain a 2.5 L solution. A sample of the solution is taken from the equipment before each mass transfer experiment to measure its $p$H. The $p$H is around 4.5 for the 3 experiments. This value is taken to fully prevent precipitation of nickel hydroxide in the equipment. The system is at ambient temperature, which varied between 23°C and 26°C. The same aqueous solution is kept in the equipment for all 3 measurements. As there is 2.5 L in total of the aqueous solution in the equipment that is pumped through the system from a storage tank and as less than 0.005 g of nickel is extracted in total from the experiment, the aqueous metal concentration variation between the measurements is considered negligible. This is especially true when the aqueous phase is pumped in and out from a tank where the aqueous phase can be homogenized.

The organic phase is composed of 10%-vol of D2EHPA and of 90%-vol of kerosene. It is filling a nozzle of 1.5 mm of diameter. By assuming the drops are spherical, the drop diameter is 3.22 mm. Three different residence times are considered: 40 s, 60 s and 90 s. The volume flowrate of the continuous phase is set between 40 and 45 L/h in the equipment software settings.

Once 250 drops are obtained for one residence time, the nickel is back-extracted from the organic phase. The volume ratio between the aqueous and the organic phase is 1. The back-extraction is made at 25°C in the basket rotating at 74 rpm for 30 minutes. The aqueous phase is hydrochloric acid at 5 M. From literature and by consulting the extraction curve in section 4.2.1, a hydrochloric acid solution at 5 M allows to strip 100% of the nickel from the organic phase (Nogueira and Delmas, 1999; Cheng, 2000). Indeed, the $p$H at equilibrium after the back-extraction is well under 1. Seeing the extraction curve in Figure 4-7, virtually no metallic cation remains in the organic phase.

The nickel concentration in the organic phase is computed from the nickel concentration in the aqueous phase after back-extraction, knowing the volume ratio of the two phases and assuming that 100% of nickel is back-extracted.

Equilibrium concentration is computed using the equilibrium constant obtained in section 4.2.1. Several assumptions are made. The $p$H and the metal concentration of the continuous phase are considered constant. It is plausible because the volume of continuous phase is much larger than the volume of dispersed phase in the equipment and the continuous phase is mixed when it is pumped through the equipment. The equilibrium constant is obtained for 25°C. It is assumed that its variation due to temperature change between 23°C and 26°C is negligible.

The equilibrium concentration in the dispersed phase is computed for $p$H 4.5, a 0.58 g/L nickel concentration in the continuous phase and 10 %-vol of D2EHPA in the dispersed phase. It is 3.44 g/L of nickel. The dimensionless mass transfer $y^+$ is computed from the concentrations in organic phase at different residence times and the calculated equilibrium concentration. The results are plotted in Figure 4-13 and compared with the mass transfer of zinc from Altunok, Kalem and Pfennig, (2012).
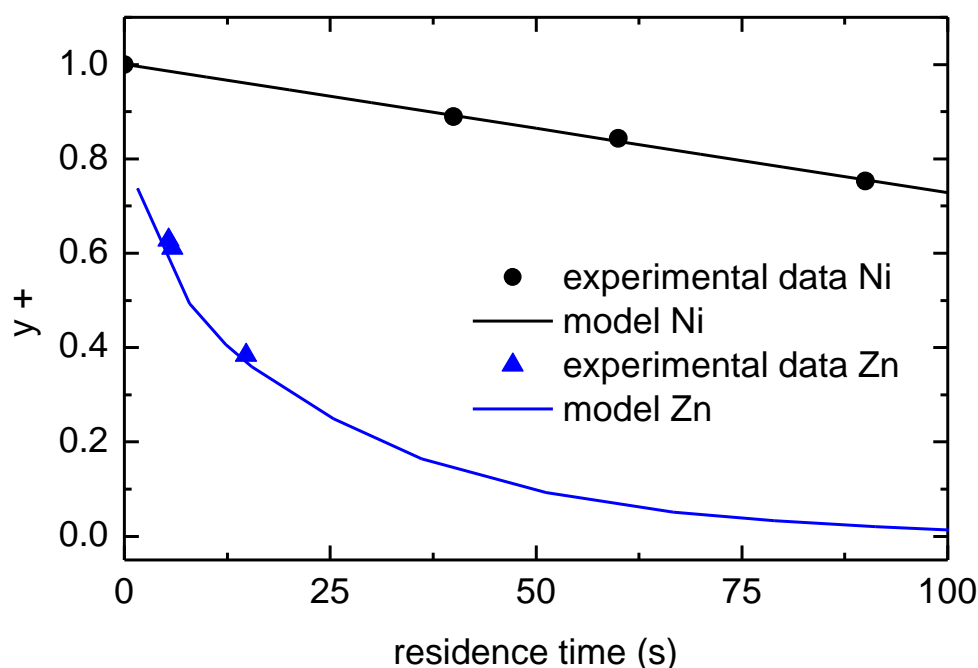


Figure 4-13: Mass transfer of nickel in 10%-vol D2EHPA compared with mass transfer of zinc in 10%-wt D2EHPA (Altunok, Kalem and Pfennig, 2012)

In Altunok et al., 30 mmol/L of zinc in sulfate media is extracted using 10%-wt D2EHPA in isododecane (Altunok, Kalem and Pfennig, 2012). The $p$H value is 4.7 and the extraction is made at 20°C. The drops released have a 3.22 mm diameter, which is similar to this work. As both isododecane and kerosene are aliphatic diluents, we assume that D2EHPA extraction is very similar between the two. Both works are thus compared, here, keeping in mind that the metals considered are different.

The general behavior of nickel, which is increasing mass transfer for longer residence time, is coherent with theory and with the results obtained for zinc extraction. However, the rate at which extraction proceeds is very different for both metals. Extraction of zinc is much faster than for nickel. For 20 s of residence time, already 40% of the equilibrium value is extracted for zinc, while not even 10% is transferred for nickel. It has to be noted in this comparison that the initial molar concentration in the aqueous phase is smaller for the nickel than for zinc. A smaller concentration in the continuous phase can slow down the mass transfer because the concentration gradient between the continuous phase and the organic phase would be smaller. However, the difference in mass transfer is far too great for this to be the only reason. Moreover, extraction kinetics of nickel is known to be slower than for zinc (Dreisinger and Cooper, 1989), so the reasons for this difference must therefore be sought in the mass transfer mechanism itself.

Mass-transfer kinetics can be slowed down for three reasons. First there can be resistance for the outer mass transfer, which corresponds to the slowing down of the metal ions from the bulk aqueous phase to reach the extractant at the interface. The extraction reaction kinetics can also be slow, if the metal ion needs a long time to form a complex with the extractant. Finally, the inner mass transfer can be slow, if the metal complex takes a lot of time to move from the interface to the inside of the drop.

The reaction kinetics is suspected to be slower for nickel than for zinc. Indeed, zinc forms a complex with 3 D2EHPA monomeric molecules (Dreisinger and Cooper, 1989), while nickel requires 6 D2EHPA monomeric molecules. It seems logical that the reaction is slower for nickel than for zinc, though by how much cannot be determined without a more in-depth study that would be beyond the scope of this thesis. Dreising and Cooper did find in their own investigations that the extraction reaction for nickel

was slower than for zinc. The reaction kinetics may thus be an explanation for the difference observed in mass-transfer rate between nickel and cobalt.

Computing the mass-transfer coefficient in both the continuous and the dispersed phase could hint on the resistance to mass transfer on both sides of the interface. Comparing their orders of magnitude would indicate whether the mass-transfer kinetics is slowed down mainly by the inner or outer mass-transfer resistance. The computation of the two mass-transfer coefficients is carried out following the calculations presented in Henschke (2004).

In Henscke (2004), the mass-transfer coefficient is expressed as $\beta_c$ in the continuous phase and $\beta_d$ in the dispersed phase. The coefficients are expressed in m/s. The correlations are different for the inner mass-transfer coefficient, inside the drop, and for the outer mass-transfer coefficient, in the bulk continuous phase surrounding the drop. First, the mass transfer in the continuous phase is evaluated. As the metal concentration in the continuous phase is 10 mmol/L, which is very low, the continuous phase is considered to be pure water in the following calculations.

The Sherwood number indicates whether the convective or the diffusive mass transfer has more influence. It is expressed on a characteristic length scale for the mass transfer. In this case, it is the diameter of the drop $d$. The drop is $3.22 \times 10^{-3}$ m of diameter. The Sherwood number $Sh_c$ is expressed as follows (Henschke, 2004):

$$Sh_c = \frac{\beta_c d}{D_c} \quad .$$

(4-14)

The diffusion coefficient in the continuous phase $D_c$ is obtained from literature. The ionic diffusion coefficient of nickel ions $6.79 \times 10^{-10}\,m^2/s$ in water at 25 °C (Sato, Yui and Yoshikawa, 1996). Several formulas are proposed for the Sherwood number in Henschke's work. Each is only valid for a fixed range of value for the Sherwood number. The adequate correlation for these calculations is (Henschke, 2004):

$$Sh_c = -178 + 3.62 Re_\infty^{1/2} Sc_c^{1/3} \quad \text{for } Sh_c > 50 \quad .$$

(4-15)

The Reynolds number $Re_\infty$ and the Schmidt number $Sc_c$ are needed for this equation. The Schmidt number computed for water is the following (Henschke and Pfennig, 1999):

$$Sc_c = \frac{\eta_c}{\rho_c D_c} \quad , \tag{4-16}$$

$$Sc_c = 1.48 \times 10^3 \quad . \tag{4-17}$$

The dynamic viscosity $\eta_c$ of water at 25°C is taken as 0.001 Pa s. The density $\rho_c$ of water at 25°C is taken as $997 \, kg/m^3$. The Reynolds number is calculated with the drop diameter as the characteristic length. It is expressed as following (Pfennig, 2021):

$$Re_\infty = \frac{\rho_c v_\infty d}{\eta_c} \quad . \tag{4-18}$$

The parameter $v_\infty$ is the sedimentation velocity of the drop in the equipment. Assuming that the drop is a rigid sphere, the Reynolds number can be expressed in function of the Archimedes number Ar and of the drag coefficient $c_d$. The equations are the following (Pfennig, 2021):

$$Ar = \frac{\rho_c (\rho_c - \rho_d) g d^3}{\eta_c^2} \quad , \tag{4-19}$$

$$Ar = 54{,}869.17 \quad , \tag{4-20}$$

$$c_d = \frac{432}{Ar} + \frac{20}{Ar^{0.33}} + \frac{0.51 Ar^{0.33}}{140 + Ar^{0.33}} \quad \text{for } 0 < Re_\infty < 3 \times 10^5 \quad , \tag{4-21}$$

$$c_d = 56.76 \quad , \tag{4-22}$$

$$Re_\infty = \sqrt{\frac{4 Ar}{3 c_d}} \quad , \tag{4-23}$$

$$Re_\infty = 35.90 \quad . \tag{4-24}$$

The *g* parameter is the gravity, equal to 9.81 $m/s^2$. The density of the dispersed phase $\rho_d$ is approached by the weighted volume average of the densities of its components. The dispersed phase is made of 10%-vol D2EHPA and 90%-vol kerosene. The average density of the continuous phase is 828.97 $kg/m^3$.

Now that both the Reynolds number and the Schmidt number are available, the Sherwood number can be computed with the equation (4-15). Its value is 69.03. From its definition given in equation (4-14), the mass transfer coefficient in the continuous phase can be computed:

$$\beta_c = \frac{Sh_c D_c}{d} \quad , \tag{4-25}$$

$$\beta_c = 1.46 \times 10^{-5} \frac{m}{s} \quad . \tag{4-26}$$

For the calculation of the inner mass-transfer coefficient, Henschke (2004) recommends different formulas to compute the mass-transfer coefficient, depending on the duration of the contact time. The Fourier number $Fo_d$ involves that contact time and determines the correlation to be used. As the diffusion occurs from the outside of the drop to its center, the length scale is the drop radius $R$. The formula is given as follows (Henschke and Pfennig, 1999):

$$Fo_d = \frac{D_d t}{R^2} \quad . \tag{4-27}$$

The contact time $t$ is taken as 40 s. It is the shortest residence time taken in the experiment. Compared with the residence times for zinc mass transfer, it is already quite a long time. The diffusion coefficient of the dispersed phase $D_d$ is computed using the Wilke-Chang correlation. This correlation approximates the interdiffusion coefficient $D_{12}$ of the solute 1 in the solvent 2 for an infinitely dilute solution. In this case, the solvent is a mix of 10% D2EHPA and 90% kerosene. The solute is the D2EHPA-Ni complex. The correlation is written as such (Wilke and Chang, 1955):

$$D_{12} = 7.4 \times 10^{-8} \frac{T \sqrt{\varphi_2 M_2}}{\eta_2 v_1^{0.6}} \quad . \tag{4-28}$$

The temperature $T$ is taken as 298 K. The properties of the solvent 2 are approximated by a weighted volume average of the components. That means 90% contribution from kerosene and 10% from D2EHPA. The dynamic viscosity of the solvent $\eta_2$ is thus assumed to be $4.986 \times 10^{-3}$ kg/$(ms)$, expressed as 4.986 cP in the correlation. The necessary data are taken from literature (Rout, Mishra and Ramanathan, 2020). The solvent molecular mass $M_2$ is computed in the same way. It is 321 g/mol. The solvent association parameter $\varphi_2$ is used to express that solutes that are associated to the solvent are slowed down for diffusion, compared to non-associated solutes. Kerosene is assumed to be a non-associated solvent, so this parameter is 1. The parameter $v_1$ is the molar volume at boiling point of solute 1, in cm$^3$/mol. It is computed using the

Schroeder's law. It is calculated by summing the volume increments specific to each atom of the solute. The volume increments are given in the literature (Gulliver, 2007; Aqua-calc.com, 2022). In section 4.2.1, the stoichiometry of the Ni-D2EHPA complex is established. Six D2EHPA molecules are bounded to one nickel cation. The parameter $v_1$ is equal to $2{,}543.39 \, cm^3 / mol$. The diffusion coefficient $D_{12}$, which corresponds to $D_d$, can then be computed with Wilke-Chang correlation and is equal to $7.17 \times 10^{-7} \, cm^2 / s = 7.17 \times 10^{-11} \, m^2 / s$.

The Fourier's number can now be computed. It is equal to 0.0011. From Henschke (2004), if Fourier's number is lower than 0.1584, the contact time is considered to be short. The suitable formula for the mass transfer coefficient in the dispersed phase $\beta_d$ is the following (Henschke, 2004):

$$\beta_d = \sqrt{\frac{D_d}{\pi t} + \frac{4\pi^4 D_d^2}{9 d^2}} \quad , \tag{4-29}$$

$$\beta_d = 7.70 \times 10^{-7} \frac{m}{s} \quad . \tag{4-30}$$

Based on these calculations, the mass-transfer coefficient in the dispersed phase $\beta_d = 7.70 \times 10^{-7}$ m/s and the one in the continuous phase $\beta_c = 1.46 \times 10^{-5}$ m/s. The outer mass-transfer coefficient being greater than the inner one, the resistance to mass transfer is higher on the dispersed phase side of the interface. It is thus very probable that a combination of inner mass-transfer resistance and of a slower reaction kinetics is responsible of the very slow mass transfer of nickel.

## 4.3.2  Neodymium and D2EHPA

In this experiment, a problem was encountered in releasing consistent drops and collecting them. Hereafter is the description of the operational conditions and of the issues met, as well as their possible causes.

Neodymium oxide is solubilized in deionized water using hydrochloric acid. This stock solution is then diluted to a 10 mmol/L neodymium solution. The equipment is filled with this solution and it is pumped around for one hour before the $p$H is measured. A sample collected in the single-drop cell after one hour has a $p$H of 2.37.

The organic phase is prepared by diluting D2EHPA in kerosene. Drops of organic phase of 3.22 mm of diameter are injected into the single-drop cell using a 1.5 mm diameter nozzle. Unfortunately, the viscosity of the organic phase changes when it is in contact with the neodymium solution. The organic phase left in the funnel becomes a gel. Deposition of gel accumulates on the nozzle tip. It creates an organic phase dome on the tip of the nozzle, which makes the experiment impossible to carry out.

It is highly probable that this gel is produced by polymerization of the metal-extractant complexes when the loading of the extractant becomes high enough (Anticó *et al.*, 1996; Batchu and Binnemans, 2018). The most present form in a not fully loaded extractant is one neodymium ion with six D2EHPA monomeric molecules (Scharf *et al.*, 2005). Scharf *et al* analyzed the composition of a D2EHPA-Nd gel. They drew the conclusion that for each neodymium atom, there were three D2EHPA molecules (Scharf *et al.*, 2005). The following irreversible reaction is proposed for polymerization in literature (Harada, Smutz and Bautista, 1972), where RH is the monomeric form of D2EHPA:

$$m\text{Nd}^{3+} + m\overline{\text{NdR}_3\left(\text{RH}\right)_3} \rightarrow \overline{\left(\text{NdR}_3\right)_{2m}} + 3m\text{H}^+ \quad . \tag{4-31}$$
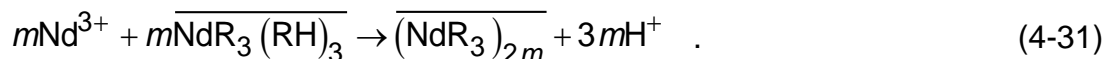
To avoid gel formation, rare earth loading must be kept suitably low. A lower loading can be achieved by adjusting several parameters. The degree of extraction can be decreased by adjusting the $p$H value to a lower value. Indeed, $p$H around 2 leads to 100% of neodymium extraction. A lower $p$H would decrease the extraction efficiency so less metal would be transferred into the drop.

Decreasing the amount of metal in contact with the extractant may also be useful too. It can be achieved by either decreasing the concentration of metal or decreasing the aqueous phase to organic phase ratio (Batchu and Binnemans, 2018). However, the volume ratio is fixed in the single-drop cell, so only the concentration can be modified.

The diluent nature also has a minor influence on loading. Aromatic components tend to decrease the metal loading (Batchu and Binnemans, 2018).

When designing another experiment with neodymium in the single-drop cell, conducting a preliminary beaker experiment is highly recommended. Indeed, gelation was not observed with a one-to-one volume ratio for the phases. A sample of the continuous

phase, around 5 mL, and another of the dispersed phase should be prepared. One drop of the dispersed phase should then be placed on the surface of the continuous phase and left for one minute. A thin rod can then be used to break the drop. Gelation is detected if some residue is left on the rod or if the organic phase at the surface does not spread in a circular shape.

The gelation of the extractant does suggest that a high loading is reached in an extremely short time. However, no precise data could be harvested because the equipment is unable to perform with gel residue on the nozzle. New experiments could be planned with an aqueous phase at $p$H 1 or lower. If the one drop beaker experiment still shows gelation, the other potential solutions listed above should be explored.

# 5 Conclusion

In this work, protocols for solvent extraction experiments are tested. Spectrophotometry is used to measure the metal concentration in the aqueous phase after extraction. Indeed, it is a fast and inexpensive method. A calibration curve is used to link concentration to absorbance for each metal. The first step of this thesis was to establish calibration curves for nickel, cobalt and neodymium.

Afterward, solvent extraction experiments in shaken tubes and in a single-drop cell are conducted. The tube experiments give the equilibrium degree of extraction per equilibrium $pH$. A so-called extraction curve can be built from these tube experiments. An attempt to model this curve is developed from the equilibrium constant equation. In all experiments, extractants are diluted in kerosene. Several well documented systems are tested out: nickel extracted with D2EHPA, nickel extracted with Cyanex 272 and cobalt extracted with Cyanex 272. The resulting extraction curves are compared with literature. The objective is to control if spectrophotometry is a suitable analysis method and to find its limitation. An extraction curve of neodymium with D2EHPA is also constructed to extend the data available for this metal.

The single-drop cell is a specific piece of equipment that allows to measure the mass-transfer kinetics of a solute transferred between two phases. In this work, a metal in aqueous solution is transferred into a drop of an organic phase that contains an extractant. The contact time between the two phases is lengthened suitably by keeping the drop in levitation in the cell. It is done by pumping the aqueous phase to counter the rise of the drop. The mass transfer experiment was conducted with nickel and D2EHPA first, then with neodymium and D2EHPA.

Spectrophotometry is an inexpensive, non-destructive and fast characterization method. However, based on the extraction curves obtained and their comparison with literature, it is concluded that it lacks precision for metal concentrations on the two edges of the extraction curve. Issues are apparent for the lower and higher degrees of extraction. At low extraction, the spectra peaks get inexplicably higher than they should according to their initial concentration. This issue worsens for higher metal concentration.

At high degree of extraction, turbidity issues make the spectrophotometry unusable. Centrifugation cannot fully take care of the turbidity. Adding modifiers to the organic phase or salts such as NaCl could be investigated to prevent turbidity, but then the system becomes different from the one studied. The spectrophotometer is thus only suitable for obtaining an order of magnitude at moderate degrees of extraction and concentrations. Other analysis methods that are not sensitive to organic molecules should be employed for precise measurements. For instance, EDTA titration or inductively coupled plasma atomic emission spectrometry (ICP-AES) could be tested out.

In the single-drop cell, nickel transfers much more slowly than zinc. Zinc extracted with D2EHPA is a standard system to develop solvent extraction models. The mass transfer is slowed down by the diffusion resistance in the organic phase of the drop more than by the resistance in the continuous phase around it. It is probable that the reaction kinetics is slower for nickel than for zinc too because more D2EHPA molecules are needed to form a complex with nickel than with zinc. A more in-depth study on the reaction kinetic could be carried out to explore this hypothesis.

A polymerization issue is met in the single-drop cell for neodymium extraction with D2EHPA. The neodymium complex forms polymers. A high metal loading is reached extremely fast in the organic phase once it is in contact with the neodymium solution. To avoid this situation, the equilibrium loading of the system should be lowered drastically. It could be achieved by lowering the aqueous phase $p$H and its concentration. An aromatic diluent tends to lower the neodymium loading too. The system should also imperatively be tested in a beaker for gelation before preparing the cell.

# 6   Bibliography

Ahmad, Z. (2006) 'Selection of materials for corrosive environment', in *Chapter 9 -Principles of Corrosion Engineering and Corrosion Control*. Butterworth-Heinemann, pp. 479–549. Available at: https://doi.org/10.1016/B978-075065924-6/50010-6.

Altunok, M.Y., Kalem, M. and Pfennig, A. (2012) 'Investigation of mass transfer on single droplets for the reactive extraction of zinc with D2EHPA', *AIChE Journal*, 58(5), pp. 1346–1355. Available at: https://doi.org/10.1002/aic.12680.

Ambaye, T.G. *et al.* (2020) 'Emerging technologies for the recovery of rare earth elements (REEs) from the end-of-life electronic wastes: a review on progress, challenges, and perspectives', *Environmental Science and Pollution Research*, 27(29), pp. 36052–36074. Available at: https://doi.org/10.1007/s11356-020-09630-2.

Anticó, E. *et al.* (1996) 'Solvent extraction of yttrium from chloride media by di(2-ethylhexyl)phosphoric acid in kerosene. Speciation studies and gel formation', *Analytica Chimica Acta*, 327(3), pp. 267–276. Available at: https://doi.org/10.1016/0003-2670(96)00103-1.

Anton Paar (2011) *Instruction manual DMA 5000 M*. Graz, Austria.

Aqua-calc.com (2022) *Nickel moles to volume & weight calculation*. Available at: https://www.aqua-calc.com/calculate/mole-to-volume-and-weight/substance/nickel (Accessed: 18 August 2022).

Ayanda, O.S. *et al.* (2013) 'Application of Cyanex extractant in Cobalt/Nickel separation process by solvent extraction', *International Journal of Physical Sciences*, 8(3), pp. 89–97. Available at: https://doi.org/10.5897/IJPS12.135.

Batchu, N.K. and Binnemans, K. (2018) 'Effect of the diluent on the solvent extraction of neodymium(III) by bis(2-ethylhexyl)phosphoric acid (D2EHPA)', *Hydrometallurgy*, 177, pp. 146–151. Available at: https://doi.org/10.1016/j.hydromet.2018.03.012.

Binnemans, K. *et al.* (2013) 'Recycling of rare earths: a critical review', *Journal of Cleaner Production*, 51, pp. 1–22. Available at: https://doi.org/10.1016/j.jclepro.2012.12.037.

Brunn, M. (2021) 'Black Mass one of the hottest issues in battery recycling', *RECYCLING magazine*, 10 September. Available at: https://www.recycling-magazine.com/2021/09/10/black-mass-one-of-the-hottest-issues-in-battery-recycling/ (Accessed: 24 May 2022).

Chauhan, S. and Patel, T. (2014) 'A Review on Solvent Extraction of Nickel', *International Journal of Engineering Research*, 3(9), p. 8.

Cheng, C.Y. (2000) 'Purification of synthetic laterite leach solution by solvent extraction using D2EHPA', *Hydrometallurgy*, 56(3), pp. 369–386. Available at: https://doi.org/10.1016/S0304-386X(00)00095-5.

Cheng, C.Y. *et al.* (2016) 'Recovery of nickel, cobalt, copper and zinc in sulphate and chloride solutions using synergistic solvent extraction', *Chinese Journal of Chemical Engineering*, 24(2), pp. 237–248. Available at: https://doi.org/10.1016/j.cjche.2015.06.002.

Choubey, P.K. *et al.* (2021) 'Development of Hydrometallurgical Process for Recovery of Rare Earth Metals (Nd, Pr, and Dy) from Nd-Fe-B Magnets', *Metals*, 11(12), p. 1987. Available at: https://doi.org/10.3390/met11121987.

Ciacci, L. *et al.* (2019) 'Recovering the "new twin": Analysis of secondary neodymium sources and recycling potentials in Europe', *Resources, Conservation and Recycling*, 142, pp. 143–152. Available at: https://doi.org/10.1016/j.resconrec.2018.11.024.

Daiminger, U.A. *et al.* (1996) 'Efficiency of Hollow Fiber Modules for Nondispersive Chemical Extraction', *Industrial & Engineering Chemistry Research*, 35(1), pp. 184–191. Available at: https://doi.org/10.1021/ie9502392.

Dalvin (2006) *File:Neodym Magnete.jpg*, *Wikipedia Commons*. Available at: https://commons.wikimedia.org/wiki/File:Neodym_Magnete.jpg (Accessed: 15 August 2022).

Darvishi, D. *et al.* (2005) 'Synergistic effect of Cyanex 272 and Cyanex 302 on separation of cobalt and nickel by D2EHPA', *Hydrometallurgy*, 77(3–4), pp. 227–238. Available at: https://doi.org/10.1016/j.hydromet.2005.02.002.

Davis, S. (2020) 'Rare Earth Elements Supply Uncertain for IC Fabs', *Semiconductor Digest*, 29 July. Available at: https://www.semiconductor-digest.com/rare-earth-elements-supply-uncertain-for-ic-fabs/ (Accessed: 3 May 2022).

Dehaine, Q. *et al.* (2021) 'Geometallurgy of cobalt ores: A review', *Minerals Engineering*, 160, p. 106656. Available at: https://doi.org/10.1016/j.mineng.2020.106656.

Donegan, S. (2006) 'Direct solvent extraction of nickel at Bulong operations', *Minerals Engineering*, 19(12), pp. 1234–1245. Available at: https://doi.org/10.1016/j.mineng.2006.03.003.

Dreisinger, D.B. and Cooper, C.W. (1989) 'THE KINETICS OF ZINC, COBALT AND NICKEL EXTRACTION IN THE D2EHPA-HEPTANE-HC104 SYSTEM USING THE ROTATING DIFFUSION CELL TECHNIQUE', *Solvent Extraction and Ion Exchange*, 7(2), pp. 335–360. Available at: https://doi.org/10.1080/07360298908962312.

Elwert, T. *et al.* (2015) 'Current Developments and Challenges in the Recycling of Key Components of (Hybrid) Electric Vehicles', *Recycling*, 1(1), pp. 25–60. Available at: https://doi.org/10.3390/recycling1010025.

Eramet (2022) *Lithium-ion battery recycling: The ReLieVe project confirms the success of the technology developed by Eramet.* Available at: https://www.eramet.com/en/lithium-ion-battery-recycling-relieve-project-confirms-success-technology-developed-eramet (Accessed: 22 May 2022).

European Commission. Joint Research Centre (2018) *Cobalt: demand supply balances in the transition to electric mobility.* LU: Publications Office. Available at: https://data.europa.eu/doi/10.2760/97710 (Accessed: 18 April 2022).

European Commission. Joint Research Centre. and Roskill. (2021) *Study on future demand and supply security of nickel for electric vehicle batteries.* LU: Publications Office. Available at: https://data.europa.eu/doi/10.2760/212807 (Accessed: 18 April 2022).

Flett, D.S. (2004) 'Cobalt-Nickel Separation in Hydrometallurgy: a Review', *Chemistry for Sustainable Development*, 12, pp. 81–91.

Fortum (2022) *Lithium-ion Battery Recycling Technology*, *Fortum*. Available at: https://www.fortum.com/products-and-services/fortum-battery-solutions/recycling/lithium-ion-battery-recycling-technology (Accessed: 25 May 2022).

Georgi-Maschler, T. *et al.* (2012) 'Development of a recycling process for Li-ion batteries', *Journal of Power Sources*, 207, pp. 173–182. Available at: https://doi.org/10.1016/j.jpowsour.2012.01.152.

Goonan, T.G. (2011) *Rare Earth Elements - End Use and Recyclability*. 2011–5094. Denver, U.S.: U.S. Geological Survey Scientific Investigations, p. 15. Available at: https://pubs.usgs.gov/sir/2011/5094/ (Accessed: 2 May 2022).

Grand View Research (2021) *Neodymium Market Size & Share Report, 2021-2028*. Available at: https://www.grandviewresearch.com/industry-analysis/neodymium-market-report (Accessed: 2 May 2022).

Gulliver, J.S. (2007) *Introduction to Chemical Transport in the Environment*. Cambridge: Cambridge University Press. Available at: https://doi.org/10.1017/CBO9780511808944.

Gupta, C.K. and Krishnamurthy, N. (2005) *Extractive metallurgy of rare earths*. Boca Raton, Fla: CRC Press.

Habashi, F. (ed.) (1997) *Handbook of extractive metallurgy*. Weinheim ; New York: Wiley-VCH.

Habashi, F. (2013) 'Extractive metallurgy of rare earths', *Canadian Metallurgical Quarterly*, 52(3), pp. 224–233. Available at: https://doi.org/10.1179/1879139513Y.0000000081.

Hach (2020) *DR 3900 User Manual*. Loveland, U.S.A. Available at: https://fr.hach.com/dr3900-spectrophotometre-avec-technologie-rfid/product-downloads?id=24821420586 (Accessed: 13 April 2022).

Harada, T., Smutz, M. and Bautista, R.G. (1972) 'Characterization of iron and rare-earth polymers of di(2-ethylhexyl)phosphoric acid', *Journal of Chemical & Engineering Data*, 17(2), pp. 203–204. Available at: https://doi.org/10.1021/je60053a052.

Henschke, M. (2004) *Auslegung pulsierter Siebboden-Extraktionskolonnen*. Aachen: Shaker (Berichte aus der Verfahrenstechnik).

Henschke, M. and Pfennig, A. (1999) 'Mass-transfer enhancement in single-drop extraction experiments', *AIChE Journal*, 45(10), pp. 2079–2086. Available at: https://doi.org/10.1002/aic.690451006.

INRS (2014) *Sulfure d'hydrogène*. Fiche Toxicologique Synthétique 32. France: INRS, p. 3. Available at: https://www.inrs.fr/publications/bdd/fichetox/fiche.html?refINRS=FICHETOX_32&section=generalites (Accessed: 29 May 2022).

Jayanti, S. (2017) '7 Main Types of Tool Steels | Metallurgy', *Engineering Notes India*, 24 October. Available at: https://www.engineeringnotes.com/metallurgy/tool-steels/7-main-types-of-tool-steels-metallurgy/26566 (Accessed: 21 April 2022).

Jeffery, G.H. *et al.* (1989) *Vogel's textbook of quantitative chemical analysis*. 5th ed. Harlow, Essex, England : New York: Longman Scientific & Technical ; Wiley.

Jha, M. *et al.* (2021) 'Recovery of Rare Earth Metals (REMs) from Nickel Metal Hydride Batteries of Electric Vehicles', *Minerals*, 12(1), p. 34. Available at: https://doi.org/10.3390/min12010034.

Judge, W.D. and Azimi, G. (2020) 'Recent progress in impurity removal during rare earth element processing: A review', *Hydrometallurgy*, 196, p. 105435. Available at: https://doi.org/10.1016/j.hydromet.2020.105435.

Kippenhan, N. and Gschneidner, K.A. (1970) *RARE-EARTH METALS IN STEELS.* IS-RIC--4, 4092302. Ames, Iowa, US: Rare Earth information center, p. IS-RIC--4, 4092302. Available at: https://doi.org/10.2172/4092302.

Kursunoglu, S. and Kaya, M. (2019) 'Hydrometallurgical processing of nickel laterites - A brief overview on the use of solvent extraction and nickel/cobalt project for the separation and purification of nickel and cobalt', *Bilimsel Madencilik Dergisi*, pp. 131–144. Available at: https://doi.org/10.30797/madencilik.580147.

Leeheng, K. (2014) *Simultaneous measurement of sedimentation and mass transfer of single drops*. Master Thesis. Technische Universität Graz.

Lewis, A.E. (2010) 'Review of metal sulphide precipitation', *Hydrometallurgy*, 104(2), pp. 222–234. Available at: https://doi.org/10.1016/j.hydromet.2010.06.010.

MarketWatch (2022) *Cobalt Sputtering Target Market Product Type Purity 99%,Purity 99.9%,Purity 99.99%,Purity 99.999% Sales, Revenue, Manufacturers, Suppliers, Key Players 2022 to 2028*, *MarketWatch*. Available at: https://www.marketwatch.com/press-release/cobalt-sputtering-target-market-product-type-purity-99purity-999purity-9999purity-99999-sales-revenue-manufacturers-suppliers-key-players-2022-to-2028-2022-05-19 (Accessed: 24 May 2022).

Mohammadi, M. *et al.* (2015) 'Separation of ND(III), DY(III) and Y(III) by solvent extraction using D2EHPA and EHEHPA', *Hydrometallurgy*, 156, pp. 215–224. Available at: https://doi.org/10.1016/j.hydromet.2015.05.004.

Neumann, J. *et al.* (2022) 'Recycling of Lithium-Ion Batteries—Current State of the Art, Circular Economy, and Next Generation Recycling', *Advanced Energy Materials*, 12(17), p. 2102917. Available at: https://doi.org/10.1002/aenm.202102917.

Nguyen, V.N.H., Nguyen, T.H. and Lee, M.S. (2020) 'Review on the Comparison of the Chemical Reactivity of Cyanex 272, Cyanex 301 and Cyanex 302 for Their Application to Metal Separation from Acid Media', *Metals*, 10(8), p. 1105. Available at: https://doi.org/10.3390/met10081105.

Nogueira, C.A. and Delmas, F. (1999) 'New flowsheet for the recovery of cadmium, cobalt and nickel from spent Ni–Cd batteries by solvent extraction', *Hydrometallurgy*, 52(3), pp. 267–287. Available at: https://doi.org/10.1016/S0304-386X(99)00026-2.

Noori, M. *et al.* (2014) 'Selective recovery and separation of nickel and vanadium in sulfate media using mixtures of D2EHPA and Cyanex 272', *Separation and Purification Technology*, 136, pp. 265–273. Available at: https://doi.org/10.1016/j.seppur.2014.08.038.

Olivier, M.C. (2011) *Developing a solvent extraction process for the separation of cobalt and iron from nickel sulfate solutions*. Master of Sciences in Engineering. Stellenbosch University. Available at: https://core.ac.uk/download/pdf/37345124.pdf (Accessed: 12 May 2022).

Parhi, P.K. *et al.* (2015) 'Liquid-liquid extraction and separation of total rare earth (RE) metals from polymetallic manganese nodule leaching solution', *Journal of Rare Earths*, 33(2), pp. 207–213. Available at: https://doi.org/10.1016/S1002-0721(14)60404-X.

Pfennig, A. (2021) 'Process Intensification and Hybridation'. Liège, Belgium.

Porvali, A. *et al.* (2020) 'Nickel Metal Hydride Battery Waste: Mechano-hydrometallurgical Experimental Study on Recycling Aspects', *Journal of Sustainable Metallurgy*, 6(1), pp. 78–90. Available at: https://doi.org/10.1007/s40831-019-00258-2.

Pradhan, S., Nayak, R. and Mishra, S. (2022) 'A review on the recovery of metal values from spent nickel metal hydride and lithium-ion batteries', *International Journal of Environmental Science and Technology*, 19(5), pp. 4537–4554. Available at: https://doi.org/10.1007/s13762-021-03356-5.

Rickelton, W.A., Flett, D.S. and West, D.W. (1984) 'Cobalt-nickel separation by solvent extraction with bis(2,4,4 trimethylpentyl)phosphinic acid', *Solvent Extraction and Ion Exchange*, 2(6), pp. 815–838. Available at: https://doi.org/10.1080/07366298408918476.

Rombach, E. and Friedrich, B. (2014) 'Recycling of Rare Metals', in *Handbook of Recycling*. Elsevier, pp. 125–150. Available at: https://doi.org/10.1016/B978-0-12-396459-5.00010-6.

Roskill Consulting Group, commissioned by the Cobalt Institute (2021) *'State of the Cobalt market' report*. Guildford, UK: Cobalt Institute, pp. 1–20. Available at: https://www.cobaltinstitute.org/wp-content/uploads/2021/05/CobaltInstitute_Market_Report_2020_1.pdf (Accessed: 21 April 2022).

Rout, A., Mishra, S. and Ramanathan, N. (2020) 'Investigations on the physicochemical properties of a combined extractant system under unirradiated and irradiated conditions', *Journal of Molecular Liquids*, 313(113498). Available at: https://doi.org/10.1016/j.molliq.2020.113498.

Sato, H., Yui, M. and Yoshikawa, H. (1996) 'Ionic Diffusion Coefficients of $Cs^{+}$, $Pb^{2+}$, $Sm^{3+}$, $Ni^{2+}$, $SeO_4^{2-}$ and $TcO_4^{-}$ in Free Water Determined from Conductivity Measurements', *Journal of Nuclear Science and Technology*, 33(12), pp. 950–955. Available at: https://doi.org/10.1080/18811248.1996.9732037.

Sato, T. (1989) 'Liquid-liquid extraction of rare-earth elements from aqueous acid solutions by acid organophosphorus compounds', *Hydrometallurgy*, 22(1–2), pp. 121–140. Available at: https://doi.org/10.1016/0304-386X(89)90045-5.

Scharf, C. *et al.* (2005) 'Investigation of the structure of neodymium-di-(2-ethylhexyl) phosphoric acid combinations using electrospray ionization and matrix-assisted laser desorption ionization mass spectrometry and nuclear magnetic resonance spectroscopy', *Metallurgical and Materials Transactions B*, 36(4), pp. 429–436. Available at: https://doi.org/10.1007/s11663-005-0033-0.

Shibata, J. and Nishimura, S. (1977) 'Effect of Sulphate and Chloride Ions on the Solvent Extraction of Some Metal Ions with Liquid Cation Exchangers', *Transactions of the Japan Institute of Metals*, 18(11), pp. 794–802. Available at: https://doi.org/10.2320/matertrans1960.18.794.

Statista (2021) *Global primary nickel consumption by industry share 2020*, *Statista*. Available at: https://www.statista.com/statistics/545041/distribution-of-nickel-consumption-worldwide-by-industry/ (Accessed: 20 April 2022).

Statista (2022a) *Cobalt global mine production volume 2021*, *Statista*. Available at: https://www.statista.com/statistics/339759/global-cobalt-mine-production/ (Accessed: 21 April 2022).

Statista (2022b) *Distribution of rare earth element consumption worldwide in 2020, by end use*, *Statista*. Available at: https://www.statista.com/statistics/604190/distribution-of-rare-earth-element-consumption-worldwide-by-end-use/ (Accessed: 2 May 2022).

Statista (2022c) *Nickel production top countries 2021*, *Statista*. Available at: https://www.statista.com/statistics/264642/nickel-mine-production-by-country/ (Accessed: 18 April 2022).

Statista (2022d) *Rare earth mine production worldwide 2021*, *Statista*. Available at: https://www.statista.com/statistics/1187186/global-rare-earths-mine-production/ (Accessed: 3 May 2022).

Tait, B.K. (1993) 'Cobalt-nickel separation: the extraction of cobalt(II) and nickel(II) by Cyanex 301, Cyanex 302 and Cyanex 272', *Hydrometallurgy*, 32(3), pp. 365–372. Available at: https://doi.org/10.1016/0304-386X(93)90047-H.

Talebi, A. *et al.* (2015) 'Nickel ion coupled counter complexation and decomplexation through a modified supported liquid membrane system', *RSC Advances*, 5(48), pp. 38424–38434. Available at: https://doi.org/10.1039/C5RA00156K.

Umicore (2022) *Our recycling process*. Available at: https://csm.umicore.com/en/battery-recycling/our-recycling-process/ (Accessed: 22 May 2022).

Wilke, C.R. and Chang, P. (1955) 'Correlation of diffusion coefficients in dilute solutions', *AIChE Journal*, 1(2), pp. 264–270. Available at: https://doi.org/10.1002/aic.690010222.

Xun, F. and Golding, J.A. (1987) 'Solvent extraction of cobalt and nickel in bis (2,4,4-tri-methylpentyl) phosphinic acid, "CYANEX -272"', *Solvent Extraction and Ion Exchange*, 5(2), pp. 205–226. Available at: https://doi.org/10.1080/07366298708918562.

Yin, S.-H. *et al.* (2015) 'Study on the aqueous solution behavior and extraction mechanism of Nd( III ) in the presence of the complexing agent lactic acid with di-(2-ethylhexyl) phosphoric acid', *RSC Advances*, 5(79), pp. 64550–64556. Available at: https://doi.org/10.1039/C5RA09928E.

Zhang, Y. *et al.* (2020) 'Hydrometallurgical Recovery of Rare Earth Elements from NdFeB Permanent Magnet Scrap: A Review', *Metals*, 10(6), p. 841. Available at: https://doi.org/10.3390/met10060841.

# 7 Annexes

## 7.1 Protocol

### 7.1.1 Experiment codes

- 2 capital letters for the operator initials
- 4 numbers for the experiment index
- 2 capital letters for the type of experiment
    - SS: aqueous stock solution
    - SO: solvent stock solution
    - SP: spectrometry curve
    - PH: $p$H modification curve
    - SX: solvent extraction
    - SD: mass transfer in the single-drop cell
    - T: titration
- Metals used
- Ex: ST 0001 SS Ni

### 7.1.2 Experiment preparation

- Make sure to have density measurement for each extractant and kerosene
- Make sure to have the physical properties for all chemicals used
- Clean all glassware the day before. Everything must be dry and clean for the experiment.
- Check the analytical balance:
    - Plate is clean
    - Balance is level

### 7.1.3 Cleaning

#### 7.1.3.1 Routine cleaning:
- Rinse with DI three times
- Leave to dry upside down

#### 7.1.3.2 Organic solvent:
- Rinse with 50 mL acetone three times
- Rinse with DI three times

- Leave to dry upside down

## 7.1.4   Preparation of stock solutions

## 7.1.4.1   Salt stock solution

Supplies:

- Analytical balance
- Volumetric flask and stopper
- Plastic boats
- Funnel with a wide opening
- Micropipette and tips
- Deionized water (DI)
- Metal salt
- Printed "Aqueous stock solution template"

Process:

- Concentration must be fixed at the highest value of the range studied
- Note down: date, time, room temperature, supplier and batch number of the chemical(s), name of the apparatus used and the name of the operator
- To avoid contamination of the chemicals in the original package, transfer a small quantity of the required chemical to another container for use. <u>Don't pour back the remaining chemical to the supplier bottle!</u> The chemical that remains in the container will be used later for other experiments.
- Compute the quantity of reagent or chemical required for the stock solution
- At the analytical balance, tare a new plastic boat and weigh the quantity of reagent required
- Tare the analytical balance.
- Weigh the empty volumetric flask with a stopper. It stays on the balance.
- Remove the stopper, put the funnel into place.
- Pour progressively the salts into the volumetric flask. Careful of not pouring too much at once and blocking the funnel.
- Remove the funnel. Put back the stopper.
- Weigh the volumetric flask with the salts and the stopper. Write it down.
- Remove the volumetric flask from the analytical balance.

- Fill the volumetric flask with DI mid-way, close with a stopper and shake vigorously to dissolve the solids completely.

- Fill the volumetric flask up to the neck with DI.

- Using a micropipette, fill the volumetric flask with DI until the meniscus has its lower point on the mark

- Close the volumetric flask with a stopper and homogenize.

- Weigh the filled volumetric flask with the stopper and note the weight.

- Ready to use, prepare samples of the stock solution to measure density and $p$H

## 7.1.4.2   Solvent stock solution

Supplies:

- Analytical balance

- Glass bottle with a screw cap

- Micropipette and tips

- Kerosene

- Extractant

- Printed "Organic stock solution template"

Process:

- Note down: date, time, room temperature, apparatus used, supplier and batch number of chemicals and name of operator

- Choose the volume fraction of extractant to use and which extractant

- Pour some extractant in a glass bottle, label it. Do not pour it back into the supplier bottle! Proceed in the same way for kerosene.

- Compute the weight of extractant and kerosene required for the desired volume, write the calculations in the laboratory notebook

- Tare the analytical balance

- Use a clean glass bottle with a screw cap

- Weigh the bottle, it stays on the same balance for the whole process.

- With a micropipette, add the required quantity of extractant in the new vessel. Write the final extractant weight in the template.

- With the micropipette, add the required quantity of kerosene. Note the final kerosene weight in the template.

- Close the bottle and shake

## 7.1.4.3 NaOH/HCl for *p*H modification

Supplies:

- Analytical balance
- *p*H-meter with stand
- Micropipette with tips
- Magnetic stirrer with magnetic rod
- 100 mL beaker
- Burette with stand
- Waste beaker
- Metal stock solution
- NaOH or HCl stock solution (named PS)
- Printed "*p*H curve template"

Process:

- Tare the analytical balance
- Put the magnetic rod in the beaker. Weigh the beaker with the magnetic rod, note down the weight
- With a micropipette, add 50 mL of the metal stock solution, weigh
- Rinse 3 times the burette with DI and 2 times with 10 mL of the PS above a waste beaker
- Fill the burette with the PS and place it vertically on the stand
- Place the beaker on the magnetic stirrer with the burette above
- Rinse and blot drops off the *p*H probe. Fix it vertically in the beaker with a stand.
- Start stirring.
- Take the *p*H measurement once it is stable.
- Add 0.5 mL of PS at once, take the *p*H measurement once it is stable and keep going until a *p*H of 13 or 1 is reached.

## 7.1.5 Sample preparation

## 7.1.5.1 Dilution

Supplies:

- Analytical balance

- Tube with a screw cap

- Micropipette and tips

- DI

- Stock solution

- Printed "Calibration curve template" or "Extraction template"

Process:

- From the concentration of the stock solution, compute the volume of stock solution and water needed. Write the calculation in the laboratory notebook.

- Note the temperature of the room, date, time, name of the operator, apparatus used

- Use a new tube for the diluted solution, label it

- Tare the analytical balance

- On an analytical balance, weigh the tube, the tube stays on the analytical balance for the whole dilution

- Use a micropipette to transfer the exact quantity of stock solution in the tube. Weigh on the analytical balance, note the value

- Use a micropipette to pour the exact quantity of DI needed, weigh and write the value in the template

- Close the tube and shake to homogenise

## 7.1.5.2   Solvent extraction

For each batch of solvent extraction, one tube should contain only DI and the organic phase.

Supplies:

- Analytical balance

- Water bath

- Timer

- Tube with a cap

- Micropipette and tips

- Solvent solution

- Aqueous solution

- *p*H changer solution (NaOH or acid solution)
- Syringes and needles
- Printed "Extraction Template"

Process:

- Choose the volume ratio between aqueous and organic phase. Calculate the mass and volume of organic phase needed in the laboratory notebook
- Choose the temperature of extraction, write it in the template.
- Note down the date, time, room temperature, name of operator, apparatus and stock solutions used on the template
- Warm up the water bath to the desired temperature
- Tare the analytical balance
- Take a clean tube with a cap, weigh it and keep the tube on the analytical balance.
- With a micropipette, perform the needed dilution from stock solution and add a fixed volume of NaOH or HCl solution for *p*H adjustment. Weigh and write in the template.
- With a micropipette, add the required quantity of organic stock solution, weigh and write the mass on the template.
- Screw the cap tightly on
- Place the tube vertically in the rotating basket. Be sure it won't move around and close the basket tightly.
- Start rotating for the prescribed time.
- Clock the time elapsed. Once time is up, stop the motor and unplug the wire
- Move the rotating basket to a drip tray and place it so that the extraction tube is upright again.
- Carefully open the basket and put it back in the water bath, with the tube still upright.
- Wait for the phase separation to happen
- Dry the exterior of the tube
- Remove carefully the cap. Be sure to prevent water from the bath from entering the tube.

- Remove carefully the organic phase with a single-use syringe, put it in a new tube if it is needed for further measurements or experiments
- With the same syringe, suck the remaining organic phase left with a bit of the aqueous phase, discard it.
- Take another syringe, suck the aqueous phase in and pour it in a new tube. Label it
- Wash the extraction tube
- Measure the concentration of metal by spectrometry and based on the calibration curve
- Measure $p$H from the aqueous phase

## 7.1.6   Analysis

### 7.1.6.1   $p$H meter calibration
Supplies:

- $p$H-meter
- Tube
- Buffer solutions
- DI
- Paper towel

Process:

- Calibration done once a day for weakly acid or weakly basic solution.  If the solution contains a strong acid or base, calibration done after each measurement.
- The $p$H of the buffer solution must frame the expected $p$H of the solution to be measured
- Take the $p$H probe out of its storage solution
- Rinse the probe with DI
- Blot water drops off from $p$H probe with a paper towel
- Press "CAL" and follow the order of buffer solution
- Once the probe is in the buffer solution, press "CAL" and stir until the calibration is done
- Rinse the probe with DI, dab and repeat in the other buffer solutions

- Note: If there is an error at the calibration, start again but let the probe soak in the buffer solution one or two minutes before pressing "CAL"
- The list of errors that can occur can be found at the back of the *p*H-meter
- "Error 14" only means that the clock of the *p*H-meter is not properly set; it doesn't influence the calibration and *p*H-measurement

## 7.1.6.2   *p*H measurement

- Warning: *p*H measurement is the last analysis to be done on a solution. The solution is unusable afterward.

Supplies:

- *p*H-meter
- Tube
- Solution to measure
- DI
- Paper towel

Process:

- In a clean tube, pour enough volume of the solution to be measured to immerse the *p*H sensor hole (it could be 5-10 mL in a small tube, 20 mL in a big one).
- Rinse the probe with DI 3 times, blot water drops off with a clean paper towel
- Dip the probe in the solution to measure and stir until the *p*H value is stabilised.
- Write the result in the template of the solution
- Once the measurement is done, rinse the probe with DI and put away the *p*H probe in its storage solution.
- Discard the solution used for the pH-measurement, it cannot be used again for an experiment/analysis

## 7.1.6.3   Density measurement

Supplies:

- Densitometer
- Syringe
- Solution to measure
- Acetone

- DI
- Paper towel

Process:

- Use Density & sound method to measure density and speed of sound
- Take a new syringe, fill it with solution, remove bubbles
- Inject the solution in the machine until there is no more bubble in the circuit
- Choose the temperature, press Start, wait
- Note the results on the template of the sample
- Once the measurement is ended, clean the machine and dry
- with the syringe full of air, push the sample out
- rinse the capillaries with 20 mL water
- rinse with 20 mL acetone twice, the second last with back-and-forth movements
- Connect the tube, start the ventilator of the machine to dry the capillaries
- Once the machine is clean, another liquid can be measured

## 7.1.6.4   Spectrometry

Supplies:

- Spectrometer
- Adapter
- Measurement cell
- Micropipette with tips
- Solution to measure
- DI

Process:

- Switch on the spectrophotometer about 15 min before using it
- Put the adapter into place
- A micropipette is used to fill the cells
- Each time the machine was shut down, make the zero from air
- Make a measure of DI for each measure set.
- Use the disposable cuvettes as it is without additional cleaning
- For each sample to be analysed

- Fill a new cell with the solution to measure, only touch the non-transparent parts at the top. 1 to 2 mL are needed
- Put the cell in the machine, the arrow drawn on the cell should be in front of the arrow of the adapter
- Close the "door" above the cell, press READ
- Check the plausibility of the result by pointing the metal wavelength on the signal
    - Nickel: 393 nm for upper signal, 501 nm for lower signal
    - Cobalt: 510 nm for upper signal, 754 nm for lower signal
- Put a USB key in the slot, send data to USB memory after each measurement, write down the file name generated by the spectrometer for the experiment on the template of the sample
- Discard the solution and the cell
- Switch off the device

## 7.1.7  Mass transfer experiment

## 7.1.7.1  Washing the equipment
Supplies:
- DI
- Thermostatic bath
- Vessels for DI
- Vessels for washing liquid
- Carboy labelled "Liquide spéciaux"


Process:
- Stop the pump
- Remove the nozzle from the cell
- Empty the nozzle in a waste beaker and disconnect it from the capillary
- Empty the syringes
- Empty the equipment from the continuous phase. Store the metal solution in a closing carboy labelled "Liquide spéciaux". Write the metal on the top of the carboy.

- If there is some precipitate on the wall of the equipment, prepare an acidic solution. The $pH$ depends on the metal hydroxide: it must be low enough to solubilize it. Wash the equipment once with the acidic solution. Make sure there is no precipitate remaining in the equipment. Empty it.

- Wash the equipment three times with 3 L of distilled water (DI) at 40°C. Between the second and the third washing, the heat exchanger is washed separately.

- Measure $pH$ on the third rinse water to control the cleaning quality

- Take one sample of the third rinse water before it is poured in the equipment.

- Take water samples of the third rinse water after the cleaning step,

- One at the bottom of the settling cell

- One at the bottom of the heat exchanger.

- Measure the $pH$ of all samples. If the $pH$ is the same for the three samples, the washing is considered to be finished. Otherwise, keep cleaning with hot DI and take samples as explained until $pH$ is the same in the entire equipment.

- The following sequence must be observed for each wash with DI

- Ensure that the valves V2, V4, V5, V6 and V8 on the bottom are closed, the valve at the top V1 is open, the screw at the top of the Single-drop cell (SD) is loose

- Fill the settling cell (SC) to the top, wait 5-10 min for the DI to reach up to the heat exchanger (HTX) and the rotameter (R)

- Start the pump at 10 L/h and wait until the level in R and HTX stays the same.

- Stop the pump

- The water level in the SC has decreased since the beginning. Add more DI to reach the top of the SC.

- Wait until the DI level in the HTX and R has finished rising

- Ensure that the DI level in the SD has reached the top and screw the top tightly on

- Start the pump at 10 L/h

- Once the flow is established between the R and the HTX, close V1

- Step up the volume rate to 50 L/h and let it flow for 1 h

- Stop the pump

- Open V1

- Open the valves V4, V5 and V6. Let the water drain.

- Unscrew the top of the SD
- Ensure no DI is left anywhere in the pipes by opening all the valves
- To wash the heat exchanger:
- Unscrew the connector between R and the pipe on the cap of HTX.
- Rotate carefully the HTX cap on a vertical axis to pop the pipe out of the connector
- Take out the cap of the HTX
- Close the V8 valve to prevent the DI getting out or in the pump
- Fill the HTX to the top with hot DI
- Open the V8 valve to drain the DI without the DI getting in the pump
- Repeat the filling and draining thrice
- Disconnect the funnel from the capillary
- Open the top of the SD and remove the funnel from the equipment
- Wash the funnel inside and outside thrice with acetone and then with DI. Let it dry.
- Wash thrice the inside and the outside of the nozzle with acetone. Let it drain and repeat with DI.
- Wash the capillaries
- Suck acetone in the syringe via the capillaries. An acetone volume equivalent to 400 steps must pass through each capillary
- Suck air through each capillary until they are empty
- Leave the capillaries to dry
- Remove the syringes from the syringe pump
- Empty the syringes and disassemble them
- Rinse three times the inside of the syringes and the plungers
- Leave them to dry
- Once the syringes, the capillaries and the funnel are dry, put them back in place.
- The equipment is ready

## 7.1.7.2   Experiment preparation

Supplies:

- Vessel filled with 3 L DI
- Diluent

- Organic stock solution
- Volumetric flask
- Metal salt
- Analytical balance
- *p*H-meter

Process:

- 12 h in advance, prepare the dispersed phase and saturated deionized water. To saturate the phases, add a thin layer of the diluent to DI and some DI to the dispersed phase.
- Prepare the continuous phase
- Prepare a metal stock solution more concentrated than the desired continuous phase concentration
- Remove the dispersed phase from the saturated DI
- Use the saturated DI and the stock solution to prepare 3 L of the continuous phase at the fixed *p*H
- Take a sample of the continuous phase in the beaker and measure *p*H. Adjust *p*H if needed.
- The following sequence is observed to fill the equipment
- Ensure that the valves V2, V4, V5, V6 and V8 on the bottom are closed, the valve at the top V1 is open, the screw at the top of the Single-drop cell (SD) is loose
- Fill the settling cell (SC) to the top, wait 5-10 min for the solution to reach up to the heat exchanger (HTX) and the rotameter (R)
- Start the pump at 10 L/h and wait until the level in R and HTX stays the same.
- Stop the pump
- The water level in the SC is lower. Add more solution to reach the top of the SC.
- Wait until the DI level in the HTX and R finished rising.
- Ensure that the DI level in the SD reached the top and screw the top tightly on.
- Start the pump at 10 L/h.
- Once the flow is established between the R and the HTX, close V1
- Sep up the volume rate to 50 L/h and let it flow for 1 h
- Stop the pump

- Collect a sample of the continuous phase through V2 and check if the *p*H is as expected. This step must be done before starting any experiment,

- Separate the saturated organic phase from the DI by transferring carefully the dispersed phase in another bottle, leaving the DI at the bottom of the first bottle

- Follow the instructions of the file "Manual small single drop cell - 2013.docx" for filling the nozzle and making the measurements at different residence times

## 7.2 Calibration curve nickel

| Sample concentration [g/L] | Delta Absorbance [-] | Exact metal mass fraction [-] | Computed metal mass fraction [-] | Relative error [%] |
|---|---|---|---|---|
| 30 | 1.077 | 0.0289 | 0.0288 | -0.44 |
| 27 | 0.97 | 0.0262 | 0.0261 | -0.06 |
| 24 | 0.862 | 0.0234 | 0.0235 | 0.23 |
| 21 | 0.755 | 0.0206 | 0.0207 | 0.78 |
| 18 | 0.646 | 0.0177 | 0.0179 | 0.94 |
| 15 | 0.543 | 0.0150 | 0.0152 | 1.43 |
| 12 | 0.395 | 0.0120 | 0.0112 | -6.68 |
| 9 | 0.324 | 0.0090 | 0.0092 | 2.23 |
| 6 | 0.210 | 0.0060 | 0.0060 | 0.13 |
| 3 | 0.107 | 0.0030 | 0.0031 | 2.93 |
| 1 | 0.031 | 0.0009 | 0.0009 | 0.65 |
| 0 | 0.000 | 0.0000 | 0.0000 | - |

Table 7-1: Relative errors relative to the calibration curve of nickel

## 7.3  Calibration curve of cobalt

| Sample concentration [g/L] | Delta Absorbance [-] | Exact metal mass fraction [-] | Computed metal mass fraction [-] | Relative error [%] |
|---|---|---|---|---|
| 10 | 1.703 | 0.0097 | 0.0096 | -0.62 |
| 10 | 1.712 | 0.0097 | 0.0097 | -0.13 |
| 8 | 1.371 | 0.0078 | 0.0078 | 0.47 |
| 8 | 1.373 | 0.0078 | 0.0079 | 0.61 |
| 6 | 1.025 | 0.0059 | 0.0060 | 0.84 |
| 6 | 1.021 | 0.0059 | 0.0059 | 0.47 |
| 4 | 0.665 | 0.0040 | 0.0039 | -1.81 |
| 4 | 0.683 | 0.0040 | 0.0040 | 0.77 |
| 2 | 0.334 | 0.0020 | 0.0020 | 0.25 |
| 2 | 0.317 | 0.0020 | 0.0019 | -4.78 |
| 1 | 0.167 | 0.0010 | 0.0010 | -3.94 |
| 1 | 0.167 | 0.0010 | 0.0010 | -3.94 |
| 0.2 | 0.025 | 0.0002 | 0.0002 | -19.29 |
| 0.2 | 0.026 | 0.0002 | 0.0002 | -16.07 |
| 0 | 0.000 | 0.0000 | 0.0000 | - |

Table  7-2: Relative error for the calibration curve of cobalt

## 7.4   Calibration curve of neodymium

| Sample concentration [g/L] | Delta Absorbance [-] | Exact metal mass fraction [-] | Computed metal mass fraction [-] | Relative error [%] |
|---|---|---|---|---|
| 7.0 | 0.251 | 0.0070 | 0.0068 | -2.7 |
| 7.0 | 0.256 | 0.0070 | 0.0069 | -0.8 |
| 5.0 | 0.183 | 0.0052 | 0.0050 | -5.1 |
| 5.0 | 0.195 | 0.0052 | 0.0053 | 1.2 |
| 4.5 | 0.175 | 0.0047 | 0.0047 | 0.8 |
| 4.5 | 0.176 | 0.0047 | 0.0048 | 1.4 |
| 4.0 | 0.156 | 0.0042 | 0.0042 | 0.8 |
| 4.0 | 0.157 | 0.0042 | 0.0043 | 1.5 |
| 3.5 | 0.132 | 0.0037 | 0.0036 | -2.3 |
| 3.5 | 0.137 | 0.0037 | 0.0037 | 1.4 |
| 3.0 | 0.116 | 0.0032 | 0.0031 | -0.1 |
| 3.0 | 0.118 | 0.0032 | 0.0032 | 1.6 |
| 2.5 | 0.098 | 0.0026 | 0.0027 | 1.0 |
| 2.5 | 0.096 | 0.0026 | 0.0026 | -1.1 |
| 2.0 | 0.08 | 0.0021 | 0.0022 | 2.9 |
| 2.0 | 0.08 | 0.0021 | 0.0022 | 2.9 |
| 1.5 | 0.059 | 0.0016 | 0.0016 | 0.6 |
| 1.5 | 0.06 | 0.0016 | 0.0016 | 2.3 |
| 1.0 | 0.039 | 0.0011 | 0.0011 | -0.1 |

| Sample concentration [g/L] | Delta Absorbance [-] | Exact metal mass fraction [-] | Computed metal mass fraction [-] | Relative error [%] |
|---|---|---|---|---|
| **1.0** | 0.039 | 0.0011 | 0.0011 | -0.1 |
| **0.5** | 0.021 | 0.0006 | 0.0006 | 2.2 |
| **0.5** | 0.019 | 0.0006 | 0.0005 | -7.5 |
| **0.0** | 0 | 0.0000 | 0.0000 | - |

Table 7-3: Relative error for the calibration curve of neodymium

## 7.5   Extraction curve nickel and D2EHPA

| pH [-] | Metal in aqueous [g] | Metal out aqueous [g] | Metal in organic [g] | Metal out organic [g] | degree of extraction [-] |
|---|---|---|---|---|---|
| 2.4 | 0.0303 | 0.0307 | 0.0000 | -0.0004 | -0.0131 |
| 2.72 | 0.0284 | 0.0240 | 0.0000 | 0.0044 | 0.1556 |
| 2.97 | 0.0302 | 0.0211 | 0.0000 | 0.0092 | 0.3031 |
| 3.19 | 0.0297 | 0.0158 | 0.0000 | 0.0139 | 0.4685 |
| 3.45 | 0.0303 | 0.0074 | 0.0000 | 0.0229 | 0.7569 |
| 3.72 | 0.0299 | -0.0018 | 0.0000 | 0.0316 | 1.0590 |

Table  7-4: Mass balance extraction of nickel by D2EHPA

## 7.6   Extraction curve nickel and Cyanex 272

| pH [-] | Metal in aqueous [g] | Metal out aqueous [g] | Metal in organic [g] | Metal out organic [g] | degree of extraction [-] |
|---|---|---|---|---|---|
| 2.89 | 0.0303 | 0.0313 | 0.0000 | -0.0010 | -0.0323 |
| 4.75 | 0.0303 | 0.0265 | 0.0000 | 0.0037 | 0.1234 |
| 5.14 | 0.0303 | 0.0173 | 0.0000 | 0.0130 | 0.4284 |
| 5.29 | 0.0299 | 0.0208 | 0.0000 | 0.0091 | 0.3032 |
| 5.32 | 0.0303 | 0.0126 | 0.0000 | 0.0177 | 0.5836 |
| 5.47 | 0.0300 | 0.0074 | 0.0000 | 0.0226 | 0.7543 |

Table  7-5: Mass balance extraction of nickel by Cyanex 272

## 7.7 Extraction curve neodymium and D2EHPA

| $p$H [-] | Metal in aqueous [g] | Metal out aqueous [g] | Metal in organic [g] | Metal out organic [g] | degree of extraction [-] |
|---|---|---|---|---|---|
| 0.5 | 0.0706 | 0.0613 | 0.0000 | 0.0093 | 0.1316 |
| 0.54 | 0.0708 | 0.0589 | 0.0000 | 0.0119 | 0.1676 |
| 0.55 | 0.0706 | 0.0576 | 0.0000 | 0.0129 | 0.1834 |
| 0.6 | 0.0707 | 0.0553 | 0.0000 | 0.0154 | 0.2181 |
| 0.62 | 0.0709 | 0.0536 | 0.0000 | 0.0173 | 0.2444 |
| 0.67 | 0.0710 | 0.0445 | 0.0000 | 0.0265 | 0.3727 |
| 0.75 | 0.0704 | 0.0419 | 0.0000 | 0.0285 | 0.4047 |
| 0.85 | 0.0720 | 0.0374 | 0.0000 | 0.0346 | 0.4808 |
| 0.93 | 0.0718 | 0.0297 | 0.0000 | 0.0420 | 0.5856 |
| 0.98 | 0.0715 | 0.0268 | 0.0000 | 0.0447 | 0.6248 |
| 1.03 | 0.0716 | 0.0236 | 0.0000 | 0.0480 | 0.6708 |
| 1.12 | 0.0715 | 0.0227 | 0.0000 | 0.0487 | 0.6818 |
| 1.19 | 0.0716 | 0.0165 | 0.0000 | 0.0551 | 0.7698 |
| 1.29 | 0.0715 | 0.0129 | 0.0000 | 0.0586 | 0.8196 |
| 1.41 | 0.0713 | 0.0088 | 0.0000 | 0.0625 | 0.8767 |
| 1.59 | 0.0710 | 0.0038 | 0.0000 | 0.0672 | 0.9459 |

Table 7-6: Mass balance extraction of neodymium by D2EHPA